The John A. Moran Eye Center is committed to the goal that no person with a blinding condition, eye disease or visual impairment should be without hope, understanding and treatment.

The John A. Moran Eye Center

Research and Clinical Abstracts 2009 - 2010

Contents

Photos Courtesy of Bryan William Jones and Ann Torrence. Collaborators: Brenda Stringham, Greg Jones, Bryan William Jones, and Nathan Galli.

Randall J. Olson, MD

Chair, Presidential Professor

The John Moran Eye Center was born as the new home for the Department of Ophthalmology and Visual Sciences at the University of Utah School of Medicine in July of 1993. The one person Division of Ophthalmology in the Department of Surgery in 1979 had grown to need this new 82,000 square feet facility. Sadly, we had dedicated only 20,000 square feet to research and the space was obviously inadequate after living in our new building only a few short years. After years of planning and fund raising we were able to move into our present building in August of 2006. This time we dedicated over half of a 210,000 square feet building to research, which space includes over 30,000 square feet roughed in and ready for program expansion. With the new building, the research program has expanded nicely, and we are very proud of our research team. This publication is our opportunity to showcase some of the work and effort ongoing here. While the work represented spans the field from very clinical to very basic, major emphasis has been placed on retinal research. As part of this we are pleased to announce our new Center for Translational Medicine under our John A. Moran Presidential Endowed Professor, Greg Hageman. We will be announcing soon other members that will be joining his team.

As Chair of the Department and CEO of the John A. Moran Eye Center, I am most pleased with the research effort and the proposed expansion as we look to the future. The size of the research mission now represents close to half our budget and our total NIH funding for the next academic year will exceed $10 million a year. Our real hope is that our institution takes the translational mission to heart and that our research effort here will lead to new treatments for our patients as we look to the future.

Sincerely,
Randall J Olson, MD

Robert Marc, PhD

Director of Research

The Moran Eye Center houses researchers whose studies span the development of the eye to the organization of cortex; the basis of phototransduction to the genetics of retinal diseases; the synaptology of the retina to neuroprosthetics. These efforts are enhanced by strong graduate programs and a tradition of interdepartmental collaboration. Our principles include maintaining basic science expertise, fostering research alliances, and accelerating the evolution of translational science programs.

Paul Bernstein, MD, PhD

Director of Clinical Research

The Clinical Research Group at the Moran Eye Center focuses on research that directly impacts the patient. Whether this means working with industry sponsors to run a clinical trial investigating a new drug or a clinician initiated study to systematically compare standard of care treatments, the Clinical Research Group is focused on finding the optimal in patient care. In this year alone, we have 45 clinical trials and research studies underway involving more than 550 patients. This work is shared with the global ophthalmic community in over 27 publications just this year.

Gregory Hageman, PhD

Director of Translational Research

The Moran Center for Translational Medicine (CTM) was recently created to expedite the pace at which basic scientific discoveries are translated into clinically effective diagnostics and therapies for the treatment of devastating eye disorders such as age-related macular degeneration and glaucoma, as well as other diseases. The conceptual framework for the CTM derived from a growing realization that seemingly disparate diseases likely share common etiologies and thus, common therapeutic targets. The CTM will draw upon the collective strengths and expertise of a collaborative team of cell biologists, molecular microbiologists, pathologists and clinicians to expedite its translationalmission. The unique resources, clinical acumen and scientific expertise of the CTM will complement the core competecies of collaborating corporate and academic partners to insure its success.

ARVO 2010

The Association for Research in Vision and Ophthalmology Honors the ARVO Fellows Inaugural Class of 2009

2009 Silver Fellows	• Wolfgang Baehr, PhD • Robert E. Marc, PhD
Class of 2010	
2010 Gold Fellow	• Gregory S. Hageman, PhD
2010 Silver Fellow	• Paul S. Bernstein, MD, PhD

2010 ARVO Abstracts

Antisense Morpholine Oligonucleotide Against FLT Splice Junction Inhibits Murine Corneal Hemangiogenesis (HA) and Lymphangiogenesis (LA)

Y. Qazi[1,2], H. Uehara[1], B.K. Ambati[1].
[1]Ophthalmology, John Moran Eye Center/University of Utah, Salt Lake City, UT;
[2]Ophthalmology, Emory Eye Center/Emory University, Atlanta, GA

Purpose. To design and test a molecular tool to convert the pro-angiogenic microenvironment of vascularised corneas by manipulating post-transcriptional processing of the FLT gene towards its anti-angiogenic isoform, sFLT-1.

Methods. Antisense morpholino oligonucleotide (morpholino, MO) was designed complementary to a sequence within the FLT splice junction of exon13-intron13 at the 5' splice site. Gene Tools LLC. prepared the morpholino. Fluorescein-tagged standard morpholino (STD MO) was transfected (electroporation) into HUVECs to test and confirm delivery of morpholinos into the nucleus using fluorescence microscopy.

A suture-induced model of corneal neovascularization (KNV) was used. BALB/CJ mice had 3 sutures placed intrastromally.1 week after suture placement, the mice were randomly divided into 3 groups, their corneas photographed and each of the groups received one of the following interventions intracorneally: 200ng sFlt-MO; 200ng STD MO; 5ul phosphate-buffered saline (PBS).1week post-injection, the corneas were photographed and the mice sacrificed. The harvested corneas were were used for flatmounts, ELISA and RT-PCR. Immunostaining was performed for vascular endothelial cells (CD31) and lymphatic endothelial cells (LYVE1). Scion Image was used to quantitate HA and LA from flatmounts imaged by fluorescence microscopy.

KNV was induced in mice as above and 1 week after suture placement, the mice were randomly divided into 2 groups, each of which received an intracorneal injection of a combination of either 2ug siRNA.sFlt + 200ng sFlt-MO, or, 2ug siRNA negative control + 200ng sFlt-MO. 1 week post-injection, the corneas were harvested and processed as mentioned above.

Results. Morpholinos designed to increase sFlt-1 (sFlt-MO) significantly inhibited the progression of both blood and lymph vessels.Treated corneas had 6.9% HA ($p= 0.017$, $n=8$) and 4.6% LA ($p<0.01$, $n=8$) compared to control STD MO with 65.6% HA and 52.9%. Regression of KNV was also seen.sFlt-MO increased its RNA transcript on RT-PCR and reduced free VEGF-A expression on ELISA. pSEC.siRNA. sFlt-1 abolished the effects of sFlt-MO, confirming specificity of mechanism.

Conclusions. sFlt-MO promotes alternative splicing of the murine FLT gene to sFLT-1 rendering an anti-angiogenic microenvironment in the cornea. The 5' splice site of FLT gene at e13-i13 junction may be a promising target in the development of molecular antiangiogenic strategies.
Program#/Poster#: 2038

Designing and Manufacturing a Refillable Multi-Drug Capsule Ring Platform

C.J. Bishop[1A], H.J. Sant[1B], S.A. Molokhia[2], R.M. Burr[1A], B.K. Gale[1B], B.K. Ambati[2].
[A]Biomedical Engineering, [B]Mechanical Engineering, [1]University of Utah, Salt Lake City, UT; [2]Ophthalmology, Moran Eye Center, Salt Lake City, UT.

Purpose. AMD treatment requires monthly intravitreal injections which are uncomfortable, risky, and costly. Because glaucoma is treated using topical polypharmaceutic regimens, patient compliance and drug-target interactions are low. A controlled delivery device would benefit both ocular diseases and transcend the patient interface. Our Capsule Drug Rings (CDR) are implanted in the capsule bag periphery during IOL placement. The CDRs are to be refilled every 6 months to 1 year in situ.

Methods. CDRs are made of well-established biocompatible materials. The inflatable shell of the CDR is a flexible polycarbonate-based polyether urethane which resists hydrolytic degradation improving longevity in vivo. A CO2 laser was used to laminate the shell edge of the CDR. Refilling Ports were made of polyimide tubing and resealing polydimethylsiloxane plugs acting as a one-way valve. One side of the shell consisted of a 1 mm2 oval window, covered by a 30 nm diameter pore-size polyethersulfone filter. Islets were placed at the ends of the device for surgical manipulation. CDRs were implanted in rabbits during intraocular lens implantation.

Results. Each port re-seals and holds at least 40 mm Hg up to 30 insertions. The carbothane shell's inner and outer diameters are 11.0 and 13.0 mm, respectively. The thickness of the shell pre and post-inflation is 200 µm and 750 µm, respectively. The drug reservoir holds 80 µL. Significantly, various sections of the CDR shell were laminated using different laser parameters. The edges with greater curvature required greater speed or less power. Radial lamination (vs horizontal or vertical) due to the symmetry and curvature of the ring device was far superior for proper sealing.

Conclusions. The CDR multi-drug platform is a promising device for treating multiple diseases simultaneously (AMD, Glaucoma, etc.). The CDR filter placement, thickness, pore size/density, window size, and drug concentration can be altered to optimize near zero order pharmacokinetics for a given drug molecule.
Program#/Poster#: 5331/A259

Higher Levels of Soluble NRP-1 May be Associated With Lesser Corneal Neovascularization in MRL6/MPJ Mice Compared to Their Background Strain C57BL/6J Mice

N. Singh, L. Luo, J.M. Simonis, B.K. Ambati
Ophthalmology-University of Utah, John Moran Eye Center, Salt Lake City, UT.

Purpose. To determine whether soluble neuropilin-1 is elevated in MRL6/MpJ mice compared to their background strain C57BL/6J mice.

Methods. C57BL/6J and MRL6/MpJ mice corneas were injected with plasmid expressing SiRNA against soluble NRP. The corneas were imaged after every 3 days and harvested 10 days after injections. C57BL6 mice developed significant higher level of blood vessels compared to MRL/MpJ mice. Corneas were immunostained with the CD31 antibodies and confocal images were obtained using an Olympus confocal microscope. RNA was isolated from the MRL6/MpJ and C57BL/6 mice and Real time PCR was performed using primers designed against N- terminal region present in soluble NRP-1 and C-terminal end present only in membrane NRP-1.

Results. Normal MRL6/MpJ mice had significant higher levels of soluble NRP 1 compared to background strain C57BL/6J mice ($p=0.00018$). Vascularization of cornea leads to significant decrease in soluble NRP-1 ($p=0.0153$) with a concurrent increase in membrane NRP-1 ($p=0.0374$) in C57BL/6J mice, while there was no significant change in levels of soluble NRP-1 is MRL6/MpJ mice.

Conclusions. Higher level of soluble NRP1 may be associated with a resistance to injury-induced corneal neovascularization in MRL6/MpJ mice.
Program#/Poster#: 5701/D865

In vitro Diffusion and Permeability of a Novel Intraocular Drug Delivery Implant

R.M. Burr[1A], S.A. Molokhia[1B], C.J. Bishop[1A], H.J. Sant[1C], J.M. Simonis[1B], B.K. Gale[1C], B.K. Ambati[2].
[A]Bioengineering, [B]Ophthalmology, [C]Mechanical Engineering, [1]University of Utah, Salt Lake City, UT; [2]Ophthalmology, John Moran Eye Center, Salt Lake City, UT.

Methods. To control the release of Avastin® we have investigated 3 commercially available hydrophilic and biocompatible membranes: Polyethersulfone (PES), Polycarbonate (PC), and Polyvinylidene Fluoride. The membrane is attached to a 1 - 4 mm2 hole that has been previously cut in a controlled drug delivery ring (CDR). An rhVEGF ELISA with known concentrations for calibration was used to assay samples collected. Side by side diffusion chambers of 2 ml each (donor and receiver) were used to identify the permeability coefficients of our Avastin® formulation for each membrane. 1 ml samples were taken from the receiver and replaced with an equal volume of fresh PVA every 2 to 6 hours for a maximum of 24 hours. We also conducted drug release studies using the PES and PC membranes to determine diffusion coefficients for later translation into a suitable in vivo Avastin® formulation. Samples were taken and replaced with an equal volume of fresh BSS daily for the first week and 1 - 2 times per week thereafter until no Avastin® was detected.

Results. The CDR will provide long-term sustained release of drug from a 100 µl reservoir. One candidate drug that we are investigating is Avastin® which is currently administered via intravitreal (IV) injections at 1.25 mg/month. We have formulated Avastin® with a polyvinyl alcohol (PVA) polymer to increase Avastin® stability and slow the release rate from the CDR. CDRs were filled with 50 - 100 µl of 12.5 and 25 mg/ml Avastin® solutions and placed in 4 ml of balanced salt solution. We found continuous elution for >2 months and therefore the CDR is a plausible alternative to monthly IV injections.

Conclusions. In vitro diffusion studies confirm long-term release of Avastin® from the CDR.
Program#/Poster#: 5299/A227

Nanoparticles Delivering Anti-VEGF-A Plasmid Regress Murine Corneal Neovascularization

B.C. Stagg[1], Y. Qazi[2], S. Singh[3], N. Singh[2], E. Pearson[1], U. Kompella[3], B.K. Ambati[2]. [1]University of Utah School of Medicine, Salt Lake City, UT; [2]Moran Eye Center, Salt Lake City, UT; [3]Department of Pharmaceutical Sciences, University of Colorado - Denver, Denver, CO.

Purpose. To determine the efficacy of pSEC.siRNA.VEGFA loaded Poly Lactic Co-Glycolic Acid (PLGA) nanoparticles (NPs) in the regression of murine corneal neovascularization (KNV).

Methods. Plasmid-loaded nile red PLGA nanoparticles were prepared using the double emulsion solvent evaporation method. KNV was induced in BALB/C mice by mechanical-alkali injury using 2 ul of 0.15M NaOH for 10 seconds followed by scraping of the corneal epithelium with a Tooke corneal knife. Vessels were allowed to mature over 4 weeks after which the mice were randomly divided into 4 groups, each of which received one of the following interventions: pSEC.siRNA.VEGFA NR PLGA NPs (2ug plasmid), naked pSEC.siRNA.VEGFA plasmid (2ug plasmid), blank NR PLGA NPs, and DMSO. The plasmid-loaded NPs were prepared in sterile DMSO to a concentration of 1 ug/ul and 2 ul were injected intracorneally using a 33 gauge needle. 4 weeks after intervention, the mice were sacrificed and the corneas were harvested for flatmounts, RT-PCR, and VEGF-A ELISA. Flatmounted corneas were immunostained for CD31 (endothelial cell marker) and the neovascular area was quantitated using Scion Image. VEGF-A gene expression was evaluated using RT-PCR. Protein levels were determined using VEGF-A ELISA.

Results. siRNA.VEGFA loaded PLGA NPs showed significant regression of KNV compared to naked plasmid and controls. siRNA.VEGFA loaded PLGA NPs regressed KNV to 12.5%. Naked plasmid treatment resulted in a KNV area of 28%. The two control groups had highly vascular corneas with 53% KNV for DMSO and 55% KNV for blank NPs. VEGF-A protein and RNA expression were reduced significantly in siRNA.VEGFA loaded PLGA NP-treated corneas.

Conclusion. pSEC.siRNA.VEGFA -loaded PLGA NPs are an effective, non-viral, non-toxic and sustainable form of gene therapy for the regression of murine KNV.
Program#/Poster#: 440/D1144

Noncnzo10/ltj Mouse, a Model of Type 2 Diabetes, May Not Be Suitable for Diabetic Retinopathy

H. Uehara, J. Cahoon, S. Oblad, J. Simonis, L. Luo, B.K. Ambati.
Ophthalmology, University of Utah, Salt Lake City, UT.

Purpose. Diabetic retinopathy is one complication of diabetes mellitus. Many rodent models of diabetes have been used to understand the mechanism of, and improve, diabetic retinopathy. In this study, we characterized retina of NONcNZO10/Ltj males, which was recently generated as a mouse model of Type 2 diabetes mellitus.

Methods. NONcNZO10/Ltj males were obtained from Jackson laboratory and fed with a high fat diet. To observe retina vascularity in vivo, fluorescein angiography was used. Retina flatmounts were stained with isolectin GS-IB4 for vessel endothelial cells and α-SMA for pericytes. They were then observed with confocal microscopy. To determine retina thickness and examine retina layer composition, we used optical coherence tomography (OCT) and cryosection. In addition, we examined expression of PDE6α, PDE6β, and PDE6γ in the retina by RT-PCR and checked *rd1* mutation by genotyping.

Results. Fluorescein angiography and retina flat mount analysis showed that NONcNZO10/Ltj retina has less vasculature compared with control mouse, but pericytes still exist with retina blood vessels. In addition, high backgrounds were observed in NONcNZO10/Ltj mouse by fluorescein angiography. Retina thickness of NONcNZO10/Ltj was dramatically thinner than control mouse. OCT showed the thickness of NONcNZO10/Ltj and control retina as 137±13μm and 281±25 μm respectively. Cryosection of NONcNZO10/Ltj eye also showed thin retina (NONcNZO10/Ltj retina: 93±12μm; Control retina: 203±18μm). Nuclear observation indicated that the outer nuclear layer of NONcNZO10/Ltj was atrophic. From RT-PCR, PDE6α and PDE6β did not express in NONcNZO10/Ltj retina, but PDE6γ was still expressed. Genotyping for *rd1* indicated NONcNZO10/Ltj is a *rd1/rd1* mouse.

Conclusions. From these results, we confirmed NONcNZO10/Ltj mouse retina degeneration comes from rd1 mutation. Although fluorescein angiography indicated NONcNZO10/Ltj retina has leakage, which is a manifestation of diabetic retinopathy, NONcNZO10/Ltj mouse may not be suitable for diabetic retinopathy studies because the outer nuclear layer progressively atrophies.
Program#/Poster#: 118/A246

Ocular Bioimaging of a Murine Model of Macular Degeneration

C.A. Mamalis[1], L. Luo[2], S.A. Molokhia[1], K. Jackman[1], M. Romanowski[3], B.K. Ambati[4]. [1]Ophthalmology, Moran Eye Center, Salt Lake City, UT; [2]Ophthalmology, University of Utah, Salt Lake City, UT; [3]Biomedical Engineering, University of Arizona, Tucson, AZ; [4]Ophthalmology, John Moran Eye Center, Salt Lake City, UT.

Purpose. To determine if anti-Vascular Endothelial Growth Factor antibody fragments (fabs) conjugated with Indocyanine Green (ICG) and gold nanorods reveal the presence of subretinal injection -induced choroidal neovascularization (CNV) in a murine model.

Methods. Using the Thermo Scientific Fab Preparation kit (#44885), anti- mouse VEGF IgG underwent papain digestion into Fab fragments which were isolated from the remaining IgG and Fc particles. Purified Fab fragments were lyophilized and conjugated to ICG and aminated gold nanorods in separate aliquots. The prepared bioconjugates were combined and injected systemically into the tail vein of Balb/C mice which had previously been injected with AAV.siRNA.sFlt to induce CNV. The posterior segment was evaluated using Ocular Coherence Tomography (OCT) and ICG imaging capabilities of the Heidelberg Spectralis. Images were obtained immediately, 2 hours, 4 hours, 24 hours, and 2 weeks post injection, for evidence of contrast indicating focally elevated concentrations of VEGF.

Results. The bioconjugation of ICG and

gold nanorods as contrast agents to anti-VEGF Fab fragments successfully identified regions of CNV (a model of exudative macular degeneration) induced via subretinal injection in Balb/C mice. The ICG images revealed a localized signal 2 and 4 hours post injection highlighting areas of suspected CNV. OCT images were then obtained immediately in the same location in order to confirm that areas highlighted by the ICG bioconjugate were in fact areas of CNV. The OCT images confirmed that the anti-VEGF-Fab-ICG bioconjugate was in areas of induced CNV. ICG became visible in the vasculature 2 hours post injection and remained until 4 hours post-injection. The localized ICG signal faded within 24 hours after injection.

Conclusions. ICG-anti-VEGF-fab and anti-VEGF-fab-nanorod bioconjugates highlighted regions of CNV in a murine model. Using novel bio-conjugated markers with SLO technology could provide convenient detection of VEGF elevation, a key pathogenic event in age-related macular degeneration, perhaps before neovascularization has caused clinical damage.

Program#/Poster#: 6145/D657

Knock-down of GCAP1 by RNA interference delays photoreceptor degeneration in GCAP-Y99C transgenic mice

Li Jiang, Sanford L. Boye, Alexander Dizhoor, William Hauswirth, Wolfgang Baehr
Department of Ophthalmology, University of Utah Health Science Center, Salt Lake City, UT; Pennsylvania College of Optometry, Salus University, Elkins Park, PA; Department of Ophthalmology, University of Florida College of Medicine, Gainesville, FL

Purpose. Transgenic mice expressing GCAP1 carrying mutations in high affinity Ca2+ binding sites EF3 and EF4 exhibit dominant rod and cone dystrophies. Our goal was to develop a virus-mediated RNA interference that would efficiently knock down both mutant and WT Guca1a mRNA in mutant mice carrying the Y99C mutation (L53 line). The virus is predicted to delay or prevent onset of photoreceptor degeneration since GCAP knockouts have no retinal degeneration phenotype.

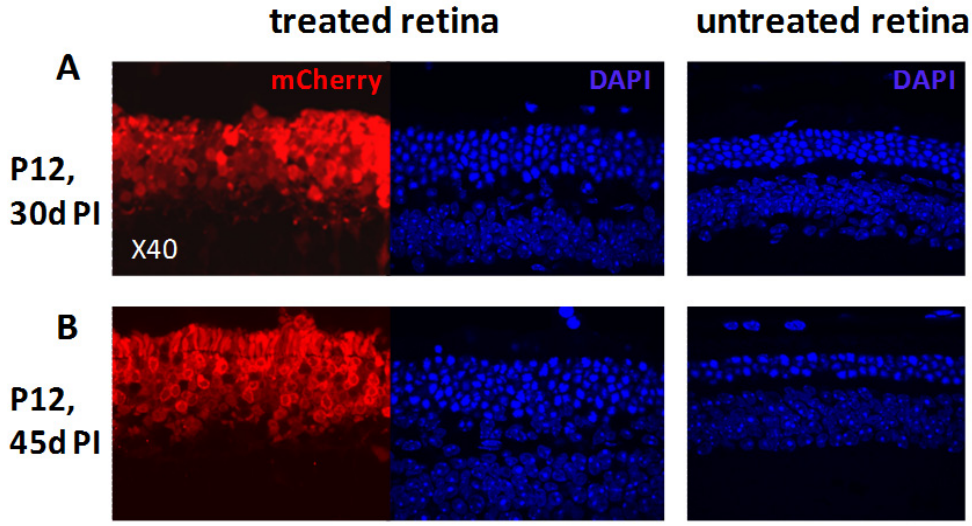

Results. Four GCAP1 specific shRNAs were cloned into an shRNA expression vector. These consisted of 21 bp sense and 21 bp antis ense strands connected by a 9 bp loop under the control of the human H1(RNA polymerase III) promoter. The constructs also expressed mCherry as a reporter driven by the CMV promoter. The most efficient GCAP1-shRNA (bG1hp4) knocked down GCAP1 with >80% efficiency as judged by western blotting and qRT/PCR. This shRNA expression cassette was cloned into a scAAV8 shuttle vector (scAAV8_bG1hp4), packaged, and subretinally injected into WT and Y99C-GCAP1 transgenic mice. The virus showed robust expression of the reporter mCherry as early as 5 days after injection. When injected into the subretinal space of GCAP1-Y99C transgenics at P12, the ONL thickness was roughly 8 nuclei 45 days post treatment while untreated mutant retinas had completely degenerated. Currently control shRNA viruses carrying mutant sense and antisense sequences are being generated and tested.

Conclusion. The results show that a rapidly progressing dominant retinal dystrophy in GCAP1-Y99C transgenic mice can be delayed by a recombinant scAAV2/8 expressing an efficient GCAP1 shRNA. Future experiments will test the virus on animal models with a slowly progressing dominant cone/rod dystrophy (GCAP1-y99c L52 line, GCAP1-L151F transgenics).

Program#/Poster#: 4488/A460

AAV-Mediated Gene Replacement Therapy in a Mouse Model of Usher Syndrome Type II Lacking Whirlin

J. H. Zou[1], L. Luo[1], B.K. Ambati[1], V.A. Chiodo[2], W. W. Hauswirth[2], J. Yang[1]
[1]Department of Ophthalmology and Visual Sciences, Moran Eye Center, University of Utah, Salt Lake City, UT; [2]Department of Ophthalmology, University of Florida, Gainesville, FL

Purpose. Whirlin, *USH2A* and *VLGR1* are the three causative genes of Usher syndrome type II, a condition with both retinitis pigmentosa and congenital deafness. It has been demonstrated that the proteins encoded by these three genes form a multiprotein complex at the periciliary membrane complex (PMC) in photoreceptors. Loss of any one of these three proteins causes disruption of this protein complex and retinal degeneration in mice. In this study, we evaluated the therapeutic effect of whirlin replacement using recombinant adeno-associated virus (AAV) in whirlin knockout mice.

Methods. Murine whirlin cDNA driven by a human rhodopsin kinase (hRK) promoter was packaged into an AAV5 vector (AAV5-hRK-whirlin) and delivered into whirlin knockout mice by subretinal injection at postnatal day 18. At 8 weeks post-injection, the localization and expression level of whirlin, USH2A and VLGR1 in the retina were examined by immunostaining and western blotting analyses. The DNA plasmid without whirlin cDNA packaged into the same AAV vector was used as a negative control.

Results. In whirlin knockout mice injected with AAV5-hRK-whirlin, the transduced whirlin was expressed throughout the entire retina at its normal cellular location, the PMC, in photoreceptors. It had a molecular size and an expression level close to those in wildtype retinas. Importantly, while USH2A and VLGR1 were mislocalized and their expression decreased in whirlin knockout retinas, expression of whirlin delivered by the AAV5 vector was found to restore both the localization and expression levels of USH2A and VLGR1. No difference in the expression of whirlin, USH2A and VLGR1 was detected in whirlin knockout mice injected with the control AAV5 vector and in uninjected whirlin knockout mice.

Conclusion. This study further confirmed that whirlin, USH2A and VLGR1 form a multi-protein complex at the PMC in photoreceptors. The successful delivery of whirlin into photoreceptors by an AAV vector and the resulting expression of whirlin driven by the hRK promoter close to the endogenous level suggest that this AAV vector gene delivery system can be an effective gene therapy approach to treat retinal degeneration in patients with Usher syndrome type II caused by whirlin mutations and, possibly, other forms of retinal degeneration as well.
Program#/Poster#: 3102/A326

Targeting of mouse guanylate cyclase 1 (Gucy2e) to Xenopus laevis rod outer segments

S. Karan[1], B. M. Tam[2], O. L. Moritz[2], W. Baehr[1],
[1]Department of Ophthalmology, John A. Moran Eye Center, University of Utah Health Science Center, Salt Lake City, UT, USA; [2]Department of Ophthalmology, University of British Columbia, Vancouver, BC, Canada

Purpose. It is unknown how guanylate cyclase 1 (GC1) targets to the outer segments where it resides. To identify a putative GC1 targeting signal, we generated a series of peripheral membrane (PM) and transmembrane (TM) constructs encoding extracellular and intracellular mouse GC1 fragments fused to eGFP for expression in *X. laevis* rod photoreceptors.

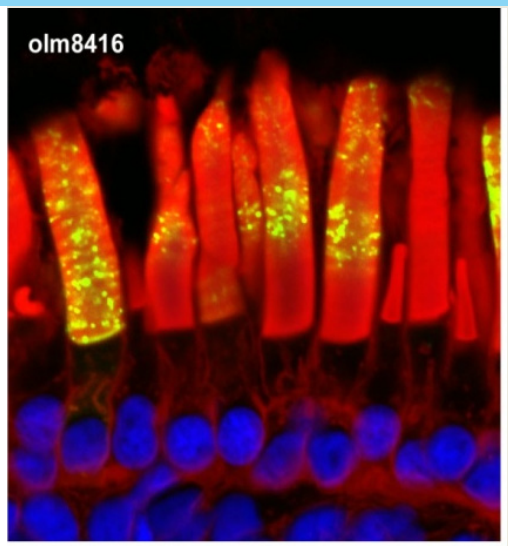

Results. GC1 consists of an extracellular domain (ECD), a transmembrane domain (TM), a kinase-like homology domain (KHD), a dimerization domain (DD), and a catalytic domain (CAT). Eight PM fusion proteins (GCct1-GCct8) contained combinations of the immediate C-terminus, CAT, DD, or KHD. Additionally, four TM constructs (GCtm9-12) consisted of GC1 fused to eGFP; in GCtm9 the ECD was replaced by eGFP; in GCtm11 the cytoplasmic domain was replaced by eGFP, and in GCtm12 the rhodopsin targeting signal TETSQVAPA was added to the C-terminus of GCtm9. Of the eight PM fusions, none targeted perfectly to the outer segments (OS), seven showed significant mislocalization to the inner segment (IS) and synapse, only one containing the entire cytoplasmic domain targeted primarily to OS. Three fusion proteins containing either C-term+CAT, KHD or KHD+DD, were excluded from the OS. Of the TM constructs, GCtm10 and GCtm9 showed near perfect targeting to the OS while GCtm11 mistargeted to the OS, IS and synapse. Addition of TETSQVSPA in GCtm12 did not prevent mistargeting in some rods, presumably because of overexpression/misfolding of the fusion protein. As a group, fusion proteins containing the entire cytoplasmic domain of GC1 (GCct4, GCtm9, GCtm10 and GCtm12) targeted to the OS nearly correctly.

Conclusions. GC1 likely has no single linear peptide-based OS targeting signal in the cytoplasmic or extracellular domains. Our results suggest targeting is due to either multiple weak signals in the cytoplasmic domain of GC1, or co-transport to the OS with another protein.
Program#/Poster#: 1103/D769

UNC119 regulates G protein trafficking in sensory neurons

H. Zhang, R. Constantine, S. Vorobiev, Y. Chen, J. Seetharaman, Y. J. Huang, R. Xiao, G. T. Montelione, M. W. Davis, G. Inana, E. M. Jorgensen, L. Tong, W. Baehr

SUMMARY. UNC119, a protein of unknown function, is expressed widely among vertebrates and invertebrates. Here we report that UNC119 recognizes the acylated N-terminus of the rod photoreceptor transducin α-subunit (Tα) as well as other Gα subunits, and that this interaction is crucial for the transport of G proteins to the sensory cilia of the neurons in which they reside. Pulldowns and isothermal titration calorimetry reveal a tight interaction between UNC119 and Gα peptides in the presence of N-terminal acylation. The crystal structure of human UNC119 at 1.95 Å resolution reveals an immunoglobulin-like β-sandwich fold, with a prominent hydrophobic cavity capable of accommodating lipids. UNC119 deletion in both mouse and *C. elegans* leads to G protein trafficking defects, ultimately resulting in photoreceptor degeneration and deficiencies in chemosensation, respectively. These results establish UNC119 as a novel cofactor/chaperone of G protein α-subunits, which is essential for their transport to sensory cilia.
Program#/Poster#: 1083/D749

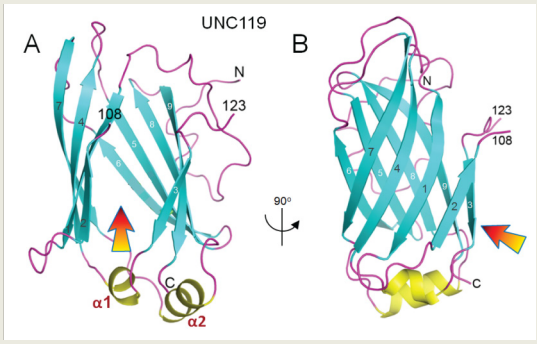

Carotenoid Bioavailability in C57BL/6 Mouse Eyes After High-Dose Supplementation

A. Liu, P.P. Vachali, Z. Shen, P.S. Bernstein.
Ophthal & Visual Sci, University of Utah/Moran Eye Center, Salt Lake City, UT.

Purpose. Lutein and zeaxanthin, the principal carotenoids in human eyes, are thought to play a protective role against age-related macular degeneration and cataract. A number of recent studies have examined carotenoid effects in various mouse models of eye disease, but no study has convincingly demonstrated that carotenoids actually accumulate in the mouse eye. After studying a variety of delivery forms and dosages, we have developed a method for reliable uptake of carotenoids into mouse eyes.

Methods. A 20% emulsion of purified marigold carotenoids (92% 3R,3'R,6'R-lutein and 8% 3R,3'R-zeaxanthin) dissolved in safflower oil was obtained from Kemin Health (Des Moines, Iowa). 2g/kg of carotenoid was orally administrated daily to 2 month old C57BL/6 mice, while control mice were fed the same volume of safflower oil. Eyes, liver, and serum were harvested after 4 weeks of supplementation. All samples were extracted with tetrahydrofuran containing 0.1% BHT. Carotenoids were then analyzed by HPLC on cyano and chiral columns with diode-array and mass spectral detection.

Results. Control mice had barely detectable lutein and zeaxanthin in serum and liver, and none was detectable in the eye. With supplementation, we could achieve serum levels ~1/5 of normal human serum, and liver levels increased substantially. Both serum and liver had lutein:zeaxanthin ratios similar to the administered material. The lutein:zeaxanthin ratio was dramatically different in the supplemented mice with 3.50 ± 1.90 ng lutein and 6.17 ± 1.67 ng zeaxanthin detected per pair of eyes. Chiral HPLC confirmed that no 3R,3'S-meso-zeaxanthin was produced.

Conclusions. These results indicate that with high-dose supplementation, carotenoids can be delivered to the mouse eye. The altered lutein:zeaxanthin ratio is consistent with the essential role of specific transport and binding proteins in mediating carotenoid uptake into the mammalian eye. With further optimization of carotenoid delivery and uptake, the mouse could serve as a useful model for lutein and zeaxanthin function in the retina.
Program#/Poster#: 1290/A102

Differential Genetic Susceptibility to Geographic Atrophy and Choroidal Neovascularization in Age-Related Macular Degeneration

L. Sobrin[1], R.C. Reynolds[2], J.A. Fagerness[3], B.M. Neale[3], N. Leveziel[4], P.S. Bernstein[5], E.H. Souied[4], M.J. Daly[3], J.M. Seddon[6].
[1]Retina/Uveitis, Mass Eye & Ear Inf., Boston, MA; [2]Ophthal. Epidem. and Genetics, Tufts Med. Ctr., Boston, MA; [3]Ctr. Human Gen. Res., Mass. Gen. Hosp., Boston, MA; [4]Creteil Univ. Hosp., Creteil, France; [5]Moran Eye Ctr., Univ. Utah Sch. Med., Salt Lake City, UT; [6]Ophthalmic Epidemiology and Genetics, Tufts University School of Medicine, Boston, MA.

Purpose. To determine if genetic variants that have been reliably associated with advanced age-related macular degeneration (AMD) have a differential effect on the risk of geographic atrophy (GA) and choroidal neovascularization (NV) in a large sample size of both phenotypes.

Methods. Participants were derived from ongoing AMD study protocols with similar procedures including the Progression of AMD Study, AMD Registry Study, Family Study of AMD, the US Twin Study of AMD, the Age-Related Eye Disease Study, University of Utah, and Hopital Intercommunal de Creteil. AMD grade was assigned based on fundus photography and ocular examination using the clinical age-related maculopathy grading system (CARMS) in which grade 4 is GA anywhere within the macula (central or non-central) and grade 5 is NV. Participants were assigned a grade based on the highest grade in either eye. All samples were genotyped on the Sequenom Iplex platform for previously associated single nucleotide polymorphism (SNPs), including *CFH rs1061170, CFH rs1410996, CFI rs10033900, CFB/C2 rs641153*, and *C3 rs2230199* in the complement pathway; *ARMS2/HTRA1 rs10490924*; and new loci *TIMP3 rs9621532*; and *LIPC rs493258*. We performed association testing comparing allele frequencies between participants with GA and participants with NV using PLINK. We performed stratified analyses by recruitment site.

Results. 748 participants with GA and 2775 participants with NV were included in the analysis. The frequency of the T allele of *ARMS2/HTRA1 rs10490924* was significantly more common in participants with NV than those with GA (odds ratio, 1.41; 95% confidence interval, 1.24 -1.60; p value = 2.5 X 10-7). This result remained statistically significant when the association testing was performed excluding individuals who had GA in one eye and NV in the contralateral eye. None of the other SNPs examined showed a differential effect for NV vs. GA.

Conclusions. Genetic variation at the *ARMS2/HTRA1* locus confers a differential risk for NV vs. GA in a well-powered sample. Future identification of other loci with similar differential effects could lead to biological insights into the mechanisms associated with development of NV vs. GA in patients with AMD.
Program#/Poster#: 1624

Genome-Wide Association Study of Advanced Age-Related Macular Degeneration Identifies a New Susceptibility Locus in the Lipid Metabolism Pathway, Hepatic Lipase (LIPC)

J.M. Seddon[1], R. Reynolds[2], J. Fagerness[3], L. Sobrin[4], E.H. Souied[5], P. Bernstein[6], M. Brantley, Jr.[7], N. Katsanis[8], R. Allikmets[9], M. Daly[3].
[1]Ophthal.Epidem. and Genetics, Tufts Univ. Sch. Med., Boston, MA; [2]Tufts Med. Ctr., Boston, MA; [3]Mass. Gen.Hosp. and Broad Inst., Boston, MA; [4]Mass. Eye & Ear Inf., Boston, MA; [5]Creteil Univ Hospital, Creteil, France; [6]Moran Eye Ctr., Univ. Utah Sch. Med., Salt Lake City, UT; [7]Wash. Univ Sch. Med., St Louis, MO; [8]Wilmer Eye Inst. Johns Hopkins, Baltimore, MD; [9]Columbia Univ., New York, NY.

Purpose. We conducted a large genome-wide association study (GWAS) of advanced age-related macular degeneration (AMD) to identify new genetic pathways contributing to the development of this complex disease.

Methods. The GWAS included 979 cases of geographic atrophy and neovascular AMD and 1709 controls all of whom were Caucasian and unrelated, and used the Affymetrix 6.0 platform (906,000 single nucleotide polymorphisms (SNPs) and 946,000 genotyped copy number variations. Replication genotyping was performed using 4337 advanced cases and 2077 controls from six independent samples with similar phenotypes and ethnicity.

Results. Our discovery scan implicated a strong association between AMD and the hepatic lipase gene *LIPC* with P=4.5 x 10 -5. We conducted several stages of replication of this and other significant findings (P < 10-4). The association with *LIPC* remained our most significant finding and was genome-wide significant with replication P= 3.3 x 10-7 for the discovery SNP and P= 1.2 x 10-8 for the functional variant in this gene. The odds ratio for the minor T allele (which raises HDL) was 0.76 (95% confidence interval 0.69-0.87) suggesting a decreased risk of AMD related to each copy of this allele, with consistent effects for geographic atrophy and neovascular disease. We also found strong associations between advanced AMD and other SNPs in the same lipid pathway including CETP and ABCA1, but these were not genome-wide significant and the direction of effect was not consistent among the lipid SNPs. We confirmed reported loci including two *CFH loci, ARMS2/HTRA1*, *CFB/C2, CFI,* and *C3*. No new copy number variations were shown to have genome-wide significant associations with AMD.

Conclusion. *LIPC*, encoding hepatic lipase, a critical enzyme in HDL metabolism, is a new gene associated with AMD. Several related mechanisms are plausible. This locus provides a new pathway for consideration in the pathogenesis of AMD, and may lead to new avenues for prevention and treatment.

Program#/Poster#: 2475

Retinal Pathology Linked to Nephropathy in Alport Syndrome

P.S. Bernstein[1], F. Ahmed[1], M. Gregory[2].
[1]Ophthal and Visual Sciences, Univ of Utah/Moran Eye Center, Salt Lake City, UT; [2]Nephrology, Univ of Utah, Salt Lake City, UT.

Purpose. Many inherited systemic diseases are associated with varying degrees of corneal, lens, and retinal degeneration. Alport syndrome is characterized by a juvenile onset of hematuria followed by changes in glomerular basement membranes (GBM). The hallmark of glomerular changes in Alport syndrome is irregular thickening, thinning, and splitting of the GBM. X-linked Alport syndrome is caused by mutations in the *COL4A5* gene. The rarer autosomal recessive form is due to mutations in other basement membrane collagen genes: *COL4A3* or *COL4A4*. Alport syndrome's best known ocular manifestation is anterior lenticonus, but retinal pathology is increasingly recognized as well, especially since retinal pigment epithelial basement membrane and GBM are structurally similar.

Methods. Subjects had complete eye examinations and retinal imaging using autofluorescence, fundus photography, and optical coherence tomography (OCT). Blood samples were collected for genotyping of *COL4A5* mutations.

Results. 21 subjects (11 female and 10 male) patients have currently enrolled in this ongoing study. Genetic analyses showed 96% of study patients have a mutation associated with the *COL4A5* gene. Of these patients, the 10 expressing L1649R and *C1654S* mutations had no retinal pathology with the exception for one patient with vitreomacular traction syndrome. Patients with other *COL4A5* mutations: G576S, G96A, G1060X, Lys1097ter, 3528+T, del ex2 had significant retinal pathology. Retinal pathology included peri-macular flecks, pigmentary changes, and reduced temporal OCT thickness.

Conclusions. The L1649R and C1564S mutations in the *COL4A5* gene, which cause a relatively mild form of Alport syndrome characterized by late onset renal failure, were not associated with substantial retinal pathology. Other *COL4A5* mutations associated with more significant renal pathology exhibited numerous retinal abnormalities including reduced temporal retina thickness and pigmentary changes. There was strong concordance of retinal phenotypes between Alport siblings. The pathological basis for Alport syndrome's retinal abnormalities remains to be explored.

Program#/Poster#: 1395/A408

Surface Plasmon Resonance (SPR) Studies of the Interactions of Carotenoids and Their Binding

P.P. Vachali1, B. Li[1], P.S. Bernstein[2].
[1]Moran Eye Center, University of Utah, Salt Lake City, UT; [2]Ophthal and Visual Sciences, Univ of Utah/Moran Eye Center, Salt Lake City, UT.

Purpose. SPR-based biosensors have drawn attention in recent years because of their ability to analyze protein-ligand interactions rapidly and sensitively. The main advantages of this technology are that assays can be performed directly and that the kinetics of analyte-target interaction can be easily determined. In this study, we explored the binding interactions of a recombinant CBP, a new member of the steroidogenic acute regulatory (StAR) protein family from silk worm (*Bombyx mori*) gland with significant homology to many human StAR proteins, and GSTP1 a xanthophyll-binding protein in human macula with different carotenoid ligands.

Methods. Purified rCBP and GSTP1 were immobilized on sensor chip (a planar mixture of hydroxyls and carboxyls in a 4:1 ratio of hydroxyl to carboxyl) using standard amine-coupling protocols to obtain a surface density of 1000-1200 RU. The carotenoids were tested in 2-fold serial dilutions. The running buffer contained 50 mM Tris pH 8 and 5% DMSO. All surface plasmon resonance measurements were recorded on a SensiQ SPR instrument (Icx Nomadics) at a controlled temperature of 25ºC.

Results. The rCBP binding responses were analyzed using Qdat Software (Icx Nomadics). Lutein showed a high affinity towards rCBP with a KD of 130 nM. The rCBP-lutein binding result is in excellent agreement with the earlier reports using Protein A -sepharose-rCBP pull down assay. The GSTP1 binding responses were analyzed with a heterogenous binding model using GraphPad Prism software. Out of the five carotenoids tested with GSTP1, (3R, 3'R)-zeaxanthin showed the highest affinity toward GSTP1 with a KD of 52.9 nM, followed by (3R, 3'S)-*meso*-zeaxanthin and astaxanthin with KD of 55.2nM and146 nM respectively. Zeaxanthin, *meso*-zeaxanthin and astaxanthin showed a second low affinity site

with a KD of 5.29 µM, 5.17 µM and 4.13 µM respectively. Beta-carotene and lutein did not show a significant affinity towards GSTP1.

Conclusions. The results demonstrate that biosensor technology can be employed to study carotenoid affinities with target proteins reliably and reproducibly. The GSTP1 results confirm our published findings that GSTP1 is the physiologically relevant binding protein for zeaxanthin in the human macula. We recently reported a Human Retinal Lutein binding protein (HR-LBP), which share many features similar to CBP. Biosensor-based assays should facilitate further study of the functional roles of xanthophyll-binding proteins in the human retina.
Program#/Poster#: 1291/A103

Determination and Assessment of Extended Haplotypes Spanning the Chromosome 1q32 CFH-To-CFHR5 Locus

E.N. Brown[1], L.S. Hancox[1], N.J. Miller[2A], J.L. Hageman[2A], C.M. Pappas[2B,2A], D.A. Hutcheson[2A], M.A. Morrison[3], M.F. Leppert[2B], M.M. DeAngelis[3], G.S. Hageman[2A].
[1]College of Medicine, University of Iowa, Iowa City, IA; [A]John A. Moran Eye Center, [B]Human Genetics, [2]University of Utah, Salt Lake City, UT; [3]Dept of Ophthalmology, Harvard Medical School, Boston, MA.

Purpose. Variations and haplotypes of the complement factor H (*CFH*) and the five *CFH*-related genes (*CFHR-1* through *CFHR-5*) are significantly associated with the risk of developing complement-mediated diseases, including age-related macular degeneration (AMD). Due to the strong homology between these six genes, and substantial copy number variation within the 1q32 region, it has been difficult to determine the causal association of individual variants, genes, and haplotypes to disease. To address this deficiency, haplotypes encompassing *CFH* and the five *CFHR* genes were determined, and their association with AMD and other diseases assessed.

Methods. Sixty-three SNPs in 1,073 white individuals were genotyped. The deletion status of the *CFHR-3/CFHR-1* genes was assessed using SSCP and a novel qPCR assay developed to detect the *CFHR-3/CFHR-1* deletion on single chromosomes. Genotypes were imputed and phased and haplotypes were subsequently constructed. Haplotype validity was confirmed in multiple three-generation families, including Utah CEPH families. Disease association was assessed by constructing haplotypes in a backwards step-wise selection method with individual SNPs, in 657 white siblings (average age = 83 yrs), who had normal maculas and the diagnosis of AREDS categories 2, 3, and neovascular AMD.

Results. Nine major haplotypes (>1% frequency) within the 260kb region were identified; they are tagged by eight SNPs. The deletion status of the *CFHR-3/CFHR-1* genes could be predicted with 97% specificity and 96% sensitivity based on the genotype of a single SNP. Fourteen percent of chromosomes in the discovery cohort contained this deletion. Haplotype fidelity was confirmed in large multi-generation families. Unique associations of six of the nine major haplotypes with different AMD risk phenotypes (both as a binary and quantitative trait) were found ($p < 10\text{-}7$), after permutation testing correction and controlling for age, sex and smoking status. In addition, haplotype associations with other complement-mediated diseases were found.

Conclusions. Haplotypes spanning the extended *CFH-to-CFHR-5* locus and including *CFHR-3/CFHR-1* deletion were determined. These 1q32 haplotypes will be valuable in refining our understanding of the causal association of individual gene variations and haplotypes in disease risk and protection.
Program#/Poster#: 1262/A44

Further Identification and Characterization of the Lutein-Binding Protein in Human and Monkey Retina

B. Li, I.L. Pop, J.M. Frederick, P.S. Bernstein.
University of Utah, Moran Eye Ctr, Salt Lake City, UT.

Purpose. We have previously reported that the lutein-binding protein in human retina is a member of the steroidogenic acute regulatory (StAR) protein family with significant cross reactivity with CBP, the StAR protein responsible for lutein uptake in the silkworm gut and silk gland (*Biochemistry*, 2009, 48 (22), pp 4798-4807). The human genome contains fifteen genes encoding StAR domain (StARD) proteins. Here we identify which StARD protein is responsible for lutein binding in the human retina.

Methods. Western blots were performed using fifteen StAR protein antibodies against total protein extracts from human and mouse retina, RPE and liver. Corresponding mRNA expressions of lutein binding protein candidates were tested by RT-PCR using human retina total RNA. Tissue distributions of lutein binding protein candidates and CBP were determined by immunohistochemistry of monkey retina sections.

Results. Immunoblots revealed that StARD3 and StARD8 are the two best lutein-binding protein candidates of the fifteen human StARD proteins. StARD3 labels human macula with a band ~48kD, while retina and RPE labeling is weak. StARD8 labels human macula, human peripheral retinal and human RPE with a band ~118kD. mRNA expressions of StARD3 and StARD8 were demonstrated by RT-PCR with bands of 728 bp and 654 bp, respectively. RT-PCR product identities were confirmed by DNA sequencing. Although broadly distributed in neurons, StARD3 and CBP colocalize prominently in photoreceptors of monkey retina. By contrast, StARD8 distribution was strong in selected cell bodies of the inner nuclear layer (INL) with axons extending into the inner plexiform layer (IPL). StARD8 did not colocalize with the Müller cell marker, glutamine synthetase.

Conclusions. StARD3 and StARD8 are both found in human retina. Based on the immunolocalization and immunoblot experiments, StARD3 is the best candidate for the human retinal lutein-binding protein, especially since it has significant sequence homology with silkworm CBP. Protein expression and quantitative binding studies are required to confirm its physiological function.
Program#/Poster#: 4814

Soluble Vascular Endothelial Growth Factor Receptor 1 (sflt-1) is Essential for Subretinal Vascular Zoning

L. Luo[1], H. Uehara[1], N. Singh[1], V. Chiodo[2], W. Hauswirth[2], N. Ferrara[3], J. Ambati[4], Y. Fu[1], W. Baehr[1], B.K. Ambati[1].
[1]Moran Eye Center, University of Utah, Salt Lake City, UT; [2]University of Florida-Gainesville, Gainesville, FL; [3]Genentech, South San Francisco, CA; [4]University of Kentucky, Lexington, KY.

Purpose. The retinal pigment epithelium (RPE)-Bruch's membrane (BrM)-choroicapillaris(CC) complex is a crucial anatomic structure for subretinal vascular zoning that presents highly vascularized, highly permeable fenestrated CC on its outer basal aspect, whereas the photoreceptor layer is completely avascular. The pathological conditions of RPE- BrM-CC arouse choroidal neovascularization(CNV) which breach the subretinal vascular barrier. The molecular underpinnings of maintaining the normal subretinal vascular zoning have remained obscure. VEGF- A is a potent stimulator of angiogenesis. sFlt-1 specifically binds VEGF and inhibits its activity. We previously showed corneal avascularity is due to sFlt-1. Here we sought to determine whether sFlt-1 in subretinal space is vital for subretinal vascular zoning.

Methods. Three independent strategies were used to test if CNV can be induced by suppressing sflt-1. First, a neutralizing antibody against sflt-1 was injected into subretinal space, isotype IgG performed as control. The second strategy was knockdown of sflt-1 using adeno-associated viral deliveryviral delivery of small RNA interference targeted to soluble VEGF receptor 1(AAV.siRNA.sFLT-1) by subretinal injection. PBS, aav.GFP and aav.nonspecific siRNA served as controls. The third strategy was genomic deletion: in FltloxP/loxP mice, subretinal NLS-Cre would reduces sFlt expression and then CNV would be expected. CNV was observed and evaluated by FA and ICG angiography and OCT using the Heidelberg Spectralis. ERG and histology were also used to evaluate functional and anatomic status after sacrifice. RT-PCR , Western blot, IHC and ELISA were performed to confirm sflt knocked down or cre expression and VEGF-A level.

Results. RPE expresses sflt-1 and suppression of this endogenous VEGF-A trap by neutralizing antibodies, RNA interference or Cre-lox-mediated gene ablation in Flt-loxp mice induced CNV($P < 0.05$). RPE secretes VEGF toward its basal side where its receptor sflt is located on the apical RPE. Free VEGF-A was elevated in these models. Subretinal pCre injection in VEGF-loxp animals prevented CNV. AAV.siRNA.sFlt-induced CNV more closely resembles human CNV than laser-induced CNV.

Conclusions. sflt-1 is essential for subretinal vascular zoning. Aav.sirna.sflt induced CNV has significant correlates to human CNV that the laser-induced CNV model does not.
Program#/Poster#: 6385

A New Era For Age-related Macular Degeneration

G.S. Hageman.
John Moran Eye Center, Ophthalmology & Visual Sciences, University of Utah, Salt Lake City, UT.

Abstract. Great strides have been made during the past ten years in the identification of genetic and environmental factors that give rise to age-related macular degeneration (AMD), as well as the ensuing cellular events that characterize the disease process. A definitive body of evidence has emerged that implicates a role for immune-mediated processes, specifically the complement system in disease pathogenesis and progression. Still unresolved are the specific roles that complement, its effector pathways and other inflammation-related pathways, including the adaptive immune system, play in the development of early AMD and its progression to late stage disease, including choroidal neovascularization and geographic atrophy. Other unresolved issues relate to the primary tissue target of AMD associated immune-mediated pathways, how to explain the fact that AMD is age-related in the context of established immune-mediated pathways, why the macula is uniquely susceptibility to degeneration and many others. These issues will be addressed in the presentation as an integrated model of AMD pathobiology.
Program#/Poster#: 1602

Müller Cells in Macular Pathology

M.B. Powner[1], M.C. Gillies[2], M. Tretiach[2], A. Scott[1], R.H. Guymer[3], G.S. Hageman[4], M. Fruttiger[1].
[1]Cell Biology, UCL Institute of Ophthalmology, London, United Kingdom; [2]Save Sight Institute, University of Sydney, Sydney, Australia; [3]Centre for Eye Research Australia, University of Melbourne, Royal Victorian Eye and Ear Hospital, Melbourne, Australia; [4]John A. Moran Eye Center, Department of Ophthalmology and Visual Sciences, University of Utah, Utah, UT

Purpose. To assess the histopathological changes in a postmortem sample derived from an eye donor with Macular Telangiectasia Type 2 (MacTel type 2) to gain further insight into the cause of the disease. MacTel type 2 affects such a specific region around the fovea that is consistent in terms of clinical observations between patients, the specificity of this region might be due to anatomical/biochemical differences in the macula compared to the rest of the retina.

Methods. Macular pigment distribution of freshly dissected eyes was photographed. Sections of the retina-RPE-choroid complex from both the macular and peripheral regions were assessed using antigen retrieval and immunohistochemistry to study the distribution of cell-specific markers for blood vessels, glial cells, microglia and photoreceptors. Using anatomical landmarks the sections were matched with the macular pigment distribution and a fluorescein angiogram that was taken before the donors' death.

Results. Macular pigment was absent in the macula. Abnormally dilated capillaries were indentified in a macula that correlated spatially with regions of fluorescein leakage in an angiogram that was taken 12 years prior to death. These telangiectatic vessels displayed a marked reduction of the basement membrane component collagen IV, indicating vascular pathology. GFAP was limited to retinal astrocytes and no reactive Müller cells were identified. Importantly, reduced immunoreactivity with Müller cell markers (vimentin, glutamine synthetase and retinaldehyde binding protein) in the macula was observed, which correlated to the region of depleted macular pigment.

Conclusions. These findings suggest that macular Müller cell loss or dysfunction is a critical component of MacTel type 2, which may have implications for future treatment strategies. Due to the spatially restricted pathology in MacTel type 2, we also conclude that the specificity of the disease area implies that there is a fundamental biological or biochemical difference between the retina in the macula and the periphery.
Program#/Poster#: 5761/D983

Retinal Plasticity and Restoration of Function After Photocoagulation

A. Sher[1], L.-S. Leung[2], T. Leng[2], H. Nomoto[2], Y. Paulus[2], R. Gariano[2], B.W. Jones[3], A.M. Litke[1], D.V. Palanker[2].
[1]Santa Cruz Institute for Particle Physic, University of California, Santa Cruz, Santa Cruz, CA; [2]Ophthalmology, Stanford University, Stanford, CA; [3]Ophthalmology, Moran Eye Center, Salt Lake City, UT.

Purpose. While retinal photocoagulation is an effective treatment for a variety of retinopathies, its side effects include secondary loss of visual field and sensitivity, and retinal scarring. Histological studies show that in laser lesions milder than those in current clinical use photoreceptors from surrounding retina fill-in the damage zone without scarring. In order to evaluate the functional significance of this phenomenon, we characterized changes in retinal visual response during the healing of photocoagulation lesions.

Methods. Retinal photocoagulation lesions of Moderate and Barely Visible clinical grades were produced in rabbits with a 532-nm Nd:YAG laser, using beam diameter of 250 and 400 μm. Retinal functional properties were characterized by in-vitro multielectrode array (512 electrodes, 1.7 mm2 area) recording of retinal ganglion cells' (RGC) responses to spatiotemporal white noise stimulus.

Results. One day after photocoagulation, the receptive fields of the RGCs had non-sensitive regions corresponding to the lesions' size and shape, confirming the photoreceptor layer destruction. At one week the non-sensitive areas significantly decreased. Finally, after 2 months sensitivity was restored for the lesions with a smaller initial size while non-responsive areas over larger lesions were retained. The results were similar for the on-set and the off-set of light sensitive RGCs.

Conclusions. Filling of the damage zone by photoreceptors in smaller lesions results in the restoration of visual sensitivity for ON and OFF retinal pathways. This may allow for significant improvements in the treatment of retinopathy by photocoagulation. The phenomenon also establishes a model for study of the dynamic changes in retinal circuitry associated with loss and restoration of the photoreceptors, thus providing a valuable insight into processes occurring in degenerated and remodeling adult retinas, important for studies of retinal rescue through surgical or genetic means. The full extent and functional consequences of the observed retinal plasticity remain to be further explored.
Program#/Poster#: 2482

Computational Molecular Phenotyping and Excitation Mapping in a Human Patient With Retinitis Pigmentosa

B.W. Jones[1], R.E. Marc[2].
[1]Ophthalmology, Moran Eye Center, Salt Lake City, UT; [2]Ophthalmology-Sch of Med, Univ of Utah/Moran Eye Center, Salt Lake City, UT.

Purpose. Evaluation of animals models of human retinitis pigmentosa have been extensively documented. However, substantive documentation of human samples of retinitis pigmentosa have not been introduced into the literature. Our goal was to assess the state and condition of the late stage human retina with retinitis pigmentosa and evaluate the dependance of retinal remodeling on cone survival.

Methods. Samples from human subjects with retinitis pigmentosa were collected post-mortem through the Utah Lions Eye Bank and incubated with 1-amino-4- guanidobutane (AGB). Retinal fragments were incubated 10 minutes at 35 degrees C in oxygenated Ames-Hepes medium with 5mM AGB with and without iGluR agonists (KA 50uM, NMDA 1mM), followed by conven-tional fixation in buffered aldehydes and embedding in epoxy resins. Tissues were sectioned at 200nm followed by classification with computational molecular phenotyping (CMP) using an array of small and macromolecular signatures (aspartate, glutamate, glycine, glutamine, glutathione, GABA, taurine, CRALBP, GS, rhodopsin, LWS1 cone opsin, tyrosine hydroxylase).

Results. As in animal models of retinitis pigmentosa and most notably the P347L transgenic rabbit, progressive rodspecific degeneration leads to complete elimination of rods and rod signaling. There is extensive survival of substantially altered cones. However, the presence of cones prevents the onset of radical remodeling in the retina, also preserving iGluR mediated signaling to surviving horizontal and bipolar cells. Those surviving bipolar and horizontal cells demonstrate neurite sprouting and potential bipolar cell and retinal reprogramming through upregulation of iGluR expression.

Conclusions. Disease progression observed in the human condition shows that animal models of retinal degeneration recapitulate the human condition. Cone mediated preservation of bipolar cell signaling, retinal reprogramming and retinal remodeling seen in the human retinitis pigmentosa retina are all duplicated in animal models.
Program#/Poster#: 4045/A438

Metabolic Biomarkers of Photoreceptor Degeneration

W.D. Ferrell, F.R. Vazquez-Chona, B.W. Jones, R.E. Marc.
Department of Ophthalmology University of Utah, John A. Moran Eye Center, Salt Lake City, UT.

Purpose. The goals of this study are to relate the classic sequelae of photoreceptor degeneration to small molecular metabolic signals and define metabolic states that define survival or apoptotic pathways in photoreceptors.

Methods. The light-induced retinal damage (LIRD) model in albino mice has been used for decades of biochemical, genetic, molecular and pharmacological investigations and ensures an adult onset, coherent timing of photoreceptor stress, built in controls in dorsal retina and extreme retinal remodeling similar to remodeling induced by age-related macular degeneration. Comparing metabolic states with specific cellular transformations is possible through the integration of high resolution,

N-dimensional metabolic profiling (Computational Molecular Phenotyping, CMP) with electron microscopy, classic photoreceptor proteome profiling, as well as assays for mitochondrial function, proliferation, and cell death.

Results. We found classic features of photoreceptor degeneration including rhodopsin mislocalization, membrane blebbing, and nuclear fragmentation correlated with specific metabolic profiles. An early metabolic anomaly was the redistribution of mitochondrial metabolites to the cytoplasm: mainly glutamate and aspartate. Late stage apoptotic events of nuclear fragmentation correlate with depletion of glutamate and aspartate in photoreceptors.

Conclusions. Current research aims to discover how changes in glutamate and aspartate distribution contribute to mitochondrial dysfunction and energy depravation. CMP is an ideal platform to integrate various levels of cell regulation (metabolism, energetics and proteomics) with high spatial resolution and quantitative analyses. Thus, CMP is paving the way toward a unified explanation of how oxidative stress imposes degeneration and ultimately cell death in photoreceptors.
Program#/Poster#: 5202

Roles of Retinoic Acid Signaling During Neuritogenesis in Light-Induced Retinal Degeneration

Y. Lin, B.W. Jones, K. Rapp, M.V. Shaw, J. Yang, C.B. Watt, R.E. Marc.
Department of Ophthalmology, University of Utah, John A Moran Eye Center, Salt Lake City, UT.

Purpose. Work in our laboratory and others has revealed striking neuritogenesis in the neural retina subsequent to photoreceptor stress and degeneration. While the initiators of this process remain unknown, our data indicate that major changes in retinoid processing occur prior to neuritogenesis. We hypothesize that alterations in retinoic acid (RA) signaling may influence the evolution of neuritogenesis and subsequent retinal remodeling.

Methods. Adult balb/c albino mice were exposed to constant intense light (24 h) by excluding one normal night cycle (12 h) to establish the light-induced retinal degeneration (LIRD) animal model. Retinas were harvested at post-light exposure day (pLX) 0, 1, 7, 30, 60, 90 and 120 for RA signaling analysis with morphological, metabolic profiling and biochemical parameters.

Results. Cellular retinoic acid-binding proteins II (CRABP II), RA receptors α, β (RARα, β), and retinoid receptors β, γ (RXRβ, γ) were expressed in inner nuclear layer (INL) and ganglion cell layer (GCL). RARγ and RXRα were not detected in control retina, but RARγ expression was immediately initiated by light stress and peaked at pLX7. The levels of CRABP II, RARβ, RXRβ, RXRγ, and müller cells marker cellular retinaldehyde-binding protein (CRALBP) were up-regulated then fluctuated in the neural retina after light stress, while RARα level had no alteration. These changes were followed by bipolar cell neuritogenesis revealed by PKCα staining in the survivor zone where the gross histology of the neural retina seemed normal. However, as expected, signals of the examined RA signaling components were reduced in INL of the LIRD zone, where photoreceptor loss and early dendritic remodeling occurred.

Conclusions. Even though the gross histology of the neural retina in the survivor zone seems normal early in LIRD, RA signaling displays large alterations, suggesting potential RA signaling pathways responsible for neuritogenesis and reactive neuronal plasticity. Deficiency of RA signaling may contribute to neurite degeneration.
Program#/Poster#: 5592/D641

The Metabolic Response of Müller Glial Cells to Photoreceptor Degeneration

F.R. Vazquez-Chona[1], W.D. Ferrell[2], B.W. Jones[2], R.E. Marc[3].
[1]Ophthalmology, Univ of Utah, Salt Lake City, UT; [2]Ophthalmology, Moran Eye Center, Salt Lake City, UT; [3]Ophthalmology-Sch of Med, Univ of Utah/Moran Eye Center, Salt Lake City, UT.

Purpose. To test the hypothesis that glial cells provide neuroprotection, we are visualizing the metabolic response of Müller glial cells to photoreceptor degeneration.

Methods. Visualizing and quantifying the metabolic states of activated glia is possible through the integration of high resolution, N-dimensional metabolic profiling (Computational Molecular Phenotyping, CMP), electron microscopy, classic glial proteome profiling, and proliferation assays. We are using the classic light-induced retinal damage model in albino mice to characterize the glial response to photoreceptor degeneration.

Results. CMP is capable of visualizing thousands of Müller cells and photoreceptors covering large stretches of retina while resolving the metabolic response of individual Müller cells and photoreceptors, preserving all histological context. We found that glial processes surrounding stressed photoreceptors exhibit changes in metabolic envelopes, displaying altered metabolic signals for glutamate metabolism, osmoregulation, anti-oxidation and retinoid metabolism. These metabolic profiles may reveal altered metabolic stabilities, altered metabolic programming or biochemical response profiles indicative of cell stress.

Conclusions. This work is aimed at investigating the metabolic relationships between Müller cells and photoreceptors in retinal stress situations. Metabolic networks are likely complex and we propose that the metabolic response of activated Müller cells assists metabolically stressed or challenged photoreceptors. The power of CMP to integrate various levels of cell regulation (metabolism, energetics and proteomics) with high spatial resolution is paving the way to discover the molecular glial transformations that confer neuroprotection.
Program#/Poster#: 4058/A451

The Viking Viewer for Connectomics: Scalable Multiuser Annotation and Summarization of Large Volume Datasets

J.R. Anderson[1], B. Grimm[2], S. Mohammed[1], B.W. Jones[1], P. Koshevoy[2,3], T. Tasdizen[2,4], R. Whitaker[2], R.E. Marc[1]
[1]Department of Ophthalmology, Moran Eye Center, University of Utah, Salt Lake City, UT, [2]Scientific Computing and Imaging Institute, University of Utah, Salt Lake City, UT, [3]Sorenson Media, Salt Lake City, UT, [4]Department Electrical and Computer Engineering, University of Utah, Salt Lake City, UT.

Abstract. Modern microscope automa-

tion permits the collection of vast amounts of continuous anatomical imagery in both two and three dimensions. These large datasets present significant challenges for data storage, access, viewing, annotation, and analysis. The cost and overhead of collecting and storing the data can be extremely high. Large datasets quickly exceed an individual's capability for timely analysis and present challenges in efficiently applying transforms, if needed. Finally annotated anatomical datasets can represent a significant investment of resources and should be easily accessible to the scientific community. The *Viking* application was our solution created to view and annotate a 16.5 TB ultrastructural retinal connectome volume and we demonstrate its utility in reconstructing neural networks for a distinctive of retinal amacrine cell class. *Viking* has several key features. (1) It works over the internet using HTTP and supports many concurrent users limited only by hardware. (2) It supports a multi-user, collaborative annotation strategy. (3) It cleanly demarcates viewing and analysis from data collection and *hosting*. (4) It is capable of applying transformations in real-time. (5) It has an easily extensible user interface, allowing addition of specialized modules without rewriting the viewer.

Calcium Stores and Glaucoma

W. Huang[1], C. Punzo[2], W. Xing[1], P. Barabas[1], G.R. Howell[3], S.W.M. John[3], D. Krizaj[1]. [1]Ophthalmology, University of Utah, Salt Lake City, UT; [2]Genetics, Harvard University, Boston, .MA; [3]Jackson Laboratory & HHMI, Boston, MA

Purpose. The rearrangement of cytoskeletal elements in any cellular remodeling is calcium-dependent. Ca release from internal stores, mediated by ryanodine receptors (RyRs) and inositol triphosphate receptors (IP3Rs) represents the hub for intracellular Ca homeostasis in both neurons and glia. Our aim was to characterize the relationship between Ca stores and the intense reorganization of neuronal-glial interfaces in glaucoma.

Methods. Expression of calcium signaling proteins together with RGC and glial markers were examined in age-matched retinas from wild type C57BL/6, DBA/2J and DBA/2J-*Gpnmb*$^{+}$ mice using quantitative RT-PCR, in situ hybridization, immunohistochemistry (IHC) and calcium imaging methods. The severity of glaucoma was assessed in PPD-labeled nerves using an established grading scheme. Eyes were classified with no or early (less than 10% axons damage), moderate (10-50% axons damage) or severe (more than 50% axons damage) glaucoma.

Results. As glaucoma severity increased, there was an upregulation of astrocyte (*Gfap*; 5.2 ± 1.2 -fold in moderate; 10.6 ± 2.5 -fold in severe glaucoma) and microglial (Iba1 and Cd11) markers and downregulation of RGC markers (*Brn3a* and *Vglut2; Vglut2* changed to 0.93 ± 0.19 in moderate; 0.13 ± 0.04 in severe glaucoma). There was a marked upregulation of RyR1 receptors in DBA/2J retinas (7.95 ± 2.56 -fold for moderate glaucoma; 6.94 ± 1.07 -fold for severe respectively). In situ hybridization and IHC revealed RyR1 expression in all retinal layers, with prominent signals in the ONL, sublamina b of the IPL and the GCL. Endfeet of Müller cells, putative astrocyte processes at the ILM and at the optic nerve head were strongly labeled by RyR1 antibodies. RyR2 was localized to GCL and proximal INL; no significant differences between controls and DBA/2J retinas were observed with respect to RyR2 isoform expression/localization (1.0 ± 0.2 in moderate; 1.5 ± 0.4 -fold in severe glaucoma). IP3R1 was localized to RGC layer and the proximal INL and was significantly more upregulated in severe (1.5 ± 0.2 -fold) and moderate (2.1 ± 0.2 -fold) glaucoma. IP3R2 was localized to RGCs and in the inner retina. Expression of IP3R2 was decreased 0.38 ± 0.02 -fold in moderate and 0.44 ± 0.08 -fold in severe glaucoma.

Conclusions. Severe glaucoma is associated with upregulation of RyR1 and IP3R1 genes in glial cells and with downregulation of IP3R2 in RGCs. This data suggests that cytoskeletal rearrangements in DBA/2J glaucomatous remodeling may be driven in part by increased Ca release from intracellular store compartments.

Program#/Poster#: 2127/A226

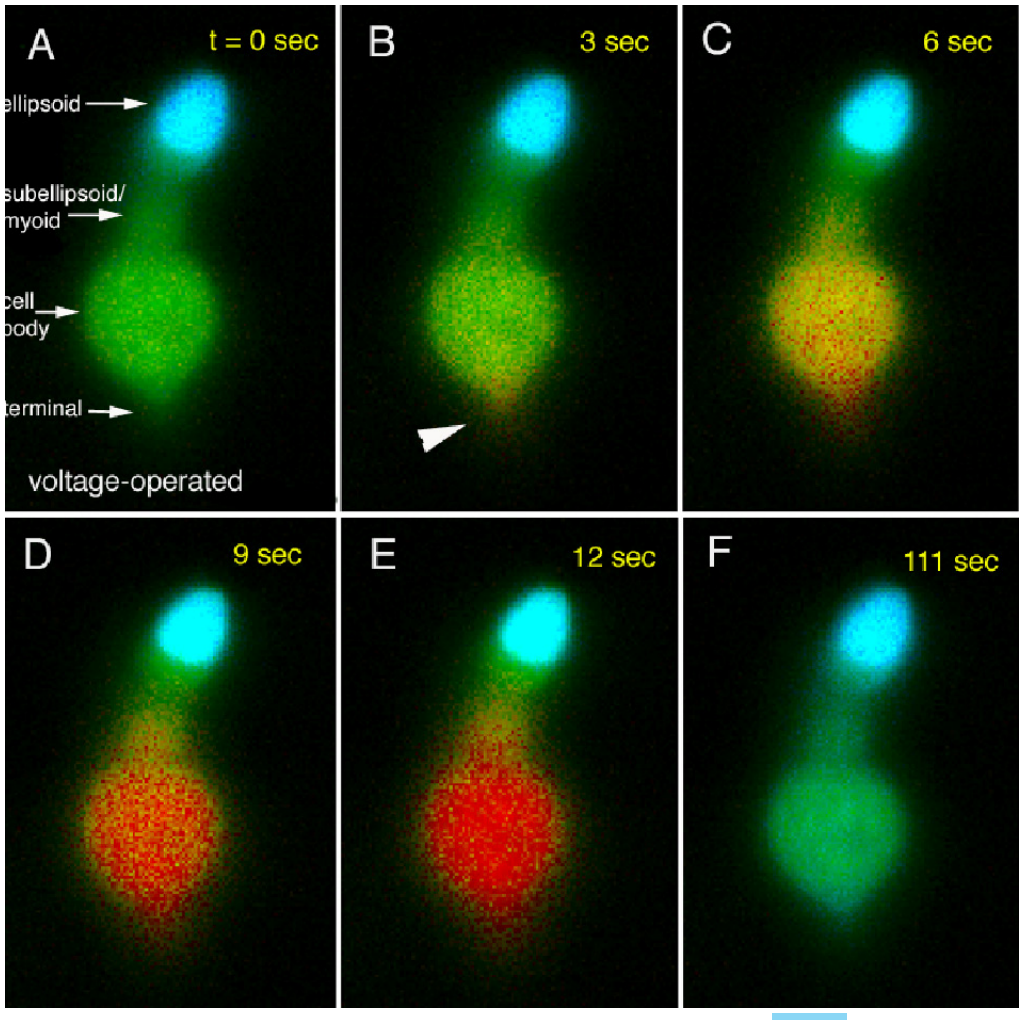

Expression and Function of TRPV4 Channels in the Vertebrate Retina

D. Krizaj[1], P. Witkovsky[2], P. Barabas[1], C. Punzo[3], R.C. Renteria[4], W. Liedtke[5], W.H. Huang[1]. [1]Ophthalmology and Visual Science, University of Utah School of Medicine, Salt Lake City, UT; [2]Ophthalmology, New York University, New York, NY; [3]Genetics, Harvard University, Cambridge, MA; [4]Physiology, Univ Texas Health Sci Ctr San Antonio, San Antonio, TX; [5]Duke University, Durham, NC.

Purpose. TRPV4 ion channels integrate extracellular signals (osmotic pressure, stretch, temperature), plasma membrane calcium fluxes with the activity of intracellular signaling pathways. TRPV4 channels are ubiquitous across the CNS where they function as osmotic and mechanosensors. We examined expression and localization of TRPV4 mRNA and protein in the mouse retina and investigated their contribution to calcium signaling and spontaneous activity in retinal ganglion neurons.

Methods. Retinas from wild type mice, DBA/2J and transgenic mice expressing GFP under the TRPV4 promoter were investigated with *in situ* hybridization, RT-PCR, immunohistochemistry, calcium imaging and multielectrode arrays (MEAs). Imaging was performed in isolated cells and slices from tiger salamander and mouse retinas. MEAs were utilized in the retinal wholemount preparation.

Results. TRPV4 mRNA was localized to the outer and inner nuclear layers and to prominently labeled RGCs. The signal in transgenic mice expressing GFP driven by the TRPV4 promotor was confined to RGC perikaryal cytoplasm. Exposure to the TRPV4 agonist 4-alpha PDD (10 uM) transiently elevated intracellular calcium concentration in subsets of putative salamander and mouse RGCs. 4 -alpha PDD-evoked increases were antagonized by 20 uM Ruthenium Red. The agonist also induced a transient increase in firing in a subset of RGCs recorded with MEAs. TRPV4 mRNA content was significantly increased in the DBA/2J mouse glaucoma model relative to age-matched control retinas.

Conclusions. These results suggest that TRPV4 is localized to retinal ganglion neurons. The upregulation of TRPV4 gene expression in DBA/2J retinas potentially implicates this calcium-permeable osmosensitive channel in cellular remodeling observed in glaucoma.

Program#/Poster#: 1860/D741

Store-Operated Calcium Entry Sustains Increased Calcium Level in Photoreceptor Cells and Affects Vision in the Mouse

P. Barabas[1], W. Huang[1], W. Xing[1], A. Rao[2], Y.-Z. Le[3], C.-K.J. Chen[4], D. Krizaj[1]. [1]Department of Ophthalmology, University of Utah, Salt Lake City, UT; [2]Department of Pathology, Harvard Medical School and Immune Disease Institute, Boston, MA; [3]Medicine, Univ of Oklahoma Hlth Sci Ctr, Oklahoma City, OK; [4]Biochemistry and Molecular Biology, Virginia Commonwealth University, Richmond, VA.

Purpose. Photoreceptor cells contain a store-operated system, which consists of Ca-permeable channels in the plasma membrane and STIM1 (stromal interaction molecule 1), a store-depletion EF sensor within the endoplasmic reticulum. Depletion of calcium stores activates store-operated calcium entry (SOCE) across plasma membrane SOC channels through STIM1 activation. We characterized the functional role of SOCE in mammalian vision by selectively eliminating STIM1 from rod and cone photoreceptors.

Methods. We developed mouse lines in which STIM1 was conditionally knocked out (cKO) in either rods or cones. STIM1 and Cre recombinase expression was determined with RT-PCR, Western blot and immunofluorescence. Fura-2 calcium imaging was performed in dissociated cells from control and cKO mouse retinas. The visual function was tested using flash ERG and the optomotor tracking response.

Results. IHC revealed photoreceptor-specific expression of Cre and deletion of the STIM1 signals from targeted photoreceptor populations. Significant changes in visual acuity were observed for both rod and cone STIM1 cKO mouse lines. Rod cKOs exhibited lower scotopic acuity (0.239 ± 0.013 c/deg) compared to wild type (0.256 ± 0.004 c/deg) and Cre+fl-/fl- control animals (0.254 ± 0.007 c/deg) with no difference in photopic acuity. Cone cKOs were characterized by a decreased photopic acuity (0.358 ± 0.007 c/deg vs 0.384 ± 0.007 c/deg in controls) and no change in scotopic acuity. Photopic vision deficits developed over 6-15 weeks after birth. Baseline [Ca2+]i in light-adapted rods was substantially decreased in cKO rods from 97 ± 6 nM in control wild type to 64 ± 11 nM in rod cKO animals whereas no such difference was observed in Müller cells. SOCE responses in isolated cKO photoreceptors were significantly decreased with respect to controls in both response amplitude and ratio of cells expressing this phenomenon.

Conclusions. Loss of STIM1 from rods selectively compromises rod vision whereas selective elimination of STIM1 from cones causes photopic vision deficits. The observed visual phenotypes suggest that STIM1-stimulated store-operated calcium entry in photoreceptors significantly contributes to the regulation of steady-state [Ca2+]i and the flow of visual information from photoreceptors to higher order visual centers.

Program#/Poster#: 4133/D629

Generation and Analysis of Two Mutant Alleles of Vsx2 That Cause Microphthalmia in Humans and Mice

C. Zou, Sr., E. Levine.
Dept. of Ophthalmology, University of Utah, Salt Lake City, UT.

Purpose. Mutations in the Vsx2 homeobox gene cause non-syndromic congenital microphthalmia in humans and mice. Because the mouse mutation, a spontaneous null mutation named ocular retardation J (orJ), is genetically distinct from those found in humans, the phenotypic profiles caused by each of the mutations might vary. To address this and to gain further insight into the etiology of human microphthalmia, we generated knock-in mice with the missense mutations Arg200Glu (R200Q) and Arg227Trp (R227W), both of which are identical to those found in humans. R200Q is located in the homeodomain and disrupts DNA binding. R227W is located in the CVC domain, which is of unknown function.

Methods. Each mouse line was generated by gene targeting. The phenotypes of these mutants and the $Vsx2^{orJ/orJ}$ mutant were examined by immunohistochemistry and quantitative RT-PCR.

Results. The extent of microphthalmia and spectrum of ocular phenotypes are similar between the orJ and R200Q mutant mice, indicating that the homeodomain is essential for Vsx2 function. Surprisingly, the phenotypes caused by the R227W mutation are more severe as indicated by smaller eyes and highly penetrant transformation of neural retina into pigmented tissue. The more severe phenotypes are attributed to novel changes in the expression levels of the transcription factor Mitf and the cyclin dependent kinase inhibitor p27Kip1, two genes previously identified as causal factors in the ocular phenotypes caused by the orJ mutation. Genetic interaction studies indicate a pathway by which p27Kip1 mediates the pigment-transforming effect of Mitf on the neural retina.

Conclusion. Our results indicate that the expression levels of Mitf or P27 in Vsx2 mutant retinal progenitor cells determine the severity of microphthalmia. Our results also reveal that the homeo- and CVC domains are essential for Vsx2 function.
Program#/Poster#: 2938

The Lim-Homeodomain Gene Lhx2 Is Required for the Self-Renewal of Retinal Progenitor Cells (RPCs) During Development

E.M. Levine, S. Yun.
Ophthalmology & Visual Science, Moran Eye Center at University of Utah, Salt Lake City, UT.

Purpose. Lhx2 is a key regulator of early eye development. Lhx2 knockout mice have anophthalmia and we recently showed that Lhx2 acts as a molecular node linking eye field specification with lens formation and the patterning of the optic neuroepithelium. Lhx2 is also expressed in the retina during the subsequent stages of eye development, but the anophthalmic phenotype precludes studying its later requirements. We therefore generated mice carrying an Lhx2 conditional allele (Lhx-2^{flox}) with the Pax6 alpha enhancer cre driver (alpha-cre) and a tamoxifen (TM) regulated cre driver active in RPCs (Hes$1^{creERT2}$) to determine the requirements of Lhx2 during retinal histogenesis.

Methods. Lhx2^{flox}; alpha-cre and Lhx-2^{flox}; Hes$1^{creERT2}$ embryos (TM exposure starting at E10.5) were harvested at several developmental timepoints. Phenotypes were examined by immunohistochemistry and in-situ hybridization.

Results. Lhx2 is expressed in the majority of RPCs during retinal histogenesis. Loss of Lhx2 resulted in an extensive depletion of RPCs due to a failure to remain in the cell cycle regardless of the cre driver utilized or the time of Lhx2 inactivation. Interestingly, the exited RPCs adopted fates that were characteristic of the stage when Lhx2 was eliminated and this occurred at the expense of later generated cell types.

Conclusions. Our results suggest that Lhx2 regulates histogenesis by preventing RPCs from exiting the cell cycle and from acquiring a state that predisposes or biases them toward the cell fates being generated at that time. By acting in this manner, Lhx2 maintains the RPC pool by actively promoting the self-renewal of an otherwise uncommitted state.
Program#/Poster#: 1231

An Anterior Chamber Toxicity Study Evaluating Besivance, Azasite and Ciprofloxacin

P.J. Ness[1], N. Mamalis[1], L. Werner[1], S. Maddula[1], D.K. Davis[1], E. Donnenfeld[2], R.J. Olson[1].
[1]Ophthalmology, Univ of Utah/Moran Eye Center, Salt Lake City, UT; [2]Ophthalmic Consultants of Long Island, Rockville Center, NY.

Purpose. We determine whether Besivance® and AzaSite® (both with DuraSite® bioadhesive), and ciprofloxacin are toxic inside the anterior chamber.

Methods. 20 New Zealand white rabbits (40 eyes) were randomized to one of four study groups: Besivance, AzaSite, ciprofloxacin and balanced salt solution (BSS). Each eye was injected with 0.1 mL of the study medication. Clinical slit lamp examinations were conducted at 24 and 48 hours post-injection. All rabbits were then sacrificed and all eyes enucleated. We randomized eyes to either corneal vital staining or histopathologic examination. The main outcome measures were clinical and pathologic signs of toxicity.

Results. The two DuraSite-based study groups (Besivance and AzaSite) showed both clinically and pathologically significant differences when compared to ciprofloxacin and BSS groups. Besivance and AzaSite eyes exhibited significantly similar and severe clinical damage, including severe corneal edema. Ciprofloxacin and BSS eyes appeared very similar and had only mild conjunctival injection and limbal vascularity. Vital staining and histopathologic evaluation revealed glaucomatous and toxic damage in eyes given DuraSite-based medications, while non-DuraSite groups showed minimal changes.

Conclusions. DuraSite blocks the trabecular meshwork and may be additionally toxic. Until the safety of these medications is established, we recommend they not be used after a clear corneal incision unless a suture is placed.
Program#/Poster#: 6420/D1038

Histopathologic Evaluation of LASIK Donor Corneal Caps in Descemet's Stripping Automated Endothelial Keratoplasty Using a Microkeratome

Y.M. Khalifa, D. Davis, M.D. Mifflin, M. Moshirfar, N. Mamalis.
Ophthalmology, University of Utah, Salt Lake City, UT.

Purpose. To compare Descemet's stripping automated endothelial keratoplasty (DSAEK) donor corneal caps from LASIK and non-LASIK donors and assess cut smoothness and LASIK flap stability.

Methods. Review of donor caps submitted for pathologic evaluation from 2005 through 2009 showed three LASIK donors and four non-LASIK donors. Tissue was prepared using an anterior chamber maintainer and Moria microkeratome. Specimens had been previously prepared with hematoxylin/eosin staining of slides following sectioning and processing for histopathologic evaluation. Examination of the LASIK flap interface and posterior cut smoothness was performed with light microscopy at 100X magnification in each specimen. Posterior cut smoothness was assessed centrally and peripherally by evaluating the number of frayed collagen fibers emanating from the posterior stromal surface. This was thought to be proportional to tissue planes invaded by the

microkeratome. Corneal cap curvature and stromal thickness were likely altered by tissue processing, and therefore, were not used as comparison criteria. Comparison of smoothness was statistically analyzed between LASIK and non-LASIK donor groups with non-parametric assays.

Results. Light microscopy revealed two of the three LASIK donor caps with large dehiscence of the flap, and the third with micro-dehiscence. Although the LASIK donor caps showed flap dehiscence anteriorly, the number of frayed posterior collagen fibers in LASIK vs. non-LASIK donor caps was not statistically significant centrally nor peripherally. Microkeratome cut smoothness appears similar between LASIK and non-LASIK donor caps.

Conclusions. LASIK donor tissue for DSAEK appears not to hinder microkeratome cut smoothness. The shearing force of the microkeratome pass does appear to create flap dehiscence.
Program#/Poster#: 780/D932

Cataract Practice Patterns and Correlation With Wound Burns

R.J. Olson.
Ophthalmology and Visual Sciences, Univ of Utah School of Medicine

Purpose. To determine the percentage of wound burns associated with various phaco machines and incision sizes in the U.S. and Canada.

Methods. Web-based survey of practices across the U.S. and Canada. Data analyzed included the number of incision wound burns, presence of ophthalmic viscosurgical devices (OVDs), phaco system employed, cataract removal technique, phaco system settings, and tip occlusion.

Results. There were a total of 957,323 phaco procedures and 415 wound burns reported (0.04%). 157 (38%) burns were associated with continuous, 140 (34%) with OZiL, 51 (12%) with pulse, 44 (11%) with hyperpulse, 4 (1%) with burst and 0 with Ellips ultrasound. For each system, the incidence was 0% for Ellips for about 12116 surgeries vs OZil incidence of 0.030% (172,723 surgeries) and 0.072% for OZil + longitudinal (173,460 surgeries). Of the wound burns, 211 occurred with incisions between 2.41-2.79mm, 132 occurred with incisions ≥ 2.8 mm. 244 (59%) of burns occurred with OVD present in the anterior chamber.

Conclusions. Although wound burn is uncommon in modern cataract surgery, the type of machine used, power modality, incision size and presence of OVD are related to this problem.
Program#/Poster#: 5452/A468

Enhanced Data Visualization In Anatomy

R.E. Marc.
Ophthalmology-Sch of Med, Univ of Utah/Moran Eye Center, Salt Lake City, UT.

Abstract. A range of data-linked tools have been developed in computer science to augment analysis, navigate data spaces, allow structured queries, facilitate annotation, and enhance didactic display. Though anatomy has made modest use of these visualizations, new web-based journal formats, “open data” models, and improved imaging standards now permit interactive, multi-dimensional and dynamic “pretty” graph displays. These provide both compact data summaries and access to real data. I will address several approaches using examples from the emerging field of retinal connectomics: (1) 3D rendering for data display, discovery and validation; (2) movies as surrogates for data mining; (3) visualization and open-data; (4) annotation as a resource to drive display and as a tool for presentation; (5) network tools from graph theory; (6) and how life in N-space has evolved towards use of projective geometries and parallel coordinate systems.

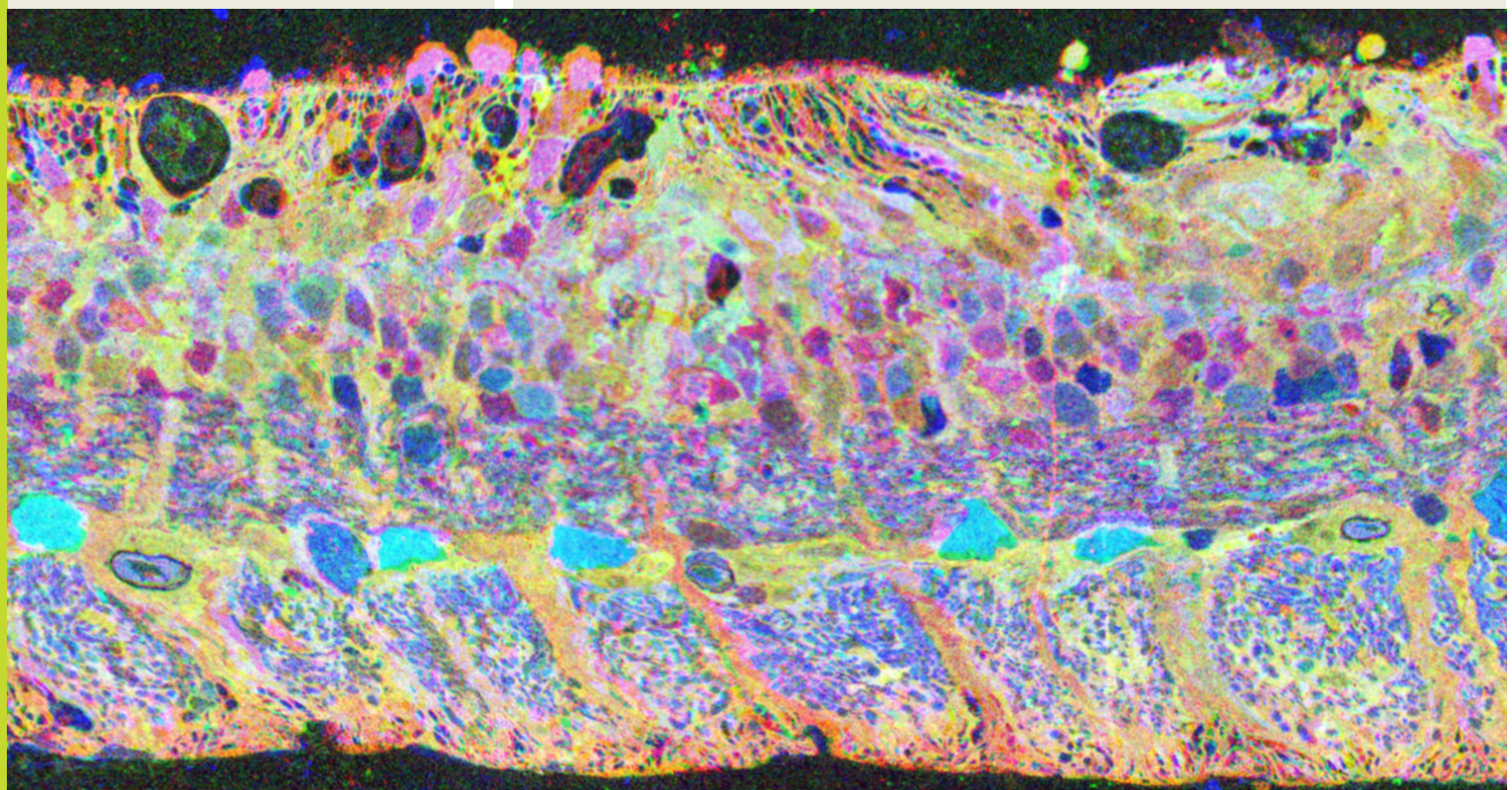

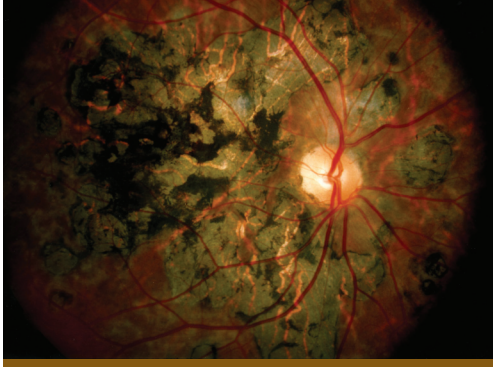
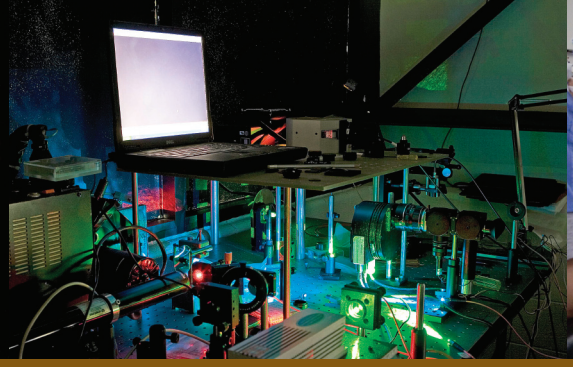


Research at the Moran Eye Center

The John A. Moran Eye Center hosts a collection of collegial and imaginative scientists whose work ranges from the development of the eye and retinal pigmented epithelium to the organization of visual cortex; from basic mechanisms of retinal phototransduction and the visual cycle, to the genetics and plasticity of retinal diseases; from synaptic interactions to immune modulation. Based in the L.S. and Aline Skaggs Research Pavilion, and joined by multiple walkways to the John A. Moran Clinical Pavilion, the Moran Eye Center research effort spans seven floors of laboratories, support resources and expansion space. Community engagement in our research programs is reflected in the establishment of the William and Pat Child and Ida Smith Vision Research Floors, and the Thomas Dee II & Family Center for Macular Degeneration Research.

The Moran Eye Center currently houses over 38,000 sq. ft. of dedicated, secure research space with primary state-of-the-art research space dedicated to individual research scientists. Each floor also houses over of core facilities including cold rooms, dark rooms, tissue culture facilities, ultracold freezer storage, office space students and fellows, conference and administrative space. Support include a dishwashing and in-house professional building management.

The Moran Eye Center houses a secure, accredited state-of-the-art vivarium managed and staffed by the University. With capacity of over 3000 mouse cages in a sealed system, the facility has procedure rooms, surgery, cage washing, and staff offices.

Major Moran Eye Center Core equipment includes two electron microscopes including an automated JEOL JEM 1400 with capacity for 5000 images/day; confocal systems; research cryostats, spectrophotometers, gel imagers, sequencing, mass spectrometry, terabyte scale data storage, optical scanning light microscopy, imaging workstations. Computational resources include a high density of gigabit ports (over 50/floor), secure wireless at all locations, and encrypted communication options.

Our basic and translational science programs include:

- The development and phenotypic maturation of the retinal pigmented epithelium
- Developmental mechanisms of cell proliferation and differentiation in the neural retina
- The genetics and biology of developmental eye defects
- The genetics, molecular and cell biology of macular degenerations
- Macular degeneration therapeutics
- Animal models of macular degeneration
- The molecular biology of phototransduction
- The molecular biology and biochemistry of retinoid metabolism
- The molecular biology and neurobiology of inherited retinal degenerations
- Gene therapy for Usher syndrome and other forms of retinitis pigmentosa
- The molecular and cellular basis of glaucoma
- Calcium signaling and regulation in the neural retina
- Regulation of vessel growth in retina and cornea
- Nanoparticle drug delivery mechanisms
- Synaptic plasticity in the developing and mature retina
- Retinal connectomics
- Retinal metabolomics
- The basis of excitatory signaling in the neural retina
- Parallel processing in visual cortex
- Cortical neuroprosthetics
- Tissue - intraocular lens implant interactions

These programs benefit from a strong collaborative tradition of the University of Utah that includes the Departments of Biology, Biochemistry, Biomedical Engineering, Electrical and Computer Engineering, Human Genetics, Internal Medicine, Mathematics, Medicinal Chemistry, Neurobiology and Anatomy, Neurology, Pediatrics, Physics, and Physiology; the School of Computing; and the Scientific Computing and Imaging Institute. In addition, strong graduate programs in Neuroscience, Biomedical Engineering and Molecular Biology, as well as MD/PhD programs through the University of Utah School of Medicine provide a vibrant collection of students for the John A. Moran Eye Center.

Our objectives in building a research team include maintaining diversity in basic science expertise, encouraging long-term research alliances among faculty, and providing an environment that supports the evolution of basic science to translational programs.

Retinal Research at Moran

Bala Ambati M.D., Ph.D, has joined the Moran faculty as a researcher and physician. We are honored to have Dr. Ambati, who has the distinction of being the world's youngest person to graduate from medical school at 17. He received his ophthalmology training at Harvard and Duke Universities. Dr. Ambati is experienced in cornea transplants, cataract extraction, keratoprosthesis (artificial cornea), LASIK, and other complex procedures of the cornea and anterior segment of the eye. He plans on building a practice welcoming patients in these areas as well as general ophthalmic issues. He has been an invited speaker at the World Ophthalmology Congress, American Society of Cataract & Refractive Surgery, International Congress of Eye Research, and other national and international conferences. He donates his time overseas on missions with ORBIS, a nonprofit organization with a Flying Eye Hospital, on which Dr. Ambati has operated and trained local surgeons in Ghana and Malaysia. With respect to clinical research, Dr. Ambati is committed to constant analysis of results of cornea transplants, LASIK, cataract extraction, and other anterior segment procedures with a view towards optimization of patient outcomes.

CCR3 is a target for age-related macular degeneration diagnosis and therapy.

Takeda A, Baffi JZ, Kleinman ME, Cho WG, Nozaki M,Yamada K, Kaneko H, Albuquerque RJ, Dridi S, Saito K, Raisler BJ, Budd SJ, Geisen P, Munitz A, Ambati BK, Green MG, Ishibashi T, Wright JD, Humbles AA, Gerard CJ, Ogura Y, Pan Y, Smith JR, Grisanti S, Hartnett ME, Rothenberg ME, Ambati J.

Journal: Nature. 2009 Jul 9; 460(7252): 225-30. Epub 2009 Jun 14.
Comment in: Nature. 2009 Jul 9;460(7252):182-3.

ABSTRACT: Age-related macular degeneration (AMD), a leading cause of blindness worldwide, is as prevalent as cancer in industrialized nations. Most blindness in AMD results from invasion of the retina by choroidal neovascularisation (CNV). Here we show that the eosinophil/mast cell chemokine receptor CCR3 is specifically expressed in choroidal neovascular endothelial cells in humans with AMD, and that despite the expression of its ligands eotaxin-1, -2 and -3, neither eosinophils nor mast cells are present in human CNV. Genetic or pharmacological targeting of CCR3 or eotaxins inhibited injury-induced CNV in mice. CNV suppression by CCR3 blockade was due to direct inhibition of endothelial cell proliferation, and was uncoupled from inflammation because it occurred in mice lacking eosinophils or mast cells, and was independent of macrophage and neutrophil recruitment.

Functional kinase homology domain is essential for the activity of photoreceptor guanylate cyclase 1

Author: Bereta G, Wang B, Kiser PD, Baehr W, Jang GF, Palczewski K.

Journal: J Biol Chem. 2009 Nov 9.

ABSTRACT: Phototransduction is carried out by a signaling pathway that links photoactivation of visual pigments in retinal photoreceptor cells to a change in their membrane potential. Upon photoactivation, the second messenger of phototransduction, cyclinc GMP, is rapidly degraded and mut be replenished during the recovery phase of phototransduction by photoreceptor guanylate cyclases (GCs), GC1 (or GC-E) and GC2 (or GC-F), to maintain vision. Here, we present data that address the role of the GC kinase homology (KH) domain in cyclic GMP production by GC1, the major cyclase in photoreceptors. First, experiments were done to test which GC1 residues undergo phosphorylation and whether such phosphorylation affects cyclase activity. Using mass spectrometry, we show that GC1 residues S530, S532, S533, and S538, located within the KH domain, undego light- and signal transduction- independent phosphorylation in vivo. Mutations in the putative Mg2+ binding site of the KH domain abolished phosphorylation, indicating that GC1 undergoes autophosphorylation. The dramatically reduced GC activity of these mutants suggests that a functional KH domai is essential for cyclic GMP production. However, evidence is presented that autophospghorylation does not regulate GC1 activity, in contrast to phsphorylation of other members of this cyclase family.

Wolfgang Baehr, Ph.D, studied organic chemistry at the University of Heidelberg. His career in retinal research was launched in the Department of Biochemistry, Princeton University, in 1976. He was recruited from the Cullen Eye Institute at Baylor College of Medicine where he was a Jules and Doris Stein Research to Prevent Blindness Professor from 1987—1994, and joined the Moran Eye Center as Professor of Ophthalmology and Director of our Foundation Fighting Blindness Center.

Dr. Baehr's career work addresses the biochemistry and molecular biology of the capture of light by photoreceptors in the eye, and the biochemistry of the key elements in that process with a focus on gene defects causative for human retinal disease.

Paul S. Bernstein, M.D., Ph.D, joined the faculty of the Moran Eye Center in 1995, where he currently divides his time equally between basic science retina research and a clinical practice devoted to medical and surgical treatment of disease of the retina and vitreous, with special emphasis on macular and retinal degenerations. His academic training at Harvard University included a summa cum laude undergraduate degree in chemistry, a Ph.D. with Robert Rando, and an M.D. from the Division of Health Sciences and Technology, and a joint program between Harvard Medical School and MIT. He did a postdoctoral fellowship with Dr. Dean Bok in retinal cell biology and a residency in ophthalmology at the UCLA Jules Stein Eye Institute.

Purification and partial characterization of a lutein-binding protein from human retina.

Author: Bhosale P, Li B, Sharifzadeh M, Gellermann W, Frederick JM, Tsuchida K, Bernstein PS.

Journal: Biochemistry. 2009 Jun 9;48(22):4798-807.

ABSTRACT: Dietary intake of lutein and zeaxanthin appears to be advantageous for protecting human retinal and macular tissues from degenerative disorders such as age-related macular degeneration. Selective concentration of just two of the many dietary carotenoids suggests that uptake and transport of the xanthophylls carotenoids into the human foveal region are mediated by specific xanthophylls-binding proteins such as GSTP1 which has previously been identified as the zeaxanthin-binding protein of the primate macula.

Here, a membrane-associated human retinal lutein-binding protein (HR-LBP) was purified from human peripheral retina using ion-exchange chromatography followed by size-exclusion chromatography. After attaining 83-fold enrichment of HR-LBP, this protein exhibited a significant bathochromic shift of approximately 90 nm in association with lutein, and equilibrium binding studies demonstrated saturable, specific binding toward lutein with a K8(D) of 0.45 muM. Examination for cross-reactivity with antibodies raised against known lutein-binding proteins from other organisms revealed consistent labeling of a major protein band of purified HR_LBP at approximately 29 KDa with an antibody raised against silkworm (Bombyx mori) carotenoid-binding protein (CBP), a member of steroidogenic acute regulatory (StAR) protein family with significant homology to many human StAR proteins.

Immunolocalization with antibodies directed against either CBP or GSTPf1 showed specific labeling of rod and cone inner segments,, especially in the mitochondria-rich ellipsoid region. There was also strong labeling of the outer plexiform (Henle fiber) layer with anti-GSTP1. Such localizations compare favorably with the distribution of macular carotenoids as revealed by resonance Raman microscopy. Our results suggest that HR-LBP may facilitate lutein's localization to a region of the cell subject to considerable oxidative stress

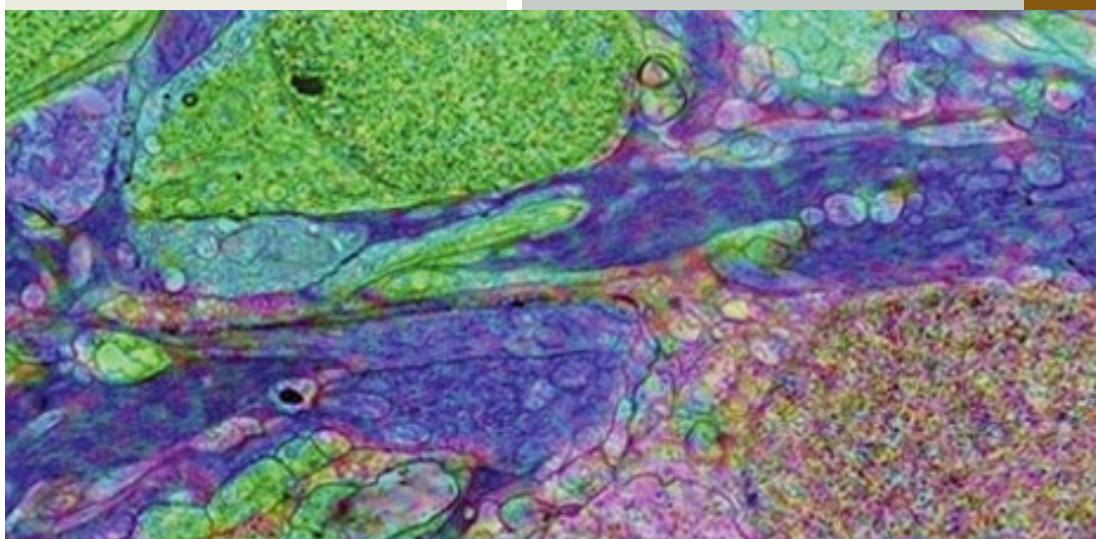

Jeanne M. Frederick, Ph.D.

Identification of genes involved in inherited human retinal disorders is the goal of research conducted by Jeanne Frederick, Ph.D. and Wolfgang Baehr, Ph.D. One of the best known heritable retinal diseases is retinitis pigmentosa (RP). Multiple genetic causes, each identified at the molecular level, are responsible for RP. The general approach to this research is twofold: to understand the molecular mechanism responsible for degeneration, and to design rational strategies to intervene and, eventually, retard or reverse disease onset. One method involves development of an animal strain that mimics a human disease. For example, knowing a specific DNA alteration in human visual pigment that is associated with RP, the same alteration can produce a comparable retinal degeneration in mice which can then be used to study the physiology, biochemistry and morphology of the retina.

Naturally occurring animal models with outer retina phenotypes.

Baehr W, Frederick JM.

Journal: Vision Res. 2009 Nov;49(22):2636-52. Epub 2009 Apr 16.

ABSTRACT: Naturally occurring and laboratory generated animal models serve as powerful tools with which to investigate the etiology of human retinal degeenerations, especially retinitis pigmentosa (RP), Leber congenital amaurosis (LCA), cone dystrophies (CD) and macular degeneration (MD). Much progress has been made in elucidating gene defects underlying disease, in understanding mechanisms leading to disease, and in designing molecules for translational research and gene-based therapy to interfere with the progression of disease. Key to this progress has been study of naturally occurring murine and canine retinal degeneration mutants. This article will review the history, phenoteypes and gene defects of select animal models with outer retina (photoreceptor and retinal pigment epithelium) degeneration phenotypes.

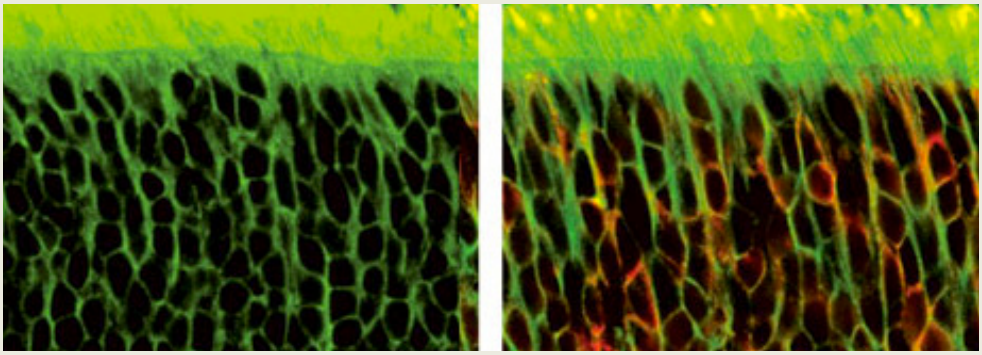

Trafficking of Membrane Proteins to Cone but not Rod Outer Segments is Dependent on Heterotrimeric Kinesin-II

Avasthi P, Watt CB, Williams DS, Le YZ, Li S, Chen CK, Marc RE, Frederick JM, Baehr W.

Journal: J Neurosci. 2009 No 11;29(45):14287-98.

SUMMARY: Heterotrimeric Kinesin-II is a molecular motor localized to the inner segment, connecting cilium and axoneme of mammalian photoreceptors. Our purpose was to identify the role of kinesin-II in anterograde intraflagellar transport (IFT) by photoreceptor-specific deletions of KIF3A, its obligatory motor subunit. In cones lacking KIF3A, membrane proteins involved in phototransduction did not traffic to the outer segments resulting in complete absence of a photopic electroretinogram and progressive cone degeneration. Rod photoreceptors lacking KIF3A degenerated rapidly between two and four weeks postnatal, but the phototransduction components including rhodopsin trafficked to the outer segments during the course of degeneration. Further, KIF3A deletion did not affect synaptic anterograde trafficking. The results indicate that trafficking of membrane proteins to the outer segment is dependent on kinesin-II in cone, but not rod photoreceptors, even though rods and cones share similar structures, and closely related photo transduction polypeptides.

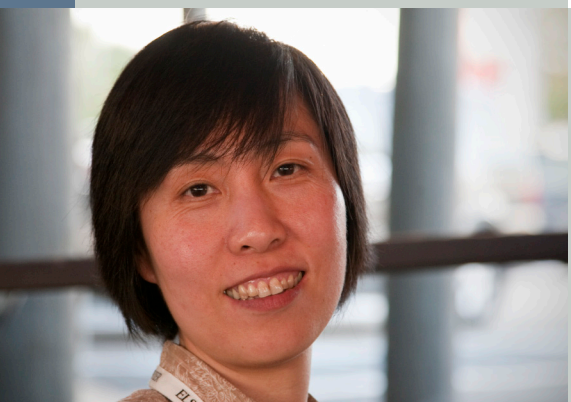

Jun Yang, Ph.D.

Dr Yang's laboratory is focused on the disease mechanisms and therapeutic treatments for retinal degenerative diseases using mouse models. Her research group investigates the biological functions of genes whose mutations are known to cause human retinal disease. Using mouse models for these diseases, the group also studies treatment of these diseases by means of gene therapy. Dr.Yang's team is also interested in the cell biology of photoreceptors, especially the cellular processes of intracellular trafficking, structural maintenance, and calcium regulation.

Yingbin Fu, Ph.D, received his B.S in Biochemistry at Peking University, Beijing, China. He received his Ph.D. in Biochemistry at Michigan State University, East Lansing, Michigan, where he was a member of the Honor Society for International Scholars. Prior to coming to the Moran Eye Center, Dr. Fu worked as a postdoc fellow at Dr. King-Wai Yau's lab at The Johns Hopkins University School of Medicine in Baltimore, Maryland.

Genetic and functional dissection of HTRA1 and LOC387715 in age-related macular degeneration.

Authors: Yang Z, Tong Z, Chen Y, Zeng J, Sun X, Zhao C, Davey L, Wang K, Chen H, London N, Muramatsu D, Salasar F, Kasuga D, Wang X, Dixie M, Zhao P, Yang R, Gibbs D, Lu F, Liu X, Li Y, Li B, Li C, Li Y, Campochiaro B, Constantine R, Zack D, Campochiaro P, Fu Y, Li D, Katsanis N, and Zhang K.

Journal: PLoS Genet. 2010 Feb 5;6(2): : e1000836. doi:10.1371/journal.pgen.1000836

ABSTRACT: A common haplotype on 10q26 influences the risk of age-related macular degeneration (AMD) and encompasses two genes, LOC387715 and HTRA1. Recent data have suggested that loss of LOC387715, mediated by an insertion/deletion (in/del) that destabilizes its message, is causally related with the disorder. Here we show that loss of LOC387715 is insufficient to explain AMD susceptibility, since a nonsense mutation (R38X) in this gene that leads to loss of its message resides in a protective haplotype. At the same time, the common disease haplotype tagged by the in/del and rs11200638 has an effect on the transcriptional upregulation of the adjacent gene, HTRA1. These data implicate increased HTRA1 expression in the pathogenesis of AMD and highlight the importance of exploring multiple functional consequences of alleles in haplotypes that confer susceptibility to complex traits.

Phototransduction: Phototransduction in Rods

Author: Fu, Y.

Encyclopedia of the Eye. Molecular Mechanisms of Visual Transduction, Chapter 206. 2010. Academic Press. ISBN-13: 978-0-12-374198-1

ABSTRACT: Rods are extremely sensitive to light to the extent that they can detect single photons. The biochemical cascade responsible for rod phototransduction is established. The exquisite sensitivity of the rod system is achieved through high quantum efficiency of photoactivation, multiple amplification steps in combination with a very low noise design. This chapter will describe the current understanding on each of these features.

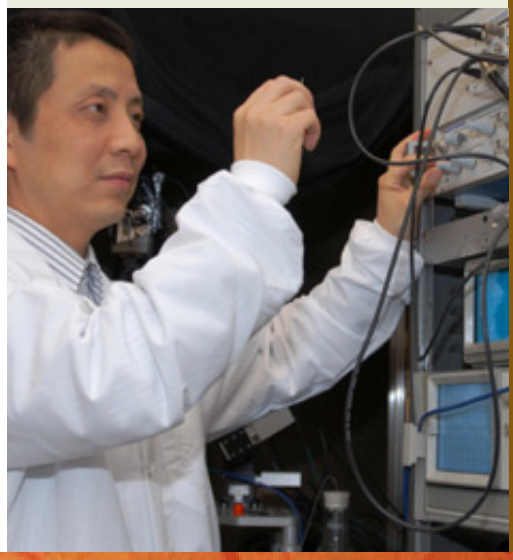

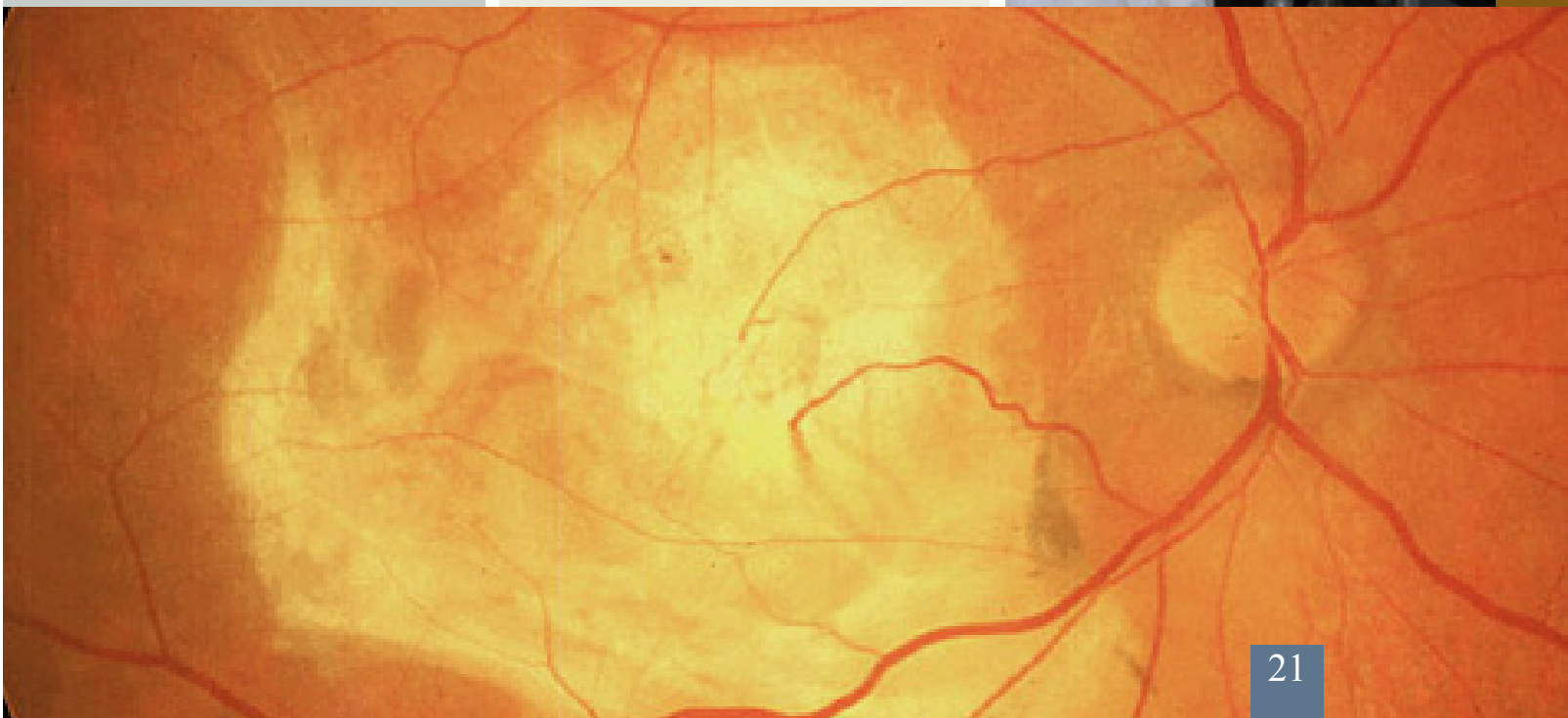

Gregory Hageman, Ph.D, is the new John A. Moran Presidential Professor of Ophthalmology and Visual Sciences, and Director of the Center for Translational Medicine. Prior to his move to the Moran Eye Center, Dr. Hageman served as the Iowa Entrepreneurial Endowed Professor and Professor of Ophthalmology & Visual Sciences at the University of Iowa, Carver College of Medicine. At Iowa he directed the Cell Biology and Functional Genomics Laboratory. He held additional appointments as a Senior Member of the University of Iowa Center for Macular Degeneration, an Associate Faculty Member in the Center for the Study of Macular Degeneration, University of California, Santa Barbara, and Honorary Professorships at Queens University, Belfast, UK and Shandong Eye Institute, Qingdao, China.

The Pivotal Role of the Complement System in Aging and Age-related Macular Degeneration: Hypothesis Re-visited.

Author: Anderson DH, Radeke MJ, Gallo NB, Chapin EA, Johnson PT, Curletti CR, Hancox LS, Hu J, Ebright JN, Malek G, Hauser MA, Rickman CB, Bok D, Hageman GS, Johnson LV.

Journal: Prog Retin Eye Res. 2010 Mar;29(2):95-112. Epub 2009 Dec 2.

ABSTRACT: During the past ten years, dramatic advances have been made in unraveling the biological bases of age-related macular degeneration (AMD), the most common cause of irreversible blindness in western populations. In that timeframe, two distinct lines of evidence emerged which implicated chonic local inflammation and activation of the complement cascade in AMD pathogenesis. First, a number of complement system proteins, complement activators, and complement regulatory proteins were identified as molecular constituents of drusen, the hallmark extracellular deposits associated with early AMD. Subsequently, genetic studies revealed highly significant statistical associations between AMD and variants of several complement pathway-associated genes including: Complement factor H (CFH), complement factor H-related 1 and 3 (CFHR1 and CFHR3), complement factor B (CFB), complement component 2 (C2), and complement component 3 (C3).

In this article, we revisit our original hypothesis that chronic local inflammatory and immune-mediated events at the level of Bruch's membrane play critical roles in drusen biogenesis and, by extension, in the pathobiology of AMD. Secondly, we report the results of a new screening for additional AMD-associated polymorphisms in a batter of 63 complement-related genes.

Third, we identify and characterize the local complement system in the RPE-choroid complex – thus adding a new dimension of biological complexity to the role of the complement system in ocular aging and AMD. Finally, we evaluate the most salient, recent evidence that bears directly on the role of complement in AMD pathogenesis and progression. Collectively, these recent findings strongly re-affirm the importance of the complement system in AMD. They lay the groundwork for further studies that may lead to the identification of a transcriptional disease signature of AMD, and hasten the development of new therapeutic approaches that will restore the complement-modulating activity that appears to be compromised in genetically susceptible individuals.

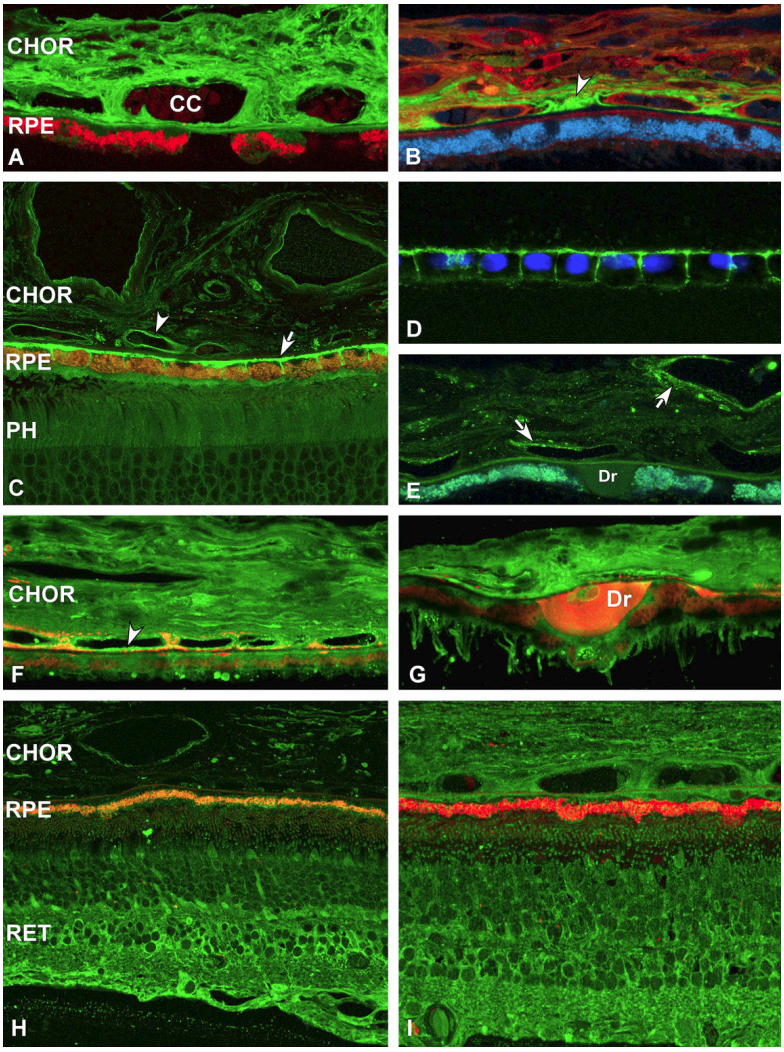

Convergence of linkage, gene expression and association data demonstrates the influence of the RAR-related orphan receptor alpha (RORA) gene on neovascular AMD: A systems biology based approach.

Silveira AC, Morrison MA, Ji F, Xu H, Reinecke JB, Adams SM, Arneberg TM, Janssian M, Lee JE, Yuan Y, Schaumberg DA, Kotoula MG, Tsironi EE, Tsiloulis AN, Chatzoulis DZ, Miller JW, Kim IK, Hageman GS, Farrer LA, Haider NB, Deangelis MM.

Journal: Vision Res. 2010 Mar 31;50(7):698-715. Epub 2009 Sep 26.

ABSTRACT: To identify novel genes and pathways associated with AMD, we performed microarray gene expression and linkage analysis which implicated the candidate gene, retinoic acid receptor-related orphan receptor alpha (RORA, 15q). Subsequent genotyping of 159 RORA single nucleotide plymorphisms (SNPs) in a family-based cohort, followed by replication in an unrelated case-control cohort, demonstrated that SNPs and haplotypes located in intron 1 were significantly associated with neovascular AMD risk in both cohorts. This is the first report demonstrating a possible role for RORA, a receptor for cholesterol, in the pathophysiology of AMD. Moreover, we found a significant interaction between RORA and the ARMS2/HTRA1 locus suggesting a novel pathway underlying AMD pathophysiology.

Complement factor H gene polymorphisms and Chlamydia pneumoniae infection in age-related macular degeneration.

Authors: Haas P, Steindl K, Schmid-Kubista KE, Aggermann T, Krugluger W, Hageman GS, Binder S.

Journal: Eye (Lond). 2009 Dec;23(12):2228-32.

PURPOSE: To investigate the association of the complement factor H gene (CFH)Y402H polymorphism and age-related macular degeneration (AMD) in the Austrian population (Caucasoid descent), and to determine whether there is an association between exposure to Chlamydia pneumoniae-responsible or up to 20% of community-acquired pneumoniae-and the AMD-associated CFH risk polymorphism.

METHODS: Genotypes were determined by polymerase chain reaction-restriction fragment length polymorphism analysis in 75 unrelated AMD patients and compared with 75 healthy, age-matched control subjects. C. pneumoniae serum IgG was tested by ELISA (R&D) in both groups. The association between the CFHY402H genetic polymorphism and the disease was examined by chi (2)ptest and logistic regression.

RESULTS: CFH Y402H genotype frequencies differed significantly between AMD patients and healthy controls (1277 TT, 22.7%; 1277 TC, 53.3%; and 1277 CC, 22.7% in the AMD group; 1277 TT, 48.0%; 1277 TC, 38.7%; and 1277 CC, 13.3% in the control group) showing a P-value <0.005 (OR:2.920/3.811). No association was found between a positive C. pneumoniae titre and AMD (P=0.192), nor was any association found between C. pneumoniae and the CH Y402H polymorphism.

CONCLUSIONS: Our data confirm that the CFHY402H polymorphism is a risk factor for the AMD in the Austrian population wth a higher frequency of the Y402 polymorphism in AMD patients. No association between preceding C. pneumoniae infection and diagnosed AMD was found.

Retinal basement membrane abnormalities and the retinopathy of Alport syndrome.

Authors: Savige J, Liu J, DeBuc DC, Handa JT, Hageman GS, Wang YY, Parkin JD, Vote B, Fassett R, Sarks S, Colville D.

Journal: Invest Ophthalmol Vis Sci.2010 Mar;51(3):1621-7. Epub 2009 Oct 22.

PURPOSE: To determine the effects of X-linked and autosomal recessive Alport syndrome on retinal basement membranes and how these result in the characteristic perimacular dot-and-fleck retinopathy, lozenge, and macular hole.

METHODS: The type IV collagen chains present in the normal retina were determined immunohistochemically. Ten patients with Alport syndrome underwent retinal photography and optical coherence tomography to determine the thickness of the internal limiting membrane (ILM) by segmentation analysis, the layers affected by the retinopathy, and any correlates of the lozenge and macular hole. Bruch's membrane was examined directly by electron microscopy in a donated Alport eye. RESULTS: The alpha3alpha4alpha5 type IV collagen network was present in the normal ILM and in the retinal pigment epithelium basement membrane of Bruch's membrane. In Alport syndrome, the ILM/nerve fiber layer and Bruch's membrane were both thinned. The dot-and-fleck retinopathy corresponded to hyperreflectivity of the ILM/nerve fiber layer in the distribution of the nerve fiber layer. The lozenge and macular hole corresponded to temporal macular thinning. The thinning across the whole retina was principally due to thinning of the ILM/nerve fiber layer and inner nuclear layer.

CONCLUSIONS: The Alport dot-and-fleck retinopathy results primarily from abnormalities in the ILM/nerve fiber layer rather than in Bruch's membrane. Thinning of the ILM/nerve fiber layer contributes to the retinopathy, lozenge, and macular hole, possibly through interfering with nutrition of the overlying retina or clearance of metabolic by-products.

Complement, age-related macular degeneration and a vision of the future.

Authors: Gehrs KM, Jackson JR, Brown EN, Allikmets R, Hageman GS.

Journal: Archives of Ophthalmology 2010 Mar;128(3):349-58.

ABSTRACT: Age-related macular degeneration (AMD) is one of the most well-characterized late-onset, complex trait diseases. Remarkable advances in our understanding of the genetic and biological foundations of this disease were derived from a recent convergence of scientific and clinical data. Importantly, the more recent identification of AMD-associated variations in a number of complement pathway genes has provided strong support for earlier, paradigm-shifting studies that suggested that aberrant function of the complement system plays a key role in disease etiology. Collectively, this wealth of information has provided an impetus for the development of powerful tools to accurately diagnose disease risk and progression and complement-based therapeutics that will ultimately delay or prevent AMD. Indeed, we are poised to witness a new era of a personalized approach toward the assessment, management, and treatment of this debilitating, chronic disease.

Mary Elizabeth Hartnett, M.D.
Our lab is using molecular techniques to study growth factor mechanisms involved in cell-cell interactions and models of retinal diseases associated with abnormal or unwanted angiogenesis.

We are investigating causes of retinal avascularity, or lack of blood vessel support in areas of the inner retina, which leads to retinal hypoxia. Retinal avascularity is a common finding prior to the formation of damaging, abnormal blood vessel growth (abnormal angiogenesis) into the vitreous gel with later blinding consequences of vitreous hemorrhage and retinal detachment. Understanding why blood vessels do not grow into the avascular and hypoxic retinal areas may allow us to find methods to promote helpful blood vessel support of the inner retina and reduce abnormal damaging blood vessel growth into the vitreous. Ultimately, this could be helpful in diseases associated with abnormal angiogenesis such as in diseases such as retinopathy of prematurity and diabetic retinopathy.

Plasma complement components and activation fragments: associations with age-related macular degeneration genotypes and phenotypes.

Authors: Reynolds R, Hartnett ME, Atkinson JP, Giclas PC, Rosner B, Seddon JM.

Journal: Invest Ophthalmol Vis Sci. 2009 Dec;50(12):5818-27. Epub 2009 Aug 6.

PURPOSE: Several genes encoding complement system components and fragments are associated with age-related macular degeneration (AMD). This study was conducted to determine whether alterations in circulating levels of these markers of complement activation and regulation are also independently associated with advanced AMD and whether they are related to AMD genotypes.

METHODS: Plasma and DNA samples were selected from individuals in our AMD registry who had progressed to or developed the advanced stages of AMD, including 58 with geographic atrophy and 62 with neovascular disease. Subjects of similar age and sex, but without AMD, and who did not progress were included as controls (n = 60). Plasma complement components (C3, CFB, CFI, CFH, and factor D) and activation fragments (Bb, C3a, C5a, iC3b, and SC5b-9) were analyzed. DNA samples were genotyped for seven single-nucleotide polymorphisms in six genes previously shown to be associated with AMD: CFB, CFH, C2, C3, and CFI and the LOC387715/ARMS2 gene region. The association between AMD and each complement biomarker was assessed by using logistic regression, controlling for age, sex, and proinflammatory risk factors: smoking and body mass index (BMI). Functional genomic analyses were performed to assess the relationship between the complement markers and genotypes. Concordance, or C, statistics were calculated to assess the effect of complement components and activation fragments in an AMD gene-environment prediction model.

RESULTS: The highest quartiles of Bb and C5a were significantly associated with advanced AMD, when compared with the lowest quartiles. In multivariate models without genetic variants, the odds ratio (OR) for Bb was 3.3 (95% confidence interval [CI] = 1.3-8.6), and the OR for C5a was 3.6 (95% CI = 1.2-10.3). With adjustment for genetic variants, these ORs were substantially higher. The alternative pathway regulator CFH was inversely associated with AMD in the model without genotypes (OR = 0.3; P = 0.01). Positive associations were found between BMI and plasma C3, CFB, CFH, iC3b, and C3a. There were also significant associations between C5a fragment and LOC387715/ARMS2 and C3 genotypes (P for trend = 0.02, 0.04), respectively. C statistics for models with behavioral and genetic factors increased to 0.94 +/- 0.20 with the addition of C3a, Bb, and C5a.

CONCLUSIONS: Increased levels of activation fragments Bb and C5a are independently associated with AMD. Higher BMI is related to increased levels of complement components. C5a is associated with AMD genotypes. C statistics are stronger with the addition of C3a, Bb, and C5a in predictive models. Results implicate ongoing activation of the alternative complement pathway in AMD pathogenesis.

The effects of oxygen stresses on the development of features of severe retinopathy of prematurity: knowledge from the 50/10 OIR model.

Author: Hartnett ME.

Journal: Doc Ophthalmol. 2010 Feb;120(1):25-39. Epub 2009 Jul 29.

ABSTRACT: The objective of this study is to determine growth factor expression and activation of signaling pathways associated with intravitreous neovascularization and peripheral avascular retina using a model of retinopathy of prematurity (ROP) relevant to today with oxygen monitoring in neonatal units. Studies using 50/10 oxygen-induced retinopathy (OIR) and 50/10 OIR+SO models were reviewed. Repeated fluctuations in oxygen increased retinal vascular endothelial growth factor (VEGF) even while peripheral avascular retina persisted and prior to the development of intravitreous neovascularization. Repeated fluctuations in oxygen increased VEGF(164) expression but not VEGF(120). Neutralizing VEGF bioactivity significantly reduced intravitreous neovascularization and arteriolar tortuosity without interfering with ongoing retinal vascularize-

tion. Repeated oxygen fluctuations led to retinal hypoxia and increased reactive oxygen species (ROS). Inhibiting ROS with NADPH oxidase inhibitor, apocynin, reduced avascular retina by interfering with apoptosis. Supplemental oxygen reduced retinal VEGF concentration and exacerbated NADPH oxidase activation to contribute to intravitreous neovascularization through activation of the JAK/STAT pathway. Oxygen stresses relevant to those experienced by preterm infants today trigger signaling of different pathways to cause avascular retina and intravitreous neovascularization. Increased signaling of VEGF appears important to the development of both avascular retina and intravitreous neovascularization.

Reduction in endothelial tip cell filopodia corresponds to reduced intravitreous but not intraretinal vascularization in a model of ROP.

Authors: Budd S, Byfield G, Martiniuk D, Geisen P, Hartnett ME.

Journal: Exp Eye Res. 2009 Nov;89(5):718-27. Epub 2009 Jul 1.

ABSTRACT: To determine the effect of a vascular endothelial growth factor receptor 2 tyrosine kinase (VEGFR2) inhibitor on intravitreous neovascularization (IVNV), endothelial tip cell filopodia, and intraretinal vascularization in a rat model of retinopathy of prematurity (ROP). Within 4h of birth, newborn Sprague-Dawley rat pups and their mothers were cycled between 50% and 10% oxygen daily until postnatal day (p)12. Pups were given intravitreous injections of VEGFR2 inhibitor, SU5416, or control (dimethyl sulfoxide, DMSO) and returned to oxygen cycling until p14, then placed into room air. Intravitreous neovascularization (IVNV), avascular/total retinal areas, and endothelial tip cell filopodial number and length were determined in lectin-labeled neurosensory retinal flat mounts. Cryosections or fresh tissue were analyzed for phospho-VEGFR1, phospho-VEGFR2, activated caspase-3, or phospho-beta3 integrin. Human umbilical venous (HUVECs) and human choroidal endothelial cells (ECs) were treated with VEGFR2 inhibitor to determine effect on VEGFR2 phosphorylation and on directed EC migration toward a VEGF gradient. Filopodial length and number of migrated ECs were also measured. Compared to control, the VEGFR2 inhibitor reduced VEGFR2 phosphorylation in HUVECs in vitro and clock hours and areas of IVNV but not percent avascular retina in vivo. Filopodial length and number of filopodia/EC tip cell were reduced in retinal flat mounts at doses that inhibited IVNV, whereas at lower doses, only a reduction in filopodial length/EC tip cell was found. There was no difference in phosphorylated beta3 integrin and cleaved caspase-3 labeling in VEGFR2 inhibitor-treated compared to control in vivo. Doses of the VEGFR2 inhibitor that reduced filopodial length and number of filopodia/migrating EC corresponded to reduced EC migration in in vitro models. VEGFR2 inhibitor reduced IVNV and filopodial number and length/EC tip cell without interfering with intraretinal vascularization. Reducing the number and length of filopodia/endothelial tip cell may reduce guidance cues for endothelial cells to migrate into the vitreous without interfering with migration into the retina toward a VEGF gradient.

The role of supplemental oxygen and JAK/STAT signaling in intravitreous neovascularization in a ROP rat model.

Authors: Byfield G, Budd S, Hartnett ME.

Journal: Invest Ophthalmol Vis Sci. 2009 Jul;50(7):3360-5. Epub 2009 Mar 5.

PURPOSE: To investigate whether oxygen stresses experienced in retinopathy of prematurity (ROP) trigger signaling through reactive oxygen species (ROS) and whether the Janus kinase-signal transducer and activator of transcription (JAK/STAT) pathway lead to intravitreous neovascularization (IVNV) in an oxygen-induced retinopathy (OIR) rat model.

METHODS: Newborn rat pups exposed to repeated fluctuations in oxygen and rescued in supplemental oxygen (28% O(2), 50/10 OIR+SO) were treated with apocynin, an NADPH oxidase and ROS inhibitor (10 mg/kg/d), AG490, a JAK2 inhibitor (5 mg/kg/d), or phosphate-buffered saline. Intraperitoneal injections were given from postnatal day (P)12 to P17 (apocynin), or from P3 to P17 (AG490). Outcomes were intravitreous neovascularization and avascular/total retinal areas, vascular endothelial growth factor, phosphorylated JAK2, and phosphorylated STAT3.

RESULTS: Apocynin significantly reduced phosphorylated STAT3 in 50/10 OIR+SO ($P = 0.04$), in association with previously reported inhibition of the IVNV area. Inhibition of JAK with AG490 significantly reduced phosphorylated JAK2 ($P < 0.001$), phosphorylated STAT3 ($P = 0.002$), and IVNV area ($P = 0.033$) in the 50/10 OIR+SO model compared with control.

CONCLUSIONS: Activation of NADPH oxidase from supplemental oxygen works through activated STAT3 to lead to IVNV. In addition, inhibition of the JAK/STAT pathway reduces IVNV. Further studies are needed to determine the effects and relationships of oxygen stresses on JAK/STAT and NAPDH oxidase signaling.

Bryan William Jones, Ph.D, joined the Research Faculty of the Moran Eye Center in 2006. Originally coming to science through the study of epilepsy and sleep medicine, he became fascinated by the beauty of the retina and the complexity of blinding diseases. His work in the laboratory of Dr. Robert E. Marc revealed the nature and extent of pathology seen in retinal degenerative diseases such as retinitis pigmentosa and macular degeneration, now known as retinal remodeling. This work helped to refine approaches to vision rescue through both bionic and biological approaches. Continued work will further define the time lines of retinal remodeling in an effort to determine windows of opportunity for intervention to limit, prevent or exploit retinal remodeling. Other work in the Marc Laboratory focuses on applying novel molecular and computational approaches to resolving the identities and connectivities of neurons in the retina to discover how the normal retina is wired, how that circuitry is altered in degenerative diseases, and how to potentially engineer artificial biological retinas.

The Viking Viewer for Connectomics: Scalable Multiuser Annotation and Summarization of Large Volume Datasets

Authors: Anderson JR, Grimm B, Mohammed S, Jones BW, Koshevoy P, Tasdizen T, Whitaker R, Marc RE.

Journal: Journal of Microscopy 2010

ABSTRACT: Modern microscope automation permits the collection of vast amounts of continuous anatomical imagery in both two and three dimensions. These large datasets present significant challenges for data storage, access, viewing, annotation, and analysis. The cost and overhead of collecting and storing the data can be extremely high. Large datasets quickly exceed an individual's capability for timely analysis and present challenges in efficiently applying transforms, if needed. Finally annotated anatomical datasets can represent a significant investment of resources and should be easily accessible to the scientific community. The Viking application was our solution created to view and annotate a 16.5 TB ultrastructural retinal connectome volume and we demonstrate its utility in reconstructing neural networks for a distinctive of retinal amacrine cell class. Viking has several key features. (1) It works over the internet using HTTP and supports many concurrent users limited only by hardware. (2) It supports a multi-user, collaborative annotation strategy. (3) It cleanly demarcates viewing and analysis from data collection and hosting. (4) It is capable of applying transformations in real-time. (5) It has an easily extensible user interface, allowing addition of specialized modules without rewriting the viewer.

A computational framework for ultrastructural mapping of neural circuitry.

Authors: Anderson JR, Jones BW, Yang JH, Shaw MV, Watt CB, Koshevoy P, Spaltenstein J, Jurrus E, U V K, Whitaker RT, Mastronarde D, Tasdizen T, Marc RE.

Journal: PLoS Biol. 2009 Mar;7(3):e1000074.

ABSTRACT: Circuitry mapping of metazoan neural systems is difficult because canonical neural regions (regions containing one or more copies of all components) are large, regional borders are uncertain, neuronal diversity is high, and potential network topologies so numerous that only anatomical ground truth can resolve them. Complete mapping of a specific network requires synaptic resolution, canonical region coverage, and robust neuronal classification. Though transmission electron microscopy (TEM) remains the optimal tool for network mapping, the process of building large serial section TEM (ssTEM) image volumes is rendered difficult by the need to precisely mosaic distorted image tiles and register distorted mosaics. Moreover, most molecular neuronal class markers are poorly compatible with optimal TEM imaging. Our objective was to build a complete framework for ultrastructural circuitry mapping. This framework combines strong TEM-compliant small molecule profiling with automated image tile mosaicking, automated slice-to-slice image registration, and gigabyte-scale image browsing for volume annotation. Specifically we show how ultrathin molecular profiling datasets and their resultant classification maps can be embedded into ssTEM datasets and how scripted acquisition tools (SerialEM), mosaicking and registration (ir-tools), and large slice viewers (MosaicBuilder, Viking) can be used to manage terabyte-scale volumes. These methods enable large-scale connectivity analyses of new and legacy data. In well-posed tasks (e.g., complete network mapping in retina), terabyte-scale image volumes that previously would require decades of assembly can now be completed in months. Perhaps more importantly, the fusion of molecular profiling, image acquisition by SerialEM, ir-tools volume assembly, and data viewers/annotators also allow ssTEM to be used as a prospective tool for discovery in nonneural systems and a practical screening methodology for neurogenetics. Finally, this framework provides a mechanism for parallelization of ssTEM imaging, volume assembly, and data analysis across an international user base, enhancing the productivity of a large cohort of electron microscopists.

David Krizaj, Ph.D, did graduate training at New York University with Paul Witkovsky focusing on synaptic signaling between retinal cells and postdoctoral work with David Copenhagen at University of California San Francisco School of Medicine, working on intracellular signaling in photoreceptors. He spent six years as faculty at the at UCSF Dept. of Ophthalmology before joining the Moran Eye Center of the University of Utah in 2007.

Calcium homeostasis and cone signaling are regulated by interactions between calcium stores and plasma membrane ion channels.

Author: Szikra T, Barabas P, Bartoletti TM, Huang W, Akopian A, Thoreson WB, Krizaj D.

Journal: PLoS One. 2009 Aug 21;4(8):e6723.

ABSTRACT: Calcium is a messenger ion that controls all aspects of cone photoreceptor function, including synaptic release. The dynamic range of the cone output extends beyond the activation threshold for voltage-operated calcium entry, suggesting another calcium influx mechanism operates in cones hyperpolarized by light.

We have used optical imaging and whole-cell voltage clamp to measure the contribution of store-operated Ca(2+) entry (SOCE) to Ca(2+) homeostasis and its role in regulation of neurotransmission at cone synapses. Mn(2+) quenching of Fura-2 revealed sustained divalent cation entry in hyperpolarized cones. Ca(2+) stores unaffected by pharmacological manipulation of voltage-operated or cyclic nucleotide-gated Ca(2+) channels and suppressed by lanthanides, 2-APB, MRS 1845 and SKF 96365.

However, cation influx through store-operated channels crossed the threshold for activation of voltage-operated Ca(+) entry in a subset of cones, indicating that the operating range of inner segment signals is set by interactions between store- and voltage-operated Ca(2+) channels. Exposure to MRS 1845 resulted in approximately 40% reduction of light-evoked postsynaptic currents in photopic horizontal cells without affecting the light responses or voltage-operated Ca(2+) currents in simultaneously recorded cones.

The spatial pattern of store-operated calcium entry in cones matched immunolocalization of the store-operated sensor STIM1. These findings show that store-operated channels regulate spatial and temporal properties of Ca(2+) homeostasis in vertebrate cones and demonstrate their role in generation of sustained excitatory signals across the first retinal synapse.

Glutamate-induced internalization of Ca(v)1.3 L-type Ca(2+) channels protects retinal neurons against excitotoxicity.

Authors: Mizuno F, Barabas P, Krizaj D, Akopian A.

Journal: J Physiol. 2010 Mar 15;588(Pt 6):953-66. Epub 2010 Feb 1.

ABSTRACT: Glutamate-induced rise in the intracellular Ca(2+) level is thought to be a major cause of excitotoxic cell death, but the mechanisms that control the Ca(2+) overload are poorly understood. Using immunocytochemistry, electrophysiology and Ca(2+) imaging, we show that activation of ionotropic glutamate receptors induces a selective internalization of Ca(v)1.3 L-type Ca(2+) channels in salamander retinal neurons. The effect of glutamate on Ca(v)1.3 internalization was blocked in Ca(2+)-free external solution, or by strong buffering of internal Ca(2+) with BAPTA. Downregulation of L-type Ca(2+) channel activity in retinal ganglion cells by glutamate was suppressed by inhibitors of dynamin-dependent endocytosis. Stabilization of F-actin by jasplakinolide significantly reduced the ability of glutamate to induce internalization suggesting it is mediated by Ca(2+)-dependent reorganization of actin cytoskeleton. We showed that the Ca(v)1.3 is the primary L-type Ca(2+) channel contributing to kainate-induced excitotoxic death of amacrine and ganglion cells. Block of Ca(v)1.3 internalization by either dynamin inhibition or F-actin stabilization increased vulnerability of retinal amacrine and ganglion cells to kainate-induced excitotoxicity. Our data show for the first time that Ca(v)1.3 L-type Ca(2+) channels are subject to rapid glutamate-induced internalization, which may serve as a negative feedback mechanism protecting retinal neurons against glutamate-induced excitotoxicity.

Edward Levine, Ph.D, joined the Moran Eye Center in 2000. His laboratory is focused on understanding the molecular and cellular mechanisms of retinal development, as well as determining the contributions of developmental mechanisms to the progression and treatment of retinal degenerative diseases. His research uses the mouse retina because its developmental progression is well understood and several genetic models of retinal degeneration are available, thus facilitating the identification and characterization of important regulatory molecules. These studies enable direct tests of the roles of these molecules in retinal degenerations.

Rlbp1 promoter drives robust Müller glial GFP expression in transgenic mice.

Author: Vázquez-Chona FR, Clark AM, Levine EM.

Journal: Invest Ophthalmoml Vis Sci. 2009 Aug;50(8):3996-4003. Epub 2009 Mar 25.

PURPOSE: Müller glia are essential for maintaining retinal homeostasis and exhibit neuroprotective and deleterious responses during retinal degeneration. Having the abililty to visualize and genetically manipulate Müller glia in vivo will facilitate a better understanding of how these cells contribute to these processes. The goal of this study was to determine whether regulatory elements of the retinaldehyde bindg protein 1 (Rlbp1; formerly Cralbp) gene can drive robust Müller glial gene expression in vivo.

METHODS: Transgenic mice were generated by pronuclear injection of a construct carrying a 3-kilobase (kb) region of the Rlbp1 gene and 5'-flanking sequences linked to the enhanced green fluorescent protein (GFP) cDNA. GFP expression was analyzed by immunohistology in regions of the central nervous system in which RLBP1 protein is expressed, in retinas from wild-type and retinal degeneration 1 (rd1) mice, and during retinal development.

RESULTS: Three transgenic lines were generated, and the one with the strongest and most consistent GFP expression was characterized further. Müller glia displayed robust GFP expression at all postnatal developmental stages and in the rd1 retina. Onset of expression occurred by birth in retinal progenitor cells.

CONCLUSIONS: Regulatory elements in a restricted region of the Rlbp1 gene are sufficient to drive GFP expression in vivo. This transgenic line provides robust GFP expression that can be used to visualize retinal progenitor cells during postnatal development and Müller glia during their differentiation and in the healthy or degenerating adult retina.

Below: Expression of Green Fluorescent Protein in Muller Glia

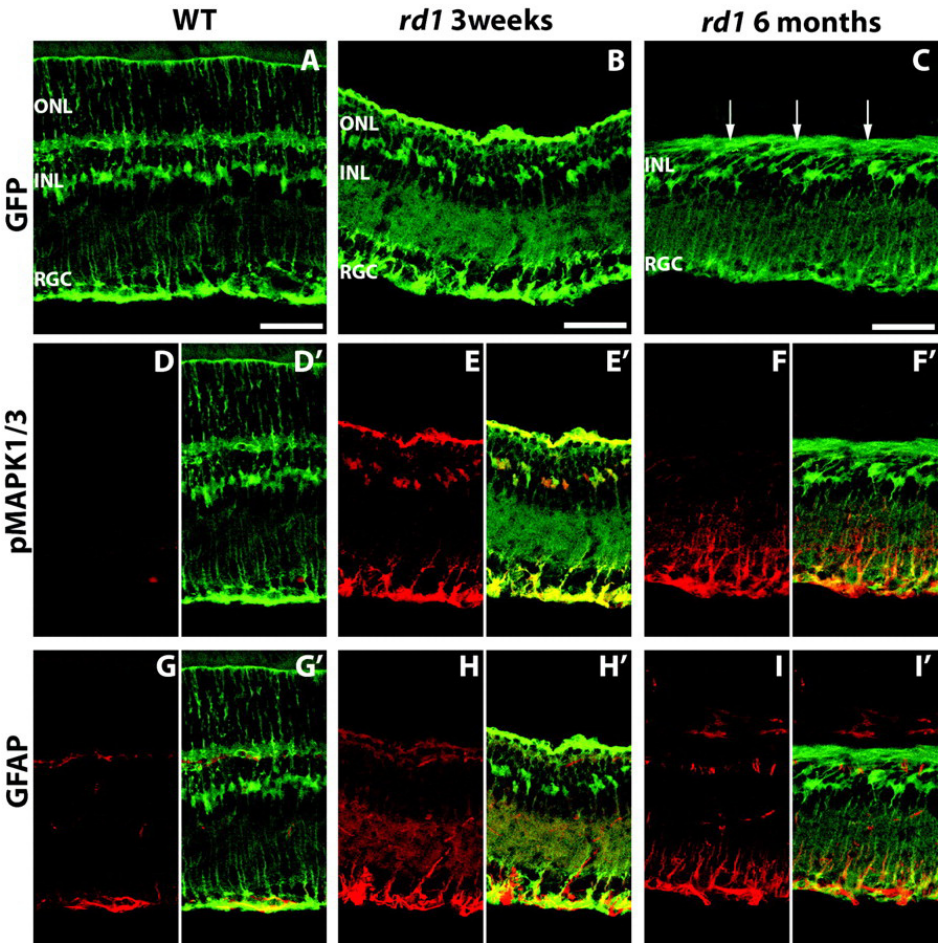

Robert Marc, Ph.D, joined the Research Faculty of the Moran Eye Center in 1993 after 15 years at the University of Texas at Houston, where he was the Robert Greer Professor of Biomedical Science. Dr. Marc's early research provided the first maps of the different color varieties of photoreceptors in the retina. It is now clear that it is this unique pattern of color sensitive cones which dictates many features of our perception of color and form. And as retinal disease inexorably disassembles the retina, these exquisite sensors are often among the first to fail.

After more than 30 years of continuous NIH funding, Dr. Marc's laboratory now exploits advanced molecular detection, imaging, and computational technologies to produce new, richer visualizations of neurons and how they are connected. These new approaches allow the Marc Laboratory to track disruptions in these connections triggered by retinal diseases such as retinitis pigmentosa and macular degeneration. The ultimate goal of this research is to learn enough about the assembly, function and disassembly of these networks to guide the development of strategies to repair defects triggered by retinal diseases.

A computational framework for ultrastructural mapping of neural circuitry.

Author: Anderson JR, Jones BW, Yang JH, Shaw MV, Matt CB, Koshevoy P, Spaltenstein J, Jurrus E, U V K, Whitaker RT, Mastronarde D, Tasdizen T, Marc RE

Journal: PLoS Biol. 2009 Mar;7(3):e1000074. Epub 2009 Mar 31.

ABSTRACT: Circuitry mapping of metazoan neural systems is difficult because canonical neural regions (regions containing one or more copies of all components) are large, regional borders are uncertain, neuronal diversity is high, and potential network topologies so numerous that only anatomical ground truth can resolve them. Complete mapping of a specific network requires synaptic resolution, canonical region coverage, and robust neuronal classification. Though transmission electron microscopy (TEM) remains the optimal tool for network mapping, the process of building large serial section TEM (ssTEM) image volumes is rendered difficult by the need to precisely mosaic distorted image tiles and register distorted mosaics Moreover, most molecular neuronal class markers are poorly compatible with optimal TEM imagine.

Our objective was to build a complete framework for ultrastructural circuitry mapping. This framework combines strong TEM-compliant small molecule profiling with automated image tile mosaicking, automated slice-to-slice image registration, and gigabyte-scale image browsing for volume annotation. Specifically we show how ultrathin molecular profiling datasets and their resultant classification maps can be embedded into ssTEM datasets and how scripted acquisition tools (SerialEM), mosaicking and registration (ir-tools), and large slice viewers (MosaicBuilder, Viking) can be used to manage terabyte-scale volumes.

These methods enable large-scale connectivity analyses of new and legacy data. In well-posed tasks (e.g., complete network mapping in retina), terabyte-scale image volumes that previously would require decades of assembly can now be completed in months. Perhaps more importantly, the fusion of molecular profiling, image acquisition by SerialEMM, ir-tools volume assembly, and data viewers/annotators also allow ssTEM to be used as a prospective tool for discovery in nonneural systems and a practical screening methodology for neurogenetics. Finally, this framework provides a mechanism for parallelization of ssTEM imaging, volume assembly, and data analysis across an international user base, enhancing the productivity of a large cohort of electron microscopists.

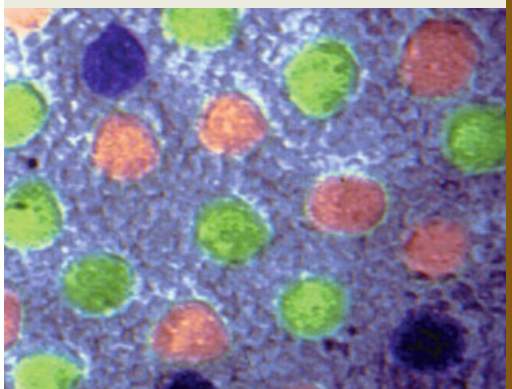

Retinal Remodeling.

Author: Marc RE.

The 114th Annual Meeting of the Japanese Ophthalmological Society

Motivation: We seek to understand the nature and scope of cellular remodeling in retinal degenerations such as RP, neovascular disease and AMD. The failure of neural integration is likely an early cause of vision loss and, ultimately, anomalous rewiring corrupts the surviving retina.

Methods: We combined advanced animal models (e.g. the transgenic P347L rabbit developed by Prof. Mineo Kondo, Nagoya University), new global molecular tagging methods, high-throughput imaging, functional imaging, computational molecular phenotyping and connectomics analysis.

Results: We have been screening response pathways triggered by photoreceptor stress and death in rodent, rabbit and human retinal degenerations and have discovered five major kinds of remodeling events. 1. Photoreceptor stress and death trigger reprogramming of retinal neurons. Retinal bipolar cells driven by dying rods switch their alliegences to cones but also switch their polarities from ON to OFF. 2. In regions of stressed retina that survive photoreceptor challenges, neurons show regulation of function. Upregulations in protective GluR2 receptor subunits and supression of non-protective GluR5 subunits, imply that the neural retina is highly plastic even in early degeneration. 3. After both rods and cones are lost, bipolar cells deconstruct their dendrites. 4. Many neurons generate new axons throughout photoreceptor degeneration and rewire into corruptive networks. The expression of retinoic acid signaling pathways may drive new this neurite growth. 5. Breakdown of the RPE-choriocapillaris interface not only permits vascular invasion, it allows Müller cells, surviving cone photoreceptors and neurons to emigrate into the choroid.

Conclusions: These tranformations show that human retinal degenerations are more than simple photoreceptor or RPE-vascular defects. The entire retina responds, similar to the brain's response to neurodegenerative challenges. It is clear that connectivity in the mature retina is as dynamically regulated as in adult hippocampus or cortex. This capacity to rewire challenges the abilities of cellular, bionic, molecular and genetic interventions to restore visual capacity. Remodeling is also an opportunity, as molecular techniques to guide and inform neurons may permit the generation of interfaces between the remnant retina and bionic devices.

Support: NIH, NSF, Research to Prevent Blindess.
Disclosure: REM is a principapl of Signature Immunologics.

Scalable Multiuser Annotation and Summarization of Large Terabyte Scale Volumes

Authors: Anderson J, Mohammed S, Marc, RE.

Janelia Farm Conference 2010. Turning Images to Knowledge: Large-Scale 3D Image Annotation, Management and Visualization conference.

ABSTRACT: Our group has assembled a suite of annotation and visualization tools as part of our project to reconstruct the rabbit retinal connectome. Our dataset is collected from both optical and transmission electron microscopy platforms and is composed of over 341,000 16 megapixel images registered into a volume. The Viking system is our solution to annotation and visualization of this multichannel multi-resolution data. Key features are support for simultaneous annotation by multiple users, user-defined annotation ontologies, an easily extensible user interface, and clean separation of hosting, viewing, and analysis functions. Its foundation is a three-tiered architecture with clients communicating to the middle-tier via HTTP. Performance is acceptable over a typical residential broadband connection. We have tested Viking with up to six users placing annotations concurrently and used this system to identify over 8000 unique structures and place over 180,000 annotations into our volume¸Äôs annotation database.

Our near-term goal is to provide web-based resources serving connectome data directly to the scientific community. All annotations can be accessed using a public web service. We have also developed a set of visualization web pages which access the web service to render morphology and high-level network diagrams.

Using the Viking system we have extensively mapped the AII amacrine cell network and discovered a number of novel AII connections, including inputs from ON cone bipolar cells and peptidergic / GABA+ amacrine cells, and outputs to OFF-layer GABA+ amacrine cells.

Our main connectome dataset was collected using serial section transmission electron microscopy (ssTEM) at an XY resolution of 2.18nm/pixel with a section thickness of 90 nm/section. The volume itself is 250Œºm in diameter and ~33Œºm tall. The cylinder begins at the inner nuclear layer, passes through the inner plexiform layer and terminates in the ganglion cell layer. Molecular identification of cell classes was embedded into the volume via periodic optical microscopy sections stained for several small molecules: GABA, Glycine, Glutamate, Glutamine, Taurine, Aspartate, and Agmatine.

Ning Tian, Ph.D, did graduate training at SUNY at Buffalo with Malcolm Slaughter focusing on synaptic transmission of retinal neurons and postdoctoral work with David Copenhagen at University of California San Francisco School of Medicine, working on developmental regulation of retinal synaptic circuitry. He was a faculty member at the UCSF, Dept of Ophthalmology for one year and a faculty member at Yale University, Department of Ophthalmology for nine years before joining the Moran Eye Center of the University of Utah in 2009.

The immune protein CD3z is required for normal development of neural circuits in the retina

Authors: Xu HP, Chen H, Ding Q, Xie ZH, Chen L, Diao L, Wang P, Gan L, Crair MC, Tian N.

Journal: Neuron. 2010 Feb 25; 65(4):503-15. Comment in: Neuron. 2010 Feb 25; 65(4):439-41.

ABSTRACT: Emerging evidence suggests that immune proteins regulate activity-dependent synapse formation in the central nervous system (CNS). Mice with mutations in class I major histocompatibility complex (MHCI) genes have incomplete eye-specific segregation of retinal ganglion cell (RGC) axon projections to the CNS. This effect has been attributed to causes that are nonretinal in origin.

We show that a key component of MHCI receptor, CD3z, is expressed in RGCs. CD3z-deficient mice have reduced RGC dendritic motility, an increase in RGC dendritic density, and a selective defect of glutamate-receptor-mediated synaptic activity in the retina. Disrupted RGC synaptic activity and dendritic motility is associated with a failure of eye-specific segregation of RGC axon projections to the CNS. These results provide direct evidence of an unrecognized requirement for immune proteins in the developmental regulation of RGC synaptic wiring and indicate a possible retinal origin for the disruption of eye-specific segregation found in immune-deficient mice.

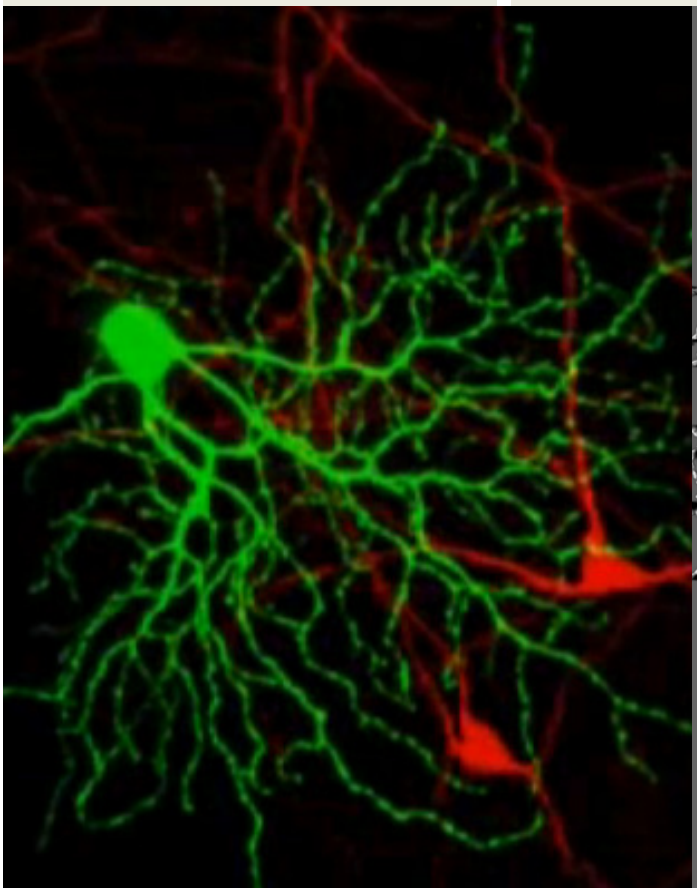

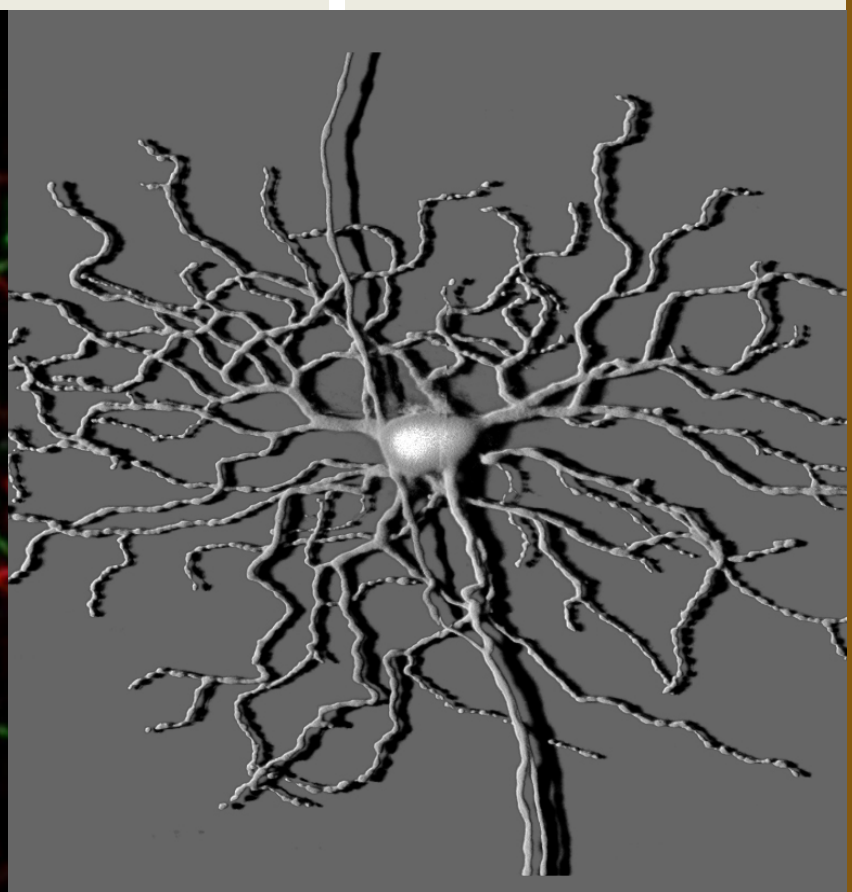

Angiogenesis Research

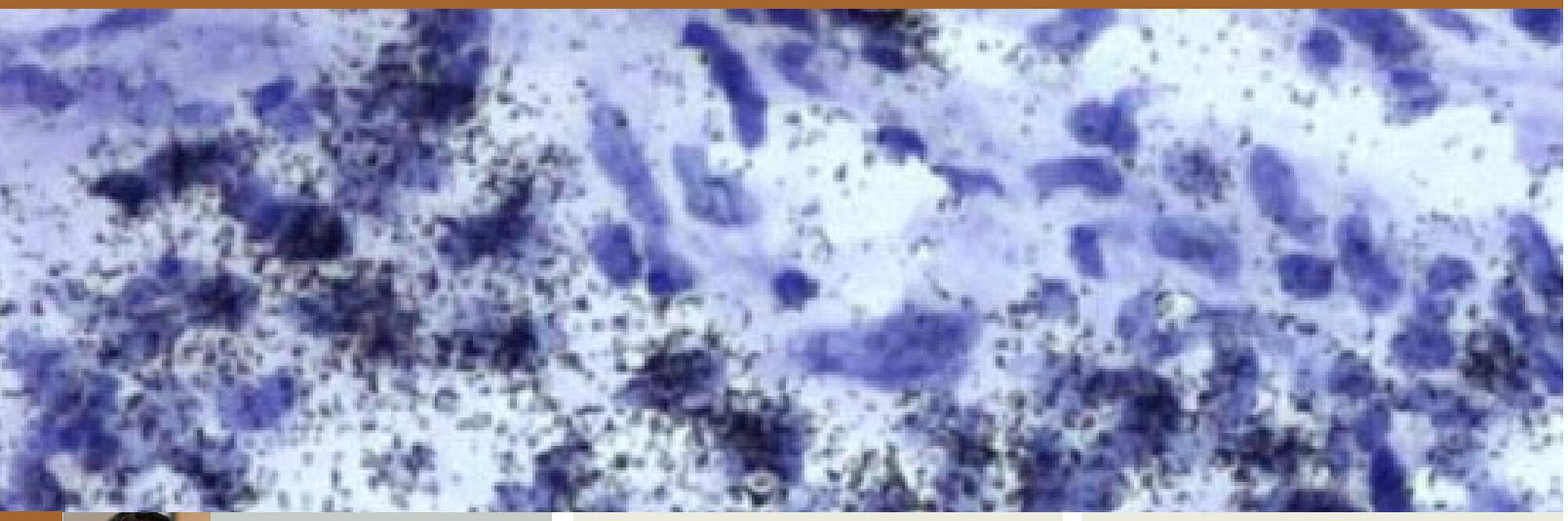

Balamurali Ambati, M.D., Ph.D.

Alternatively spliced vascular endothelial growth factor receptor-2 is an essential endogenous inhibitor of lymphatic vessel growth.

Author: Albuquerque RJ, Hayashi T, Cho WG, Kleinman ME, Dridi S, Takeda A, Baffi JZ, Yamada K, Kaneko H, Green MG, Chappell J, Wilting J, Weich HA, Yamagami S, Amano S, Mizuki N, Alexander JS, Peterson ML, Brekken RA, Hirashima M, Capoor S, Usui T, Ambati BK, Ambati J.

Journal: Nat Med. 2009 Sep;15(9):1023-30. Epub 2009 Aug 9. Comment in: Nat Med. 2009 Sep;15(9):993-4.

Disruption of the precise blanace of positive and negative molecular regulators of blood and lymphatic vessel growth can lead to myriad diseases. Although dozens of natural inhibitors of hemangiogenesis have been identified, an endogenous selective inhibitor of lymphatic vessel growth has not to our knowledge been previously desxribed. We report the existence of a splice variant of the gene encoding vascular endothelial growth factor receptor-2 (Vegfr-2) that encodes a secreted form of the protein, designeated solub le Vegfr-2 (sVegfr-2), that inhibits developmental and reparative lymphangiogenesis by blocking Vegf-c function. Tissue-specific loss of sVegfr-2 in mice induced, at birth, spontaneous lymphatic invasion of the normally alymphatic cornea and hyperplasia o skin lymphatics withut affecting blood vasculature.

Administration of sVegfr-2 inhibited lymphangiogenesis but not hemangiogenesis induced by corneal suture injury or transplantation enhanced corneal allograft survival and suppressed lymphangioma cellular proliferation. Naturally occurring sVegfr-2 thus acts as a molecular uncoupler of blood and lymphatic vessels; modulation of sVegfr-2 might have therapeutic effects in treating lymphatic vascular malformations, transplantation rejection and, potentially, tumor lymphangiogenesis and lymphedema (pages 993-994).

Mediators of ocular angiogenesis.

Authors: Qazi Y, Maddula S, Ambati BK.

Journal: J Genet. 2009 Dec;88(4):495-515.

ABSTRACT: Angiogenesis is the formation of new blood vessels from pre-existing vasculature. Pathologic angiogenesis in the eye can lead to severe visual impairment. In our review, we discuss the roles of both pro-angiogenic and anti-angiogenic molecular players in corneal angiogenesis, proliferative diabetic retinopathy, exudative macular degeneration and retinopathy of prematurity, highlighting novel targets that have emerged over the past decade.

Anti-SPARC oligopeptide inhibits laser-induced CNV in mice.

Authors: Uehara H, Luo L, Simonis J, Singh N, Taylor EW, Ambati BK.

Journal: Vision Res. 2010 Mar 31;50(7):674-9. Epub 2009 Dec 22.

ABSTRACT: It is known that SPARC gates VEGF-A signal transduction towards KDR, the primary angiogenic VEGF receptor. We sought to determine whether inhibition of SPARC activity using anti-SPARC peptide could inhibit laser-induced CNV by promoting binding of VEGF-A to FLT-1. We created anti-SPARC l-peptide and retro-inverso anti-SPARC d-peptide. Anti-SPARC peptides or PBS were injected intravitreally 1day before or after laser induction. Intravitreal injection of anti-SPARC l-peptide 1day before laser induction promotes FLT-1 phosphorylation and inhibited laser-induced CNV and anti-SPARC d-peptide had no effect. Injection 1day after laser injury did not affect size of laser-induced CNV. Inhibition of SPARC activity could be complementary to existing anti-CNV therapy.

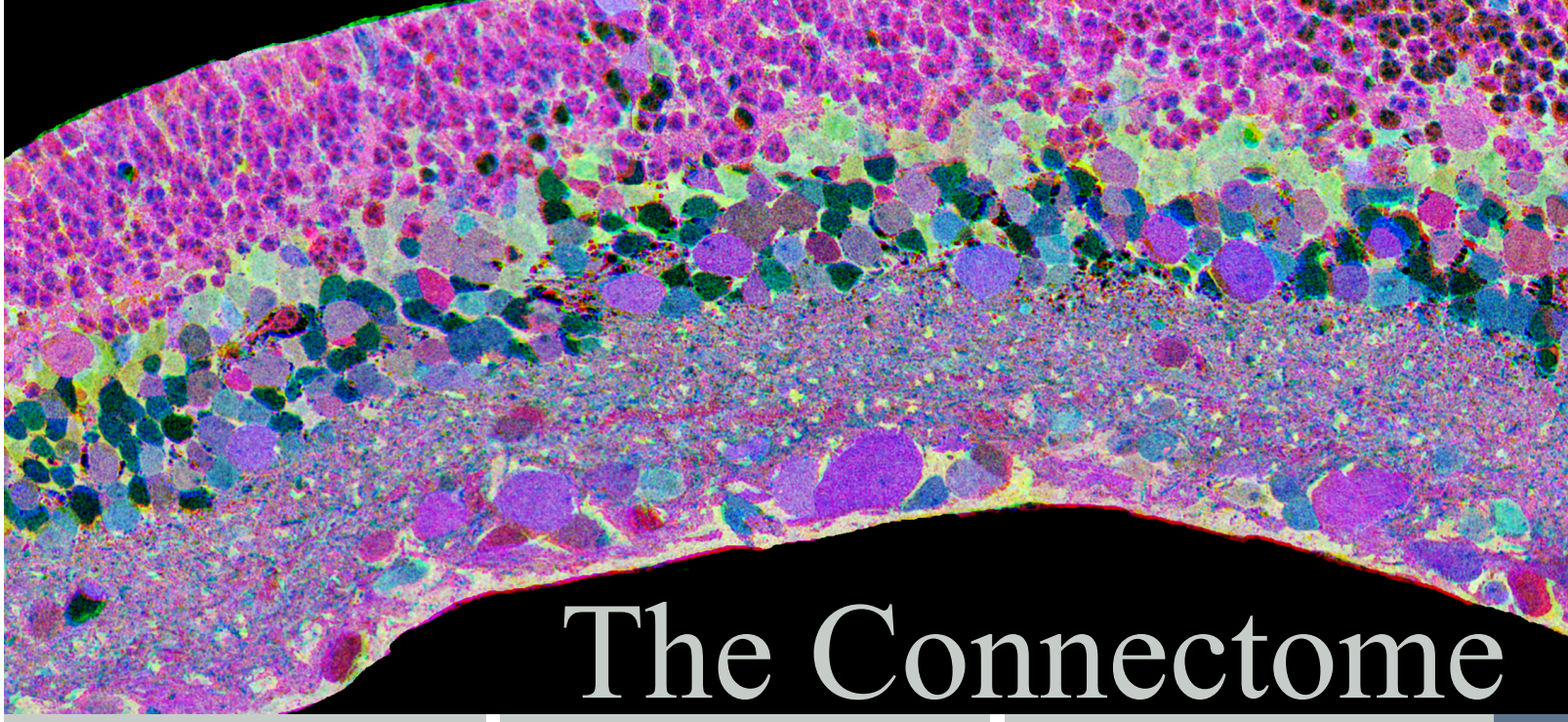

The Connectome

Putting the puzzle together

Despite substantial advances in neuroscience and medical technology, millions of Americans still suffer from blindness due to retinal degenerative diseases such as retinitis pigmentosa (RP), age-related macular degeneration (AMD), diabetic retinopathy, and glaucoma. Treatments for advanced forms of these conditions are severely limited by incomplete knowledge of associated changes in the neural retina. Efforts at the Moran Eye Center are underway to discover and describe in detail how the normal cellular networks of the eye are transformed in disease.

Over the past ten years, the Marc laboratory the Moran Eye Center has shown that RP (and possibly AMD) trigger anomalous rewiring that corrupts retinal networks and visual information processing. But with these discoveries came the realization that our knowledge of normal retinal wiring largely generic. Understanding the topological details of cellular associations and retinal networks may be essential to informing bionic, cellular and molecular strategies for rescuing advanced vision loss. Some strategies may include molecular blockade of rewiring in disease or re-patterning of ongoing rewiring in parallel with bionic or biological interventions.

The retina is a light capture and signal processing device. The scale and richness of that signal processing has made retinal network analysis challenging for many generations of scientists. Even a simple human retina contains about 70 different kinds of cells, with thousands to millions of copies of each, and up to hundreds of connections for each. We believe that each cell forms precise patterns of connections with specific partners and that hidden in these patterns are the image processing operations that create the roughly 20 different versions of the visual world that the retina transmits to our brains.

Many laboratories worldwide have contributed to our current understanding of the the patterns of cells and connections in the retina. The Marc laboratory is seeking to produce a complete catalogue of retinal neurons and a comprehensive map of their connections. While a human retina could potentially form over 100,000 unique networks, it appears that only about 20 are used. The question is: which ones? One powerful way to determine this is by high-density tracing of the connections of all the cells in a retinal region: an approach known as connectomics. Building a retinal connectome means that, for the first time, we will really know how certain image processing networks in the retina are constructed.

Many groups worldwide are pursuing similar aims for retina, fly brains, worm nerve cords, mammalian muscle innervation and now brain regions. The Utah project brings together teams of scientists and fuses new computational approaches with existing imaging technologies, to meet one of the longstanding grand challenges in neu-

roscience, the detailed elucidation of natural neural network. Indeed, the key technologies for mapping retinal structures have existed for decades, but only recently have computational power and data storage densities permitted projects of this scope. These approaches are enabling a revolution in microscopy that will lead to a seachange not just in retinal neuroscience, but in all areas of biology.

A matter of scale and sharing

Until recently, methods used to reconstruct even small portions of retina were extraordinarily time consuming and exceedingly labor intensive. The process, championed by the Sterling, Raviola and Kolb labs, is known as serial-section transmission electron microscopy (ssTEM) and involves slicing a sample of tissue into a series of extremely thin layers and then imaging each slice with an electron microscope. While new technologies for automated sectioning and imaging are emerging, ssTEM remains the gold standard in resolution. The problem has been the inability to capture large areas at high speed. But the allure of building a volume that could contain the ground truth for every kind of neuron in the retina was intense and inspired Dr. Marc and collaborators at the University of Utah Scientific Computing and Imaging (SCI) Institute at the University of Utah to create new software for a completely automated pipeline of image capture and volume assembly. The collaborative team included Dr. Robert Marc, Dr. Bryan Jones, Dr. Carl Watt, graduate student James Anderson, histologist Jia-Hui Yang, and immunochemist Maggie Shaw, all at the Moran Eye Center; Dr. Tolga Tasdizen, Dr. Ross Whitaker, graduate students Elizabeth Jurrus and developers Pavel Koshevoy and Bradley Grimm at SCI; and Dr. David Mastronarde at the Boulder Center for 3D Electron Micrscopy. These new automation technologies now drive a JEOL JEM-1400 transmission electron microscope, purchased with a generous gift from one of our donors, Ms. Martha Ann Healy. This system now permits capture of millimeter-scale structures at nanometer-scale resolution.

A number of retinal connectomes, from normal and pathologic tissue, have been or are being captured. One complete retinal dataset, RC1, represents 16.5 terabytes of raw data; 341,000 individual images of over 371 ultrathin sections of retina. About 10% of the data have been mapped in a little over a year, but the volume has already revealed many unexpected features of organization. The outcomes of these retinal reconstruction projects will be manifold, but one important feature is that these data, resources and tools are free and available to all. Such tissue maps, which lay the technology foundations to more precisely study retinal disease, also open the door for other scientists to explore structural biological questions in cancer, epilepsy, heart disease and diabetes.

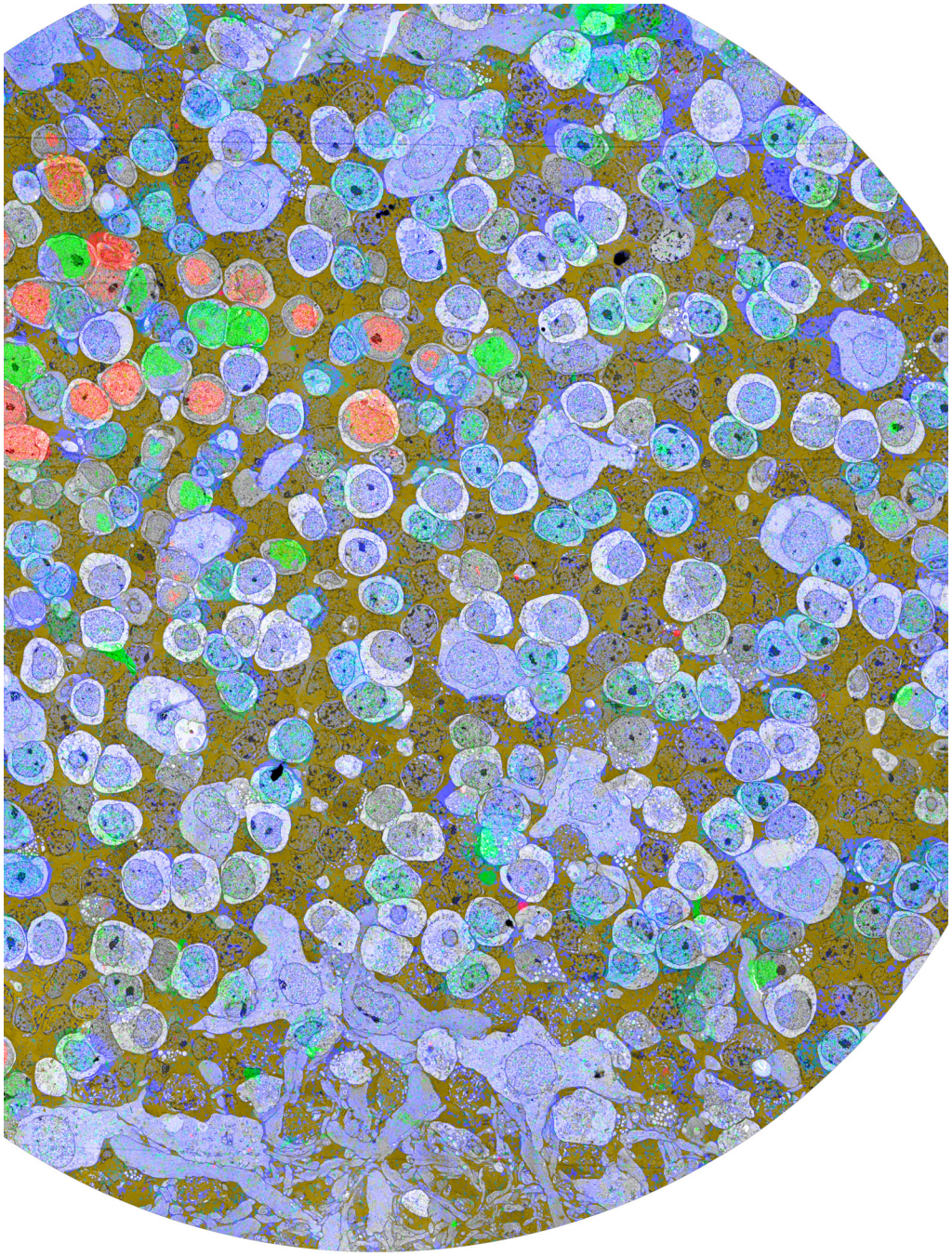

Visual Cortex Research

Alessandra Angelucci, M.D., Ph.D. Dr. Angelucci's research focuses on identifying neuronal circuits that underlie functional properties of neurons in the visual cerebral cortex and, ultimately, visual perception. The laboratory uses electrophysiological recording of cortical neurons and co-injecting neuroanatomical tracers to map neuronal response properties onto the underlying anatomical structure. To determine the broader functional organization of specific cortical circuits, optical imaging of neuronal populations is combined with injections of anatomical tracers.

Comparison of spatial summation properties of neurons in macaque V1 and V2.

Author: Shushruth S, Ichida JM, Levitt JB, Angelucci A.

Journal: J Neurophysiol. 2009 octo;102(4):2069-83. Epub 2009 Aug 5.

ABSTRACT: In visual cortex, responses to stimulation of the receptive field (RF) are modulated by simultaneous stimulation of the RF surround. The mechanisms for surround modulation remain unidentified. We previously proposed that in the primary visual cortex (V1), near surround modulation is mediated by geniculocortical and horizontal connections and far surround modulation by interareal feedback connections.

To understand spatial integration in the secondary visual cortex (V2) and its underlying circuitry, we have characterized spatial summation in different V2 layers and stripe compartments and compared it to that in V1. We used grating stimuli in circular and annular apertures of different sixes to estimate the extent and sensitivity of RF and surround components in V1 and V2. V2 RFs and surrounds were twice as large as those in V1. As in V1, V2 RFs doubled in size when measured at low contrast.

In both V1 and V2, surrounds were about fivefold the size of the RF and the far surround could exceed 12.5 degrees in radius, averaging 5.5 degrees in V1 and 9.2 degrees in V2. The strength of surround suppression was similar in both areas. Thus although differing in spatial scale, the interactions among RF components are similar in V1 and V2, suggesting similar underlying mechanisms. As in V1, the extent of V2 horizontal connections matches that of the RF center, but is much smaller than the largest far surrounds, which likely derive from interareal feedback. IN V2, we found no laminar or stripe differences in size and magnitude of surround suppression, suggesting conservation across stripes of the basic circuit for surround modulation.

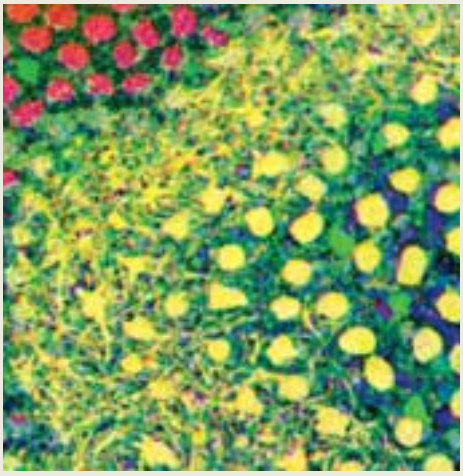

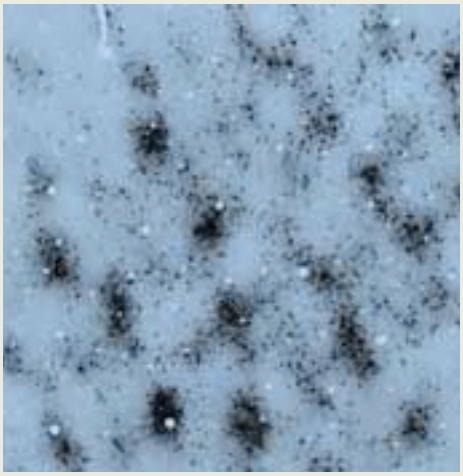

Anatomical evidence for classical and extra-classical receptive field completion across the discontinuous horizontal meridian representation of primate area V2.

Author: Jeffs J, Ichida JM, Federer F, Angelucci A.

Journal: Cereb Cortex. 2009 Apr;19(4):963-81. Epub 2008 Aug 28.

ABSTRACT: In primates, a split of the horizontal meridian (HM) repesentation at the V2 rostral border divides this area into dorsal (V2d) and ventral (V2v) halves (representing lower and upper visual quadrants, respectively), causing retinotopically neighboring loci across the HM to be distant within V2. How is perceptual continuity maintained across this discontinuous HM representation? Injections of neuroanatomical tracers in marmoset V2d demonstrated that cells near the V2d rostral border can maintain retinotopic continuity within their classical and extraclassical receptive field (RF), by making both local and long-range intra- and interareal connections with ventral cortex representing the upper visual quadrant.

Contrast-dependence of surround suppression in Macaque V1: Experimental testing of a recurrent network model.

Authors: Schwabe L, Ichida JM, Shushruth S, Mangapathy P, Angelucci A.

Journal: Neuroimage. 2010 Jan 15.

ABSTRACT: Neuronal responses in primary visual cortex (V1) to optimally oriented high-contrast stimuli in the receptive

field (RF) center are suppressed by stimuli in the RF surround, but can be facilitated when the RF center is stimulated at low contrast. The neural circuits and mechanisms for surround modulation are still unknown. We previously proposed that topdown feedback connections mediate suppression from the "far" surround, while "near' surround suppression is mediated primarily by horizontal connections. We implemented this idea in a recurrent network model of V1. A model assumption needed to account for the contrast-dependent sign of surround modulation is a response asymmetry between excitation and inhibition; accordingly, inhibition, but not excitation, is silent for weak visual inputs to the RF center, and surround stimulation can evoke facilitation. A prediction stemming from this same assumption is that surround suppression is weaker for low than for high contrast stimuli in the RF center. Previous studies are inconsistent with this prediction. Using single unit recordings in macaque V1, we confirm this model's prediction. Model simulations demonstrate that our results can be reconciled with those from previous studies. We also performed a systematic comparison of the experimentally measured surround suppression strength with predictions of the model operated in different parameter regimes. We find that the original model, with strong horizontal and no feedback excitation of local inhibitory neurons, can only partially account quantitatively for the experimentally measured suppression. Strong direct feedback excitation of V1 inhibitory neurons is necessary to account for the experimentally measured surround suppression strength.

Four projection streams from primate V1 to the cytochrome oxidase stripes of V2.

Authors: Federer F, Ichida JM, Jeffs J, Schiessl I, McLoughlin N, Angelucci A.

Journal: J Neurosci. 2009 Dec 9;29(49):15455-71.

ABSTRACT: In the primate visual system, areas V1 and V2 distribute information they receive from the retina to all higher cortical areas, sorting this information into dorsal and ventral streams. Therefore, knowledge of the organization of projections between V1 and V2 is crucial to understand how the cortex processes visual information. In primates, parallel output pathways from V1 project to distinct V2 stripes. The traditional tripartite division of V1-to-V2 projections was recently replaced by a bipartite scheme, in which thin stripes receive V1 inputs from blob columns, and thick and pale stripes receive common input from interblob columns. Here, we demonstrate that thick and pale stripes, instead, receive spatially segregated V1 inputs and that the interblob is partitioned into two compartments: the middle of the interblob projecting to pale stripes and the blob/interblob border region projecting to thick stripes. Double-labeling experiments further demonstrate that V1 cells project to either thick or pale stripes, but rarely to both. We also find laminar specialization of V1 outputs, with layer 4B contributing projections mainly to thick stripes, and no projections to one set of pale stripes. These laminar differences suggest different contribution of magno, parvo, and konio inputs to each V1 output pathway. These results provide a new foundation for parallel processing models of the visual system by demonstrating four V1-to-V2 pathways: blob columns-to-thin stripes, blob/interblob border columns-to-thick stripes, interblob columns-to-pale(lateral) stripes, layer 2/3-4A interblobs-to-pale(medial) stripes.

Implants Research

Richard Normann, Ph.D, received the B.S., M.S., and Ph.D. degrees from the University of California, Berkeley, where he used intracellular recording techniques to study rod and cone light- and dark-adaptation. At the National Institute of Health he studied the mechanisms of gain control and signal transmission in the vertebrate retina. In 1979 he moved to the Departments of Bioengineering and Ophthalmology at the University of Utah where his interests broadened and encompassed the encoding of sensory and motor information by neural ensembles in the cerebral cortex and the vertebrate retina, and the conduct of feasibility studies for motor and sensory neuroprostheses. Recent work is focused on the development of a cortically based visual neuroprosthesis for those with profound blindness.

Automated stimulus-response mapping of high-electrode-count neural implants.

Author: Wilder AM, Hiatt SD, Dowden BR, Brown NA, Normann RA, Clark GA.

Journal: IEEE Trans Neural Syst Rehabil Eng. 2009 Oct;17(5):504-11. Epub 2009 Aug 7

ABSTRACT: Over the past decade, research in the field of functional electrical stimulation (FES) has led to a new generation of high-electrode-count (HEC) devices that offer increasingly selective access to neural populations. Incorporation of these devices ito research and clinical applications, however has been hampered by the lack of hardware and software plat-

forms capable of taking full advantage of them. IN this paper, we present the first generation of a closed-loop FES platform built specifically for HEC neural interface devices.

The platform was designed to support a wide range of stimulus-response mapping and feedback-based control routines. It includes a central control module, a 1100-channel stimulator, an array of biometric devices, and a 160-channel data recording module. To demonstrate the unique capabilities of this platform, two automated software routines for mapping stimulus-response properties of implanted HEC devices were implemented and tested. The first routine determines stimulation levels that produce perithreshold muscle activity, and the second generates recruitment curves (as measure by peak impulse response). Both routines were tested on 100—electrode Utah Slanted Electrode Arrays (USEAs) implanted in cat hindlimb nerves using joint torque or emg as muscle output metric. Mean time to map perithreshold stimulus level was 16.4 s for electrodes that evoked responses (n = 3200), and 3.6 s for electrodes that did not evoke responses (n = 1800). Mean time to locate recruitment curve asymptote for an electrode (n = 155) was 9.6 s , and each point in the recruitment curve required 0.87 s. These results demonstrate the utility of our FES platform by showing that it can be used to completely automate a typically time- and effort-intensive procedure associated with using HEC devices.

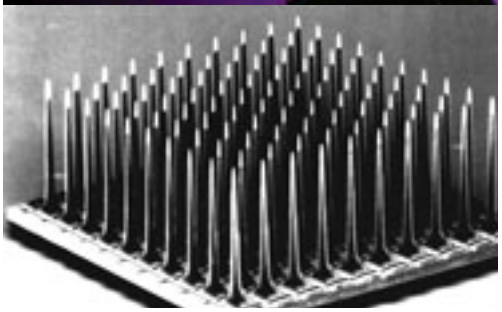

Developmental Research

Sabine Fuhrmann, Ph.D, received her Ph.D. from the University of Freiburg in Germany and postdoctoral training at the University of Washington/Seattle, investigating the role of tissue-tissue interactions during early eye development. In 2000, she joined the faculty at the Moran Eye Center. Her laboratory studies the role of extra cellular signaling pathways in regulating patterning and differentiation of ocular tissues such as the neural retina and pigmented epithelium. The molecular signals that mediate these patterning events are largely unknown. Multiple congenital eye disorders, including anophthalmia, micropthalmia, aniridia, coloboma, and retinal dysplasia, stem from disruptions in early eye development. It is thus critical to define the signals that regulate normal patterning and development of the optic vesicle. The goal of Dr. Fuhrmann's research is to elucidate the cellular and molecular mechanisms that regulate the patterning and differentiation of ocular tissues using chick and mouse as model organisms.

β-catenin controls differentiation of the retinal pigment epithelium in the mouse optic cup by regulating Mitf and Otx2 expression

Authors: Westenskow P, Piccolo S, Fuhrmann S.

Journal: Development 136, 2505-2510 (2009) doi:10.1242/dev.032136

ABSTRACT: The retinal pigment epithelium (RPE) consists of a monolayer of cuboidal, pigmented cells that is located between the retina and the choroid. The RPE is vital for growth and function of the vertebrate eye and improper development results in congenital defects, such as microphthalmia or anophthalmia, or a change of cell fate into neural retina called transdifferentiation. The transcription factors microphthalmia-associated transcription factor (Mitf) and orthodenticle homolog 2 (Otx2) are crucial for RPE development and function; however, very little is known about their regulation. Here, by using a Wnt-responsive reporter, we show that the Wnt/β-catenin pathway is activated in the differentiating mouse RPE. Cre-mediated, RPE-specific disruption of β-catenin after the onset of RPE specification causes severe defects, resulting in microphthalmia with coloboma, disturbed lamination, and mislocalization of adherens junction proteins. Upon β-catenin deletion, the RPE transforms into a multilayered tissue in which the expression of Mitf and Otx2 is downregulated, while retina-specific gene expression is induced, which results in the transdifferentiation of RPE into retina. Chromatin immunoprecipitation (ChIP) and luciferase assays indicate that β-catenin binds near to and activates potential TCF/LEF sites in the Mitf and Otx2 enhancers.

We conclude that Wnt/β-catenin signaling is required for differentiation of the RPE by directly regulating the expression of Mitf and Otx2. Our study is the first to show that an extracellular signaling pathway directly regulates the expression of RPE-specific genes such as Mitf and Otx2, and elucidates a new role for the Wnt/β-catenin pathway in organ formation and development.

Characterization of a Transient TCF/LEF-Responsive Progenitor Population in the Embryonic Mouse Retina

Authors: Fuhrmann S, Riesenberg AN, Mathiesen AM, Brown EC, Vetter ML, Brown NL.

Journal: Invest Ophthalmol Vis Sci. 2009;50:432–440

Purpose. High mobility group (HMG) transcription factors of the T-cell-specific transcription factor/lymphoid enhancer binding factor (TCF/LEF) family are a class of intrinsic regulators that are dynamically expressed in the embryonic mouse retina. Activation of TCF/LEFs is a hallmark of the Wnt/β-catenin pathway, however, the requirement for Wnt/β-catenin and noncanonical Wnt signaling during mammalian retinal development remains unclear. Our goal was to characterize more fully a TCF/LEF-responsive retinal progenitor population in the mouse embryo, and to correlate this with Wnt/β-catenin signaling. Methods. TCF/LEF activation was analyzed in the TOPgal reporter mouse (TOP: TCF optimal promoter) at embryonic ages and compared to Axin2 mRNA expression, an endogenous readout of Wnt/β-catenin signaling. Reporter expression was also examined in embryos with a retina-specific deletion of the β-catenin gene (Ctnnb1), using Six3-Cre transgenic mice. Finally, the extent to which TOPgal cells coexpress cell cycle proteins, basic-helix-loop-helix (bHLH) transcription factors and other retinal cell type markers was tested by double-immunohistochemistry. Results. TOPgal reporter activation occurs transiently in a subpopulation of embryonic retinal progenitor cells. Axin2 is not expressed in the central retina, and TOPgal reporter expression persists in the absence of β-catenin. Although a proportion of TOPgal-labeled cells are proliferative, most coexpress the cyclin-dependent kinase inhibitor p27/Kip1. Conclusions. TOPgal cells give rise to the four earliest cell types: ganglion cells, amacrines, horizontals and photoreceptors. TCF/LEF activation in the central retina does not correlate with Wnt/β-catenin signaling, pointing to an alternate role for this transcription factor family during retinal development.

Edward M. Levine, Ph.D.

Lhx2 links the intrinsic and extrinsic factors that control optic cup formation.

Author: Yun S., Saijoh Y, Hirokawa KE, Kopinke D, Murtaugh LC, Monuki ES, Levine EM.

Journal: Development. 2009 Dec;136(23):3895-906.

ABSTRACT: A crucial steop in eye organogensesis is the transition of the optic vesicle into the optic cup. Several transcription factors and extracellular signals mediate this transition, but whether a single factor links them into a common genetic network is unclear. Here, we provide evidence that the LIM homeobox gene Lhx2, which is expressed in the optic neuroepitheliaum, fulfils such a role. In Lhx2 (-/-) mouse embryos, eye field specification and optic vesicle morphogenesis occur, but development arrests prior to optic cup formatin in both the optic neuroepithelium and lens ectoderm. This is accompanied by failure to maintain or initiate the expression patterns of optic-vesicle-patterning and lens-inducing determinants. Of the signaling pathways examined, only BMP signaling is noticeably altered and Bmp4 and Bmp7 mRNAs are undetectable. Lhx2(-/-) optic vesicles and lens ectoderm upregulate Pax2, Fgf15 and Sox2 in response to BMP treatments, and Lhx2 genetic mosaics reveal that transcription factors, including Vsx2 and Mitf, require Lhx2 cell-autonomously for their expression.

Our data indicate that Lhx2 is required for optic vesicle patterning and lens formation in part by regulating BMP signaling in an autocrine manner in the optic neuroepithelium and in a paracrine manner in the lens ectoderm. We propose a model in which Lhx2 is a central link in a genetic network that coordinates the multiple pathways leading to optic cup formation.

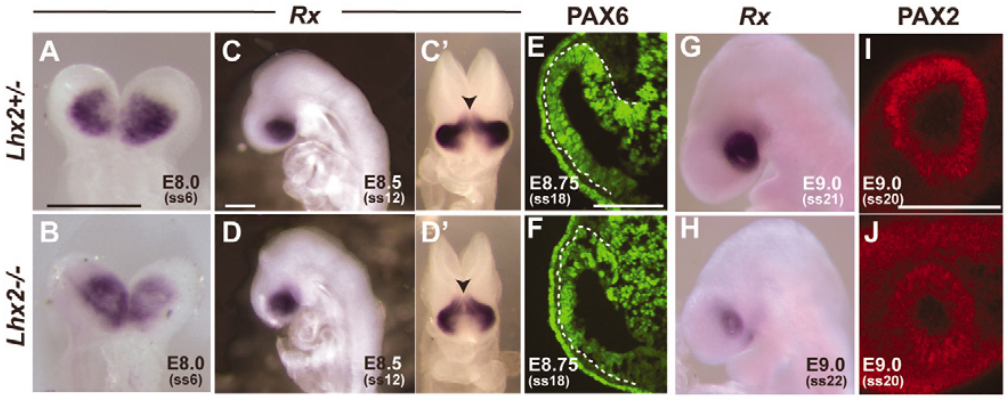

Eye field specification initiates normally in the absence of Lhx2, but the patterns of the EFTFs are altered during optic vesicle maturation. (A-D) Rx mRNA expression at ss6 and ss12. Arrowheads (C,D) indicate a lack of Rx expression at the midline. (A,B,C,D) Frontal views; (C,D) lateral views. The image in D is reflected on the vertical axis. (E,F)PAX6 protein expression at ss18. (G,H)Rx mRNA expression at ss21-22. (I,J)Single-scan confocal images of PAX2 expression at ss20.

Cyclin D1 fine-tunes the neurogenic output of embryonic retinal progenitor cells.

Author: Das G, Choi Y, Sicinski P, Levine EM.
Journal: Neural Dev. 2009 May;4:15.

BACKGROUND: Maintaining the correct balance of proliferation versus differentiation in retinal progenitor cells (RPSs) is essential for proper development of the retina. The cell cycle regulator cyclin D1 is expressed in RPCs, and mice with a targeted null allele at the cyclin D1 locu (Ccnd1-/-) have microphthalmia and hypocellulare retinas, the latter phenotype attributed to re-

duced RPC proliferation and increased photoreceptor cell death during the postnatal period. How cyclin D1 influences RPC behavior, especially during the embryonic period, is unclear.

RESULTS: In this study, we show that embryonic RPCs lacking cyclin D1 progress through the cell cycle at a slower rate and exit the cell cycle at a faster rate. Consistent with enhanced cell cycle exit, the relative proportions of cell types born in the embryonic period, such as retinal ganglion cells and photoreceptor cells, are increased. Unexpectedly, cyclin D1 deficiency decreases the proportions of other early born retinal neurons, namely horizontal cells and specific amacrine cell types. We also found that the laminar positioning of horizontal cells and other cell types is altered in the absence of cyclin D1. Genetically replacing cyclin D1 with cyclin D2 is not efficient at correcting the phenotypes due to the cyclin D1 deficiency, which suggests the D-cyclins are not fully redundant. Replacement with cyclin E or inactivation of cyclin-dependent kinase inhibitor p27Kip1 restores the balance of RPCs and retinal cell types to more normal distributions, which suggests that regulation of the retinoblastoma pathway is an important function for cyclin D1 during embryonic retinal development.

CONCLUSION: Our findings show that cyclin D1 has important roles in RPC cell cycle regulation and retinal histogenesis. The reduction in the RPC population due to a longer cell cycle time and to an enhanced rate of cell cycle exit are likely to be the primary factors driving retinal hypocellularity and altered output of precursor populations in the embryonic Ccnd1-/- retina.

Neuro-Ophthalmology Research

Kathleen B. Digre, M.D., specializes in neuro-ophthalmology. She evaluates and treats complex visual complaints which can be due to optic nerve or brain disease. Her interests include gender differences in neuro-ophthalmic disorders, pseudotumor cerebri, ischemic optic neuropathy, temporal arteritis, papilledema, episodic vision loss, headaches and eye pain, diplopia and Graves' Disease. She has worked with NANOS and the University Eccles Library to develop a Neuro-ophthalmology virtual educational library (NOVEL).

Bradley J. Katz, M.D., Ph.D, specializes in neuro-ophthalmology, and comprehensive ophthalmology. He also evaluates patients with diseases that affect the optic nerve, diseases that affect eye movements, and diseases of the brain that affect vision. Dr. Katz is also the principal investigator for a research grant from the National Institutes of Health to study optic nerve drusen.

A neural mechanism for exacerbation of headache by light.

Authors: Noseda R, Kainz V, Jakubowski M, Gooley JJ, Saper CB, Digre KB, Burstein R.

Journal: Nat Neurosci. 2010 Feb;13(2):239-45. Epub 2010 Jan 10.
Comment in: Nat Neurosci. 2010 Feb;13(2):150-1.

ABSTRACT: The perception of migraine headache, which is mediated by nociceptive signals transmitted from the cranial dura mater to the brain, is uniquely exacerbated by exposure to light. We found that exacerbation of migraine headache by light is prevalent among blind individuals who maintain non-image-forming photoregulation in the face of massive rod/cone degeneration. Using single-unit recording and neural tract tracing in the rat, we identified dura-sensitive neurons in the posterior thalamus whose activity was distinctly modulated by light and whose axons projected extensively across layers I-V of somatosensory, visual and associative cortices. The cell bodies and dendrites of such dura/light-sensitive neurons were apposed by axons originating from retinal ganglion cells (RGCs), predominantly from intrinsically photosensitive RGCs, the principle conduit of non-image-forming photoregulation. We propose that photoregulation of migraine headache is exerted by a non-image-forming13

Neuro-ophthalmologic manifestations of benign anterior skull base lesions.

Authors: Hornyak M, Digre K, Couldwell WT.

Journal: Postgrad Med. 2009 Jul;121(4):103-14.

ABSTRACT: Visual disturbance is a common presenting symptom of anterior skull base lesions. These lesions cause deterioration in visual acuity, restriction of the visual field, or reduction of ocular mobility. Common pathological entities that affect the skull base and involve vision include meningioma, pituitary adenoma, tumors of the bone, malignancy, and infection. Benign lesions are typically treated surgically with acceptable long-term results. In this article, we review the presentation, evaluation, and surgical treatment of patients with benign skull base lesions presenting with visual disturbance.

FL-41 tint improves blink frequency, light sensitivity, and functional limitations in patients with benign essential blepharospasm.

Authors: Blackburn MK, Lamb RD, Digre KB, Smith AG, Warner JE, McClane RW, Nandedkar SD, Langeberg WJ, Holubkov R, Katz BJ.

Journal: Ophthalmology. 2009 May;116(5):997-1001.

OBJECTIVE: The objective of these 2 studies was to assess the efficacy of FL-41-tinted lenses in the treatment of benign essential blepharospasm (BEB).

DESIGN: A randomized crossover study and a randomized crossover case-control study.

PARTICIPANTS: The first study included 30 subjects with BEB. The second study included 26 subjects with BEB and 26 controls.

METHODS: For the first study, subjects were randomized to wear either FL-41 or gray-tinted lenses for 2 weeks. After a 2-week washout period, the other lens was worn for 2 weeks. Questionnaires were completed at baseline, after the first lens, and after the second lens. In the second study, surface electromyography (EMG) was used to measure blink frequency, duration, and force while subjects read and wore FL-41, rose, or gray-tinted lenses.

MAIN OUTCOME MEASURES: Questionnaires were used to assess perceptions of light sensitivity and the effect of light sensitivity on activities of daily living (ADL). EMG was used to measure blink frequency, duration, and force.

RESULTS: Most participants observed improvement while wearing both FL-41 and gray-tinted lenses. FL-41-tinted lenses provided superior improvement in the areas of reading, fluorescent light sensitivity, overall light sensitivity, blepharospasm frequency, and blepharospasm severity. FL-41 lenses reduced mean blink rate compared with both rose and gray-tinted lenses, and reduced eyelid contraction force compared with rose-tinted lenses.

CONCLUSIONS: FL-41 lenses provided both subjective and objective benefit to subjects with BEB. Physicians should consider recommending this noninvasive and inexpensive lens tint to patients with BEB.

A comparison of idiopathic intracranial hypertension with and without papilledema.

Author: Digre KB, Nakamoto BK, Warner JE, Langeberg WJ, Baggaley SK, Katz BJ.

Journal: Headache. 2009 Feb;49(2):185-93

OBJECTIVE: To compare clinical features, visual characteristics, and treatment of idiopathic intracranial hypertension patients with and without papilledema.

BACKGROUND: Idiopathic intracranial hypertension does not often occur without papilledema. This study estimates the prevalence and compares the clinical characteristics of idiopathic intracranial hypertension patients with and without papilledema.

METHODS: We performed a cross-sectional analysis of all idiopathic intracranial hypertension patients diagnosed at the University of Utah Neuro-Ophthalmology Unit between 1990 and 2003. Patient records were reviewed for presence of papilledema and other signs, symptoms, and treatment characteristics. Each patient without papilledema was matched to the patient with papilledema who was closest to his/her age and sex. McNemar's and Wilcoxon-signed rank sum tests were used to compare characteristics between matched pairs.

RESULTS: Among all patients (n = 353), the prevalence of those without papilledema was 5.7% (n = 20). Patients without papilledema reported photopsias (20%), and were found to have spontaneous venous pulsations (75%), and non-physiologic visual field construction (20%) more often than did those with papilledema. Mean opening pressure, although above normal, was lower in patients without papilledema (mean = 309 mm cerebrospinal fluid) compared with those with papilledema (mean = 373 mm cerebrospinal fluid, kP = .031). Idiopathic intracranial hypertension patients without papilledema had more frequent diagnostic lumbar punctures than did patients with papilledema. Visual acuities and treatment were similar between groups.

CONCLUSIONS: The clinical presentation of idiopathic intracranial hypertension without papilledema is only somewhat different from that of idiopathic intracranial hypertension with papilledema. The lower the opening pressure in patients without papilledema may explain variations in symptoms and signs between the 2 gropus. When there are visual field changes in idiopathic intracranial hypertension without papilledema, non-physiologic visual loss should be considered.

Giant cell arteritis and mortality.

Author: Crow RW, Katz BJ, Warner JE, Alder SC, Zhang K, Schulman S, Digre KB.

Journal: J Gerontol A Biol Sci Med Sci. 2009 Mar;64(3):365-9 Epub 2009 Feb 4

BACKGROUND: Giant cell arteritis (GCA) is a systemic vasculitis of elderly individuals associated with significant mobidity, including blindness, stroke, and myocardial infarction. Previous studies have investigated whether GCA is associated with increased mortality, with conflicting results. The objective of this study is to determine whether GCA, is associated with increased mortality.

METHODS: Forty-four cases with GCA were identified from the University of Utah Health Sciences Center, the major tertiary care center for the Intermountain West. The Utah Population

Database, a unique biomedical information resource, selected cases and age- and gender-matched controls. Cases were defined as patients with a temporal artery biopsy-proven diagnosis of GCA (international classification of diseases [ICD]-9 code 446.5) between 1991 and 2005. Exclusion criteria included a negative biopsy, alternative diagnoses, or insufficient clinical data. For each of the 44 cases, 100 controls were identified; thus, 4,400 controls ($p = 0.04$). Five-year cumulative survival was 67% for the control group versus 35% for the cases ($p < .001$). Survival rates for cases and controls converged at approximately 11.12 years.

CONCLUSIONS: Patients with GCA were more likely than age- and gender-matched controls to die within the first 5 years following diagnosis.

The Intermountian Ocular Research Laboratory

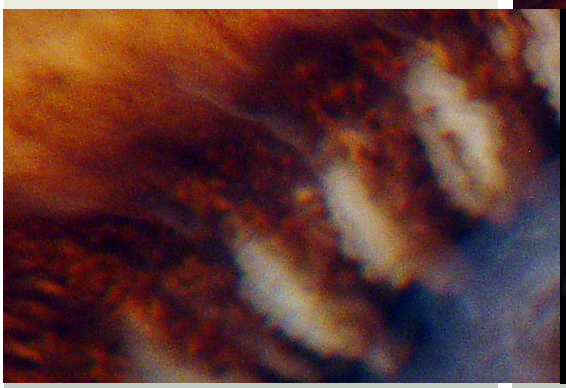

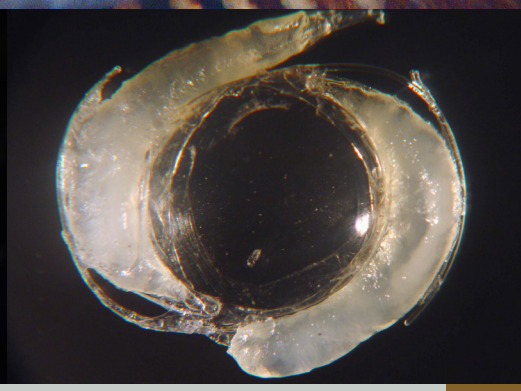

Each year approximately 1.4 million people in the United States receive intra-ocular lens (IOL) implants after surgical removal of cataracts. Though these replacement lenses improve vision, postoperative complications can occur. The Department of Ophthalmology and Visual Sciences in the University of Utah School of Medicine established a research program in 1984 to study the causes and origins of IOL-related complications. Research performed in this center has resulted in improved quality and design of IOLs, developed new surgical techniques now used by most implant surgeons, and spurred the withdrawal of poorly designed IOLs from the marketplace. We are now studying the causes, prevention, and treatment of posterior capsule opacification and development of IOLs from new soft biomaterials.

The Center functions as a national registry for removed IOLs and eye tissue with lens-induced disease. Ophthalmologists worldwide have sent over 16,000 specimens to the center and many eye banks from around the nation regularly send tissues to the center for histopathological analysis.

The Center also conducts research on exciting new technologies. Incorrect IOL power is still a problem following otherwise successful cataract surgery. We have worked with the industry to develop a light adjustable lens which allows lens power to be changed following surgery while the implant is inside the eye.

Another major area of research is the development of an "accommodative" IOL. Currently, IOLs correct distance vision following cataract surgery, but do not allow many patients to have clear near vision for reading. Our clinician-scientists have worked with ophthalmic companies in the development of an accommodative IOL that can provide good distance and near vision. In addition, the Center has established a worldwide registry for the evaluation, treatment, and prevention of toxic anterior segment syndrome (TASS) following ocular surgery.

Nick Mamalis, M.D., has directed the Intermountain Ocular Research Center, a nonprofit, independent laboratory that performs basic, in depth scientific research on intra-ocular lenses. In addition, the Center provides services and education to surgeons, clinical ophthalmologists, their patients, and intra-ocular lens manufacturers worldwide. Dr Mamalis is also Academic Appointments: Professor of Ophthalmology & Visual Sciences—University of Utah School of Medicine; Director of Ocular Pathology

Liliana Werner, M.D., Ph.D., joined the Moran Eye Center in September 2002 and co-directs the Intermountain Ocular Research Center. Dr. Werner's research is centered on the interaction between ocular tissues and different intra-ocular lens designs, materials and surface modifications. These include intra-ocular lenses implanted after cataract surgery, and also phakic lenses for refractive surgery and ophthalmic implantable devices in general.

Complications of sulcus placement of single-piece acrylic intraocular lenses: recommendations for backup IOL implantation following posterior capsule rupture.

Author: Chang DF, Masket S, Miller KM, Braga-Mele R, Little B, Mamalis N, Oetting TA, Packer M; ASCRS Cataract Clinical Committee.

Journal: J Cataract Refract Surg. 2009 Aug;35(8):1445-58.

PURPOSE: To describe complications arising from sulcus placement of single-piece acrylic (SPA) intraocular lenses (IOLs), evaluate IOL options for eyes that lack adequate capsule support, and examine the appropriateness of various IOL designs for sulcus placement.

SETTING: University and private anterior segment surgery practices.

METHODS: Patients referred for complications of SPA IOLs in the ciliary sulcus from 2006 and 2008 were identified. Demographic information, examination findings, and complications of the initial surgery were recorded. Details of surgical interventions and the most recent corrected distance visual acuity (CDVA) were noted. A thorough review of the literature was undertaken to analyze options for IOL placement.

RESULTS: Complications of sulcus SPA IOLs included pigment dispersion, iris transillumination defects, dysphotopsia, elevated intraocular pressure, intraocular hemorrhage, and cystoid macular edema. Two patients n the series of 30 patients experienced 1 complication; 8 experienced 2 complications; 13 experienced 3 complications; 4 experienced 4 complications; and 2 experienced 5 complications. Twenty-eight eyes (93%) required surgical intervention; IOL exchange was performed in 25 (83%). Postoperatively, the mean CDVA improved, with most eyes attaining 20/20.

CONCLUSIONS: Intraocular lenses designed solely for the capsular bag should not be placed in the cililary sulcus. Backup IOLs in appropriate powers, sized, and designs should be available for every cataract procedure. The development, investigation, and supply of IOLs specifically designed for placement in eyes that lack adequate capsule support represent clinically important endeavors for ophthalmology and the ophthalmic industry.

Clinical and Histopahtologic Evaluation of Six Human Eyes Implanted with the Bag-in-the-Lens.

Author: Werner L, Tassignon MJ, Zaugg BE, De Groot V, Rozema J.

Journal: Ophthalmology. 2010 Jan;117(1):55-62. Epub 2009 Nove 5.

PURPOSE: To describe the clinical and histopathologic features of eyes implanted with the bag-in-the-lens (BIL), which involves the use of a twin capsulorhexes.

DESIGN: Case series with clinicopathologic correlation.

PARTICIPANTS: Six eyes implanted with the foldable, hydrophilic arylic BIL, obtained postmortem at different postoperative times, from 4 patients were studied.

METHODS: On the patients' death, the eyes were enucleated, immersed in fixative, and submitted for analyses under a high-frequency ultrasound unit (Ar-

temis, Ultralink, St. Petersburg, FL; 50 MHz), gross analyses, and histopathologic analyses. Clinical data in each case were obtained by chart review.

MAIN OUTCOME MEASURES: Clinical data obtained included patient demographics preoperative evaluatin, descriptioin of surgical implantation procedure, and postoperative outcomes. The postmortem evaluation included analyses of postoperative capsular bag opacification.

RESULTS: The patients were aged 74.6+/-12.6 years at implantation. The postoperative time in this series ranged from 4 to 39 months. In all eyes for which the surgical implantation was uneventful (N = 5), postoperative BIL decentration was insignificant. In 1 eye, the anterior capsulorhexis was torn off, and although BIL implantation was still possible, a relative lens decentration was observed postoperatively, but without clinical significance. Although progressively larger amounts of Soemmering's ring formation were observed in the specimens with larger follow-up, the central area delimitated by the rhexis openings remained perfectly clear in all 6 eyes.

CONCLUSIONS: This is the first series of human eyes implanted with the BIL, obtained postmortem at different postoperative times. IL centration depends on the performance of centered capsulorhexes of appropriate size. The results confirm the concept of the lens design in that any proliferative/regenerative material remains confined to the intercapsular space of the capsular bag remnant outside the optic rim.

FINANCIAL DISCLOSURE(S): Proprietary or commercial disclosure may be found after the references.

Intraocular pressure changes during injection of microincision and conventional intraocular lenses through incisions smaller than 3.0 mm.

Author: Kamae KK, Werner L, Chang W, Johnson JT, Mamalis N.

Journal: J Cataract Refract Surg. 2009 Aug;35(8):1430-6.

PURPOSE: Too compare intraocular pressure (IOP) during insertion of a new microincision intraocular lens (IOL) (Akreos AO MI60) and a conventional IOL (AcrySof Natural SN60AT) and to determine the minimum incision sizes for insertion in a cadaver eye model.

SETTING: John A. Moran Eye Center, University of Utah, Salt Lake City, Utah, USA.

METHODS: After phacoemulsification in phakic cadaver eyes, multiple IOL insertions were attempted through 1.8 mm to 2.5 mm wounds. The final incision size and insertion success were evaluated in each case. A pressure transducer placed in the vitreous cavity measured real-time IOP changes (100 readings per second), including the mean and peak IOP during IOL implantation.

RESULTS: The minimum incision size for the microincision IOL insertion was 1.9 mm using a wound-assisted technique and 2.2 mm using a cartridge-insertion technique. The minimum incision size for wound-assisted implantation of the conventional IOL was 2.4 mm. During successful implantation, the mean and peak IOPs were similar between the 2 IOL types. The peak IOPs exceeded 60 mm Hg (retinal perfusion pressure). In unsuccessful attempts, the mean and peak IOPs were higher for the conventional IOL, reaching 306.05 mm Hg in 1 eye.

CONCLUSIONS: Monitoring during implantation of both IOL types confirmed that IOP increases during insertion, including during microincision surgery using a wound-assisted technique. Further studies are necessary to evaluate the effect of pressure spikes on the optic nerve during IOL insertion.

Detection of pyrogens adsorbed to intraocular lenses: evaluation of limulus amoebocyte lysate and in vitro pyrogen tests.

Author: Werner L, Tetz M, Mentak K, Aldred M, Zwisler W.

Journal: J Cataract Refract Surg. 2009 Jul;35(7):1273-80.

PURPOSE: To determine the ability of the limulus amobocyte lysate (LAL) assay and the in vitro pyrogen teest (IPT) to detect pyrogens adsorbed to intraocular lenses (IOLs).

SETTING: Berlin Eye Research Institute, Berlin, Germany.

METHODS: Fifteen of each of the following IOLs were used: MicroSil MS 612 ASP, AcrySof SA60AT, Superflex, Sensar, SACT, and LS-106 IOLs. The challenge organism suspensions were 10(3) CFU/mL and 10(4) CFU/mL Escherichia coli, 10(3) CU/mL and 10(4) CFU/mL Pseudomonas putida, and 10(5) CFU/mL and 10(6) CU/mL Staphylococcus epidermidis. Two IOLs of each model were incubated at room temperature for at least 2 days in 0.6 mL of 1 of the suspensions. There were then gamma sterilized. The extract of 1 IOL was tested with the LAL assay; the other IOL was tested wit the IPT.

RESULTS: The LAL was negative for all incubated IOLs. The IPT was positive for all IOLs incubated in E coli and P putida suspensions, with the MicroSil MS 612 ASP, AcrySof SA60AT, SACT, and LS_106 IOLs showing a severe reaction. The Superflex and Sensar IOLs had a slight to moderate response for lower bacterial concentrations and a moderate to severe response for higher concentrations. For S epidermidis, all IOLs showed a slight IPT response except XACT IOLs, which showed a nonpyrogenic response.

CONCLUSIONS: Results indicate that the LAL test may fail to detect pyrogens adsorbed to IOLs and the IPT reliably detects pyrogens with a dose-dependent response. This has relevance in the investigation of toxic anterior segment syndrome outbreaks.

Evaluating and defining the sharpness of intraocular lenses: microedge structure of commercially available square-edged hydrophilic intraocular lenses.

Author: Werner L, Tetz M, Feldmann I, Bücker M.

Journal: J Cataract Refract Surg. 2009 Mar;35(3):556-66.

PURPOSE: To evaluate the microstructure of the edges of currently available hydrophilic acryli intraocular lenses (IOLs) in terms of their deviation from an idea" square as a follow-up of preliminary in vitro studies of experimental poly(methyl methacrylate) IOLs and commercially available foldable hydrophobic IOLs.

SETTING: Berlin Eye Research Institute, Berlin, Germany.

METHODS: Twenty-four designs of hydrophilic acrylic IOLs were used in this study. For each design, a +20.0 diopter (D) IOL and a +0.0 D IOL (or the lowest available plus dioptric power) were evaluated. The IOL edge was imaged under low-vacuum (0.7 torr), high-magnification scanning electron microscopy (SEM) using an environmental microscope and standardized technique. The photographs were imported to a digital computer program, and the area above the posterior-lateral edge, representing the deviation from a perfect square, was measured in square microns.

RESULTS: Currently available hydrophilic acrylic IOLs labeled as square edged had an area of deviation from a perfect square ranging from 60.84 to 871.51 microm(2) for the +20.0 D IOLs and from 35.52 to 826.55 microm(2) for the low-diopter IOLs. Although some differences in edge finishing between the IOLs analyzed were observed,, edge surfaces of hydrophilic acrylic IOLs appeared overall smooth under environmental SEM.

CONCLUSIONS: Analysis of the microstructure of the optic edge of currently available square-edged hydrophilic acrylic IOLs showed a large variation of deviation area from a perfect square.

Comparison of the corneal endothelial protective effects of Healon-D and Viscoat.

Author: Peck CM, Joos ZP, Zaugg BE, Abdel-Aziz S, Stringham JD, Werner L, Mamalis N, Olson RJ.

Journal: Clin Experiment Ophthalmol. 2009 May;37(4):397-401.

BACKGROUND: the use of dispersive ophthalmic viscosurgical devices (OVDs) has been shown to provide significant protection against air bubble damage to the corneal endothelium when compared with cohesive OVDs. We compared the corneal endothelial protective effects of a new dispersive OVD, Healon-D, with Viscoat.

METHODS: Healon-D and Viscoat were used in a randomized and masked fashion in the anterior chamber of 40 rabbit eyes during a procedure where ultrasound at 70% continuous energy was delivered for 2 min. Two milliliters of air bubbles were injected into the anterior chamber during the first minute of the procedure on each eye. Corneas were then stained with trypan blue and alizarin red and evaluated via light microscopy for endothelial injury. Both denuding of the endothelial layer, as well as damage to endothelial cells were quantified by using the Evaluation of Posterior Capsule Opaxifiation digital imaging system.

RESULTS: The denuded area for eyes treated with Healon-D and Viscoat were not significantly different (medians of 0.004167 and 0.003333, respectively , P = 0.8908). There was no significant difference in the area of endothelial cell damaged (medians of 0.02183 and 0.01433, respectively, P = 0.4565). when the denuded and damaged areas were calculated together, there was also no difference in the total injured area (medians of 0.05817 and 0.05817, respectively, P = 0.5740).

CONCLUSION: The new dispersive OVD Healon-D is equally as effective as Viscoat in protecting the corneal endothelial layer from denuding and damage from air bubbles during anterior segment surgery.

Long-term pathological follow-up of obsolete design: Pannu universal intraocular lens.

Authors: Davis D, Werner L, Strenk S, Strenk L, Yeh O, Mamalis N.

Journal: J Cataract Refract Surg. 2010 Mar;36(3):512-6.

ABSTRACT: We studied an enucleated postmortem eye from an 82-year-old white donor who had been implanted with a Pannu "universal" intraocular lens (IOL) in the anterior chamber approximately 20 years earlier. This IOL has design features characteristic of a 1-piece, C-loop posterior chamber IOL. Magnetic resonance imaging showed a relatively well-centered IOL in the anterior chamber with haptics impinging on the iris. Gross and light microscopic analyses of the eye and the IOL showed peripheral anterior synechiae enclaving one haptic, areas of angle widening, significant attenuation of the corneal endothelium, multiple areas of iris trauma secondary to optic and haptic iris abrasion, large areas of pigment dispersion in the angle, diffuse pigment accumulation within the anterior chamber, and attenuation of the ganglion cell layer. The histopathological findings were consistent with glaucoma and chronic inflammation.

Translational Research

Balamurali Ambati, M.D., Ph.D.

The capsule drug device: Novel approach for drug delivery to the eye.

Author: Molokhia SA, Sant H, Simonis J, Bishop CJ, Burr RM, Gale BK, Ambati BK.

Journal: Vision Res. 2010 Mar 31;50(7):680-5. Epub 2009 Oct 23.

ABSTRACT: Treatment of age-macular degeneration requires monthly intravitreal injections, which are ostly and have serious risks. The objective of this study was to develop a novel intraocular implant for drug delivery. The capsule drug ring is a reservoir inserted in the lens apsule during cataract surgery, refillable and capable of delivering multiple drugs. Avastin (®) was the drug of interest in this study. Prototypes were manufactured using polymethgylmetharylate sheets as the reservoir material, a semi-permeable membrane for controlled delivery and silicone check valves for refilling. The device showed near zero-order release kinetics and Avastin (®) stability was investigated with accelerated temperature studies.

Surface-functionalized nanoparticles for targeted gene delivery across nasal respiratory epithelium.

Author: Sundaram S, Roy SK, Ambati BK, Kompella UB.

Journal: FASEB J. 2009 Nov;23(11):3752-65. Epub 2009 Jul 16.

ABSTRACT: The objective of this study was to determine whether surface-modified nanoparticles enhance permeability across nasal mucosa, while retaining the effectiveness of the payload. The uptake and permeability of polystyrene nanoparticles (PS-NPs; FluoSpheres) was evauated across the various regions of the bovine nasal epithelia following conjugation with deslorelin and transferring. Uptake and transport of PS-NPs, deslorelin-PS-NPs, and treanferrin-PS-NPs exhibited regional differences in the order: inferior turbinate posterior (ITP) > medium turbinate posterior (MTP) > medium turbinate anterior (MTA). Uptake and transport also exhibited directionality and temperature dependence in these tissues.

Further, uptake as well s transport of functionaloized nanoparticles could be inhibited by excess free functionalizing ligand. Confocal microscopy indicated the presence of functionalized nanoparticles in respoiratory epithelial cells, as well as other cell types of the nasal tissue. We chose the ITP region for further studies with deslorelin or transferring-conjugated poly-I-lactide-co-glycolide nanoparticles (PLGA-NPs) encapsulating an anti-VEGF intraceptor (FLT23k) plasmid. Transport of the nanoparticles, as well as the plasmid from the nanoparticles, exhibited the following order: transferring-PLGA-NPs > deslorelin-PLGA-NPs > PLGA-NPs >> plasmid. The ability of the nanoparticles transported across the nasal tissue to retain the effectiveness of the Flt23k plasmid was evaluated by measuring transfection efficiency (percentage of cells expressing GFP) and transfection efficiency (percentage of cells expressing GFP) an VEGF inhibition in LNCaP and PC-3 prostate cancer cells. Transfection efficiencies and VEGF inhibition in LNCaP and PC-3cells exhibited the following trend: transferring-PLGA-NPs >or=deslorelin-PLGA-NPs > PLGA-NPs >> plasmid.

Further, functionalized nanoparticles exhibited transfection efficiencies and functionalized nanoparticles exhibited transfection efficiencies and VEGF inhibition significantly superior compared with the tourinely used transfecting agent, lipofectamine. Formulating plasmids into nanoparticulate delivery systems enhances the transnasal delivery and gene therapy at remote target cancer cells, which can be further enhance by nanoparticle functionalization with deslorelin or transferrin.

Targeted drug and gene delivery systems for lung cancer therapy.

Authors: Sundaram S, Trivedi R, Durairaj C, Ramesh R, Ambati BK, Kompella UB.

Journal: Clin Cancer Res. 2009 Dec 1;15(23):7299-308. Epub 2009 Nov 17.

PURPOSE: To evaluate the efficacy of a novel docetaxel derivative of deslorelin, a luteinizing hormone-releasing hormone (LHRH) agonist, and its combination in vivo with RGD peptide conjugated nanoparticles encapsulating an antiangiogenic, anti-vascular endothelial growth factor (VEGF) intraceptor (Flt23k; RGD-Flt23k-NP) in H1299 lung cancer cells and/or xenografts in athymic nude BALB/c mice.

EXPERIMENTAL DESIGN: The in vitro and in vivo efficacy of the deslorelin-docetaxel conjugate was evaluated in H1299 cells and xenografts in athymic nude mice. Coadministration of deslorelin-docetaxel conjugate and RGD-Flt23k-NP was tested in vivo in mice. Tumor inhibition, apoptosis, and VEGF inhibition were estimated in each of the treatment groups.

RESULTS: The conjugate enhanced in vitro docetaxel efficacy by 13-fold in H1299 cells compared with docetaxel at 24 hours, and this effect was inhibited following reduction of LHRH receptor expression by an antisense oligonucleotide. Combination of the conjugate with the RGD-Flt23k-NP in vivo resulted in an 82- and 15-fold tumor growth inhibition on day 39 following repeated weekly i.v. injections and a single intratumoral (i.t.) injection, respectively. These effects were significantly greater than individual targeted therapies or docetaxel alone. Similarly, apoptotic indices for the combination therapy were 14% and 10% in the i.v. and i.t. groups, respectively, and higher than the individual therapies. Combination therapy groups exhibited greater VEGF inhibition in both the i.v. and i.t. groups.

CONCLUSIONS: Docetaxel efficacy was enhanced by LHRH receptor-targeted des-

lorelin conjugate and further improved by combination with targeted antiangiogenic nanoparticle gene therapy. Combination of novel targeted therapeutic approaches described here provides an attractive alternative to the current treatment options for lung cancer therapy.

Intraveous ransferrin, RGD peptide and dual-targeted nanoparticles enhance anti-VEGF intraceptor gene delivery to laser-induced CNV.

Singh SR, Grossniklaus HE, Kang SJ, Edelhauser HF, Ambati BK, Kompella UB

Journal: Gene Ther. 2009 May;16(5):645-59. Epub 2009 Feb 5

ABSTRACT: Choroidal neovascularization (CNV) leads to loss of vision in age-related macular degeneration (AMD), the leading cause of blindness in adult population over 50 years old. In this study, we developed intravenously administered, nanoparticulate, targeted nonviral retinal gene delivery systems for the management of CNV. CNV was induced in Brown Norway rats using a 532 nm laswer. We engineered transferrin, arginine-glycineaspartic acid (RGD) peptide or dual-functionalized poly-(lactide-co-glycolide) nanoparticles to target delivery of anti-vascular endothelial growth factor (VEGF) intraceptor plasmid to CNV lesions. Anti-VEGF intraceptor is the only intracellularly acting VEGF inhibitory modality.

The results of the study show that nanoparticles allow targeted delivery to the neovascular eye but not the conrol eye on intravenouos administration. Fuctionalizing the nanoparticle surface with transferring, a linear RGD peptide or both increased the retinal delivery of nanoparticles and subsequently the intraceptor gene expression in retinal vascular endothelial cells, photoreceptor outer segments and retinal pigment epithelial cells when compared to nonfunctionalized nanoparticles. Most significantly, the CNV areas were significantly smaller in rats treated with functionalized nanoparticles as compared to the ones treated with vehicle or nonfunctionalized nanoparticles. Thus, surface-functionalized nanoparticles allow targeted gene delivery to the neovascular eye on intravenous administration and inhibit the progression of laser-induces CNV in a rodent model.

Gene delivery nanoparticles fabricated by supercritical fluid extraction of emulsions.

Authors: Mayo AS, Ambati BK, Kompella UB.

Journal: Int J Pharm. 2010 Mar 15;387(1-2):278-85. Epub 2009 Dec 16.

ABSTRACT: Non-viral polymeric gene delivery systems offer increased protection from nuclease degradation, enhanced plasmid DNA (pDNA) uptake, and controlled dosing to sustain the duration of pDNA action. Such gene delivery systems can be formulated from biocompatible and biodegradable polymers such as poly(D,L-lactic-co-glycolic) acid (PLGA). Experimental loading of hydrophilic macromolecules such as pDNA is low in polymeric particles. The study purpose was to develop a supercritical fluid extraction of emulsions (SFEE) process based on CO(2) for preparing pEGFP-PLGA nanoparticles with high plasmid loading and loading efficiency. Another objective was to determine the efficacy of pFlt23k, an anti-angiogenic pDNA capable of inhibiting vascular endothelial growth factor (VEGF) secretion, following nanoparticle formation using the SFEE process. Results indicated that the SFEE process allows high actual loading of pDNA (19.7%, w/w), high loading efficiency (>98%), and low residual solvents (<50 ppm), due to rapid particle formation from efficient solvent removal provided by the SFEE process. pFlt23K-PLGA nanoparticles were capable of in vitro transfection, significantly reducing secreted VEGF from human lung alveolar epithelial cells (A549) under normoxic and hypoxic conditions. pFlt23K-PLGA nanoparticles did not exhibit cytotoxicity and are of potential value in treating neovascular disorders wherein VEGF levels are elevated.

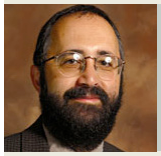

Paul Bernstein M.D., Ph.D.

The value of measurement of macular carotenoid pigment optical densities and distributions in age-related macular degeneration and other retinal disorders.

Author: Bernstein PS, Delori FC, Richer S, van Kuijk FJ, Wenzel AJ.

Journal: Vision Res. 2010 Mar 31;50(7):716-28. Epub 2009 Oct 23.

ABSTRACT: There is increasing recognition that the optical and antioxidant properties of the xanthophylls carotenoids lutein and zeaxanthin play an important role in maintaining the health and function of the human macula. In this review article, we assess the value of non-invasive quantification of macular pigment levels and distributions to identify individuals potentially at risk for visual disability or catastrophic vision loss from age-related macular degeneration, and we consider the strengths and weaknesses of the diverse measurement methods currently available.

A Genome-Wide Scan of Advanced Age-Related Macular Degeneration Suggests a Role of Lipase-C

Authors: Neale BM, Fagerness J, Reynolds R, Sobrin L, Parker M, Raychaudhuri S, Tan P, Oh EC, Merriam JE, Souied E, Bernstein PS, Li B, Frederick JM, Zhang K, Brantley MA, Jr., Lee AY, Zack DJ, Campochiaro B, Campochiaro P, Ripke S, Smith RT, Barile GR, Katsanis N, Allikmets R, Daly MJ, Seddon JM.

Manuscript Information: Classification (Biological Science; Genetics); Text Pages 22; Figures 3; Tables 3.

ABSTRACT: Advanced age-related macular degeneration (AMD) is the leading cause of late onset blindness. This neurodegenerative disorder arises from retinal damage associated with accumulation of drusen and subsequent atrophy or neovascularization that leads to central visual loss. We present results of a genome-wide association study (GWAS) of 979 advanced AMD cases and 1709 controls using the Affymetrix 6.0 platform with replication including the Michigan/Penn/Mayo GWAS and six additional cohorts (totaling 4337 cases and 2077 controls) . We also present the first comprehensive analysis of copy number variations and polymorphisms for AMD. In addition to confirming reported AMD loci, our discovery data implicated he-

patic lipase (LIPC) in the high-density lipoprotein cholesterol (HDL-c) pathway as a novel locus for AMD risk (combined discovery and replication P = 8.75 x 10-8 for SNP rs493258), with protective effect of the minor T allele for advanced wet and dry AMD. This association was strongest at a promoter variant (rs10468017, P = 9.81 x 10-9) that influences LIPC expression and serum HDL levels. We observed weaker associations with other HDL loci (CETP, P = 5.36 x 10-4 and ABCA1, P = 2.73 x 10-3). Based on lack of a consistent association between these HDL increasing or decreasing alleles and AMD risk, the LIPC association may not be the result of an effect on HDL levels, but could represent a pleiotropic effect of the same functional unit. This genetic locus implicates a novel biologic pathway and provides a new avenue for possible prevention and treatment of AMD.

Gregory Hageman Ph.D.

New era for personalized medicine: the diagnosis and management of age-related macular degeneration.

Author: Baird PN, Hagement GS, Guymer RH.

Journal: Clin Experiment Ophthalmol. 2009 Nov;37(8):814-21.

ABSTRACT: It can be argued that age-related macular degeneration is one of the best characterized complex trait diseases. Extensive information related to genetic and environmental risk factors exists, and a number of different biological pathways are strongly implicated in its aetiology. Along with recent improvements in high throughput and relatively inexpensive genetic technologies, we area now in a position to consider developing a presymptomatic, personalized approach towards the assessment, management and treatment of this disease. We explore the applicability and challenges of this approach if it is to become commonplace for guiding treatment decisions for individuals with pre-existing disease or for those at high risk of developing it.

Rapid and sensitive method for detection of Y402, H402, I62, and V62 variants of complement factor H in human plasma samples using mass spectrometry.

Author: Kelly U, Rickman CB, Postel EA, Hauser MA, Hageman GS, Arshavsky VY, Skiba NP.

Journal: Invest Ophthalmol Vis Sci. 2009 Apr;50(4):1540-5. Epub 2008 Nov 21.

PURPOSE: Variations in the complement factor H (CFH) gene are tightly associated with age-related macular degeneration (AMD) across diverse populations. Of the many nonsynonymous coding variants in CFH, two are most strongly associated with increased risk of AMD: isoleucine 62 to valine (I62V) and tyrosine 402 to histidine (Y402H). Detection of these variations in a patient's blood is important for a risk assessment of AMD and disease prognosis. However, traditional methods of genetic anaysis cannot be used for measuring CFH allotypes in some sources of human plasma and other biological fluids not containing DNA. The purpose was to develop a protein-based method of detecting CFH allotypes.

METHODS: A combination of a single-step affinity enrichment of CFH, gel separation, and mass spectrometry identification o the CFH peptides spanning amino acids at positions 62 and 402 was used to identify individual CFH allotypes.

RESULTS: The CFH isoforms V62, I62, H402, and Y402 were reliably detected based on identification of tryptic peptides with masses of 1148.59 Da, 1162.60 Da, 2031.88 Da, and 2057.88 Da, respectively, using MALDI-TOF-TOF. The presence or absence pattern of these peptides in mass spectra of different CFH samples robustly correlated with all nine genotypes of CFH, as a result of variations at positions 62 and 402.

CONCLUSIONS: A rapid and sensitive method has been developed for detection of V62, I62, H402, and Y402 variants of CFH in human plasma samples using mass spectrometry. This method can be used in clinical laboratories equipped with a basic inexpensive mass spectrometer capable of performing peptide fingerprinting.

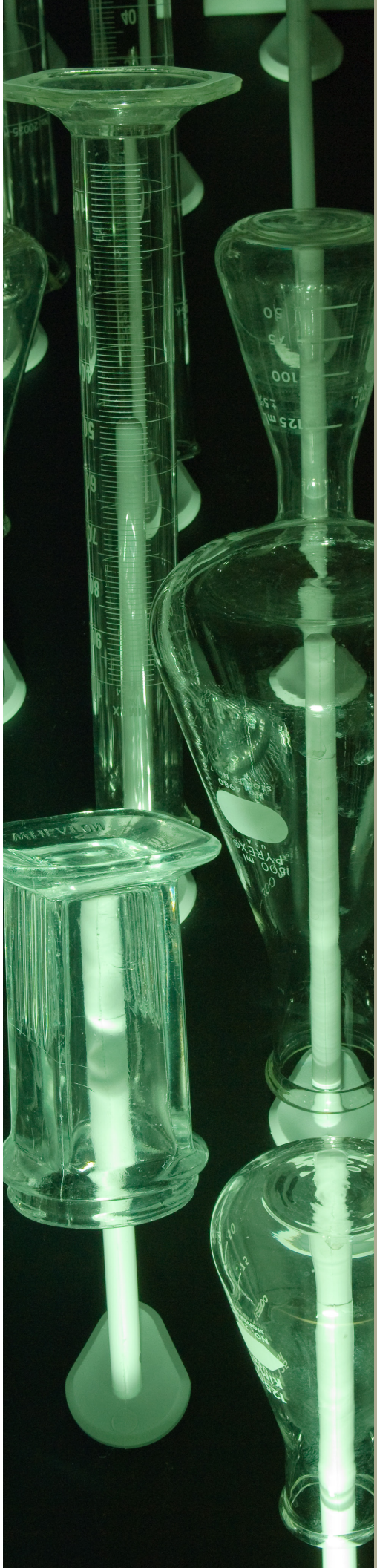

Clinical Research

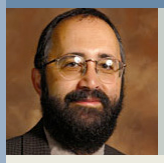

Paul Bernstein M.D, Ph.D.

Nutritional Interventions against Age-Related Macular Degeneration.

Author: Bernstein PS.

Journal: Acta Hortic. 2009 Aug 31;841:103-112.

Age-related macular degeneration (AMD) is the leading cause of irreversible visual loss in the developed world. This disease of the elderly robs them of central vision in one or both eyes leading to a devastating loss of the ability to drive, read, and recognize faces. In recent years, a number of novel treatments for the neovascular form of AMD (also known as "wet" or exudative AMD) have been introduced, and for the first time, the relentless downhill course of vision loss experienced by the majority of patients with this particularly malignant variant of AMD has been transformed to the stabilization and even improvement of visin in at least two-thirds of patients. Likewise, the slower, more insidious form of AMD known as dry AMD which leads to geographic atrophy of the macula, has become the focus of pharmaceutical firms efforts for intervention. Unfortunately, all of these novel treatments have limitations, and they tend to be very expensive. Thus, prevention of AMD is of paramount importance to reduce the healthcare burden of this blinding disorder. Accumulating evidence suggests that encouragement of increased consumption of fruits and vegetables rich in the xanthophyll carotenoids lutein and zeaxanthin is a simple, cost effective public health intervention that might help to decrease the incidence of AMD. In this review article, the scientific underpinnings for these nutritional recommendations will be surveyed.

Demographic Characteristics, Patterns, and Risk Factors for Retinal Vein Occlusion in Nepal: A Hospital-Based Case-Control Study

Thapa R, Paudyal G, Bernstein PS.

Journal: Clin Experiment Ophthalmol

PURPOSE: Retinal vein occlusion is an increasing problem leading to visual impairment in Nepal. Our study investigates the demographic characteristics, patterns, and risk factors for retinal vein occlusion (RVO) in this developing Asian country.

METHODS: This is a hospital-based case-control study conducted at the Tilganga Institute of Ophthalmology of Nepal during the period of January 2007 to January 2008. All consecutive new cases of RVO diagnosed at the Institute were included. Cases with intraocular inflammation or a prior history of intraocular injections, laser therapy, or vitrectomy for RVO were excluded from the study. Age, sex, and geographically matched subjects were recruited as a control group from patients who presented for regular eye examinations at the same hospital during the study period.

RESULTS: A total of 218 patients with RVO presented during the study period. The mean age of the patients was 61.1 years (12.3 S.D) with more males (58.3%) than females. The mean age for control groups was 61.3 years (13.0 S.D). Seventy percent of subjects had branch retinal vein occlusion (BRVO), while central retinal vein occlusion (CRVO) was present in 26.6%. 63.9% of BRVO was found in the superotemporal branch. Hypermetropia, primary open angle glaucoma, hypertension, mixed diabetes and hypertension, and heart disease were significantly higher in RVO cases as compared to the control group.

CONCLUSION: The demographic characteristics, patterns and risk factors of RVO in Nepal can help guide interventions against these blinding diseases in similar developing countries.

Alan S. Crandall, M.D., focuses on the medical and surgical management of glaucoma and cataracts.

Dr. Crandall has experience with trabeculoplasty and laser cyclophotocoagulation. He is involved in numerous clinical research studies at the Moran Eye Center. Dr. Crandall is also the Director of the Medical Education Program. Dr. Crandall lectures all over the world and was selected by Cataract and Refractive Surgery Today as one of the 50 international opinion leaders.

Late in-the-bag spontaneous intraocular lens dislocation: evaluation of 86 consecutive cases.

Author: Davis D, Brubaker J, Espandar L, Stringham J, Crandall A, Werner L, Mamalis N.

Journal: Ophthalmology. 2009 Apr;116(4):664-70.

OBJECTIVE: As techniques for cataract surgery have evolved, spontaneous intraocular lens (IOL) dislocation has decreased overall. However, since 2006 the Intermountain Ocular Research Center has received and increased number of explanted IOLs within the capsular bag forwarded for pathologic evaluation. Late, spontaneous dislocation of IOLs results from zonular insufficiency and zonulysis that has been associated with pseudoexfoliation, trauma, and other

risk factors. The findings of 86 consecutivecases of this complication, analyzed in the laboratory, are described.

DESIGN: Retrospective case series.

PARTICIPANTS: Eighty-six IOLs explanted within the capsular bag, submitted in formalin.

METHODS: Standard light microscopy of specimens, as well as questionnaire sent to explanting surgeons and patient chart review, when available.

Kathleen B. Digre, M.D.

Progress and Priorities in the Health of Women and Girls: A Decade of Advances and Challenges.

Authors: Garcia FA, Freund KM, Berlin M, Digre KB, Dudley DJ, Fife RS, Gabeau G, Geller SE, Magnus JH, Trott JA, White HF.

Journal: J Womens Health (Larchmt). 2010 Mar 4.

OBJECTIVE: Following the initial wave of federal support to address women's health, there is a need to assess successes and determine the next priorities to advance the health of women. The objective of this study was to systematically collect expert opinion on the major advances in women's health in the past decade and priorities for women's health research and service in the coming decade.

METHODS: We utilized a Delphi method to query the leadership from academic and community Centers of Excellence in Women's Health, as designated by the Department of Health and Human Services. Leaders from 36 of the 48 centers responded to a series of questions about the major advances and critical indicators to evaluate future needs in women's health. We utilized a social ecology model framework to organize the responses to each question.

RESULTS: The experts identified increased health education for women and increased empowerment of women across multiple spheres as the major advances positively impacting the health of women. The experts selected the following areas as the most important indicators to measure the status of the health of women in the future: health education and promotion, rates and impact of interpersonal violence against women, and access to healthcare.

The major advances and measures of the health of women did not focus on specific changes to individual women in illness management, clinical care, or individual behavioral change.

CONCLUSIONS: As we move to address health reform, we must be able to recognize and incorporate a broad perspective on public health and policy initiatives critical to the health and wellness of women and girls and, therefore, central to the well-being of the nation.

Gregory Hageman Ph.D.

Retinal basement membrane abnormalities and the retinopathy of Alport syndrome.

Author: Savige J, Liu J, Cabrera Debuc D, Handa JT, Hageman GS, Wang YY, Parkin JD, Vote B, Fassett R, Sarks S, Colville D.

Journal: Invest Ophthalmol Vis Sci. 2010 Mar;51(3):1621-7. Epub 2009 Oct 22.

PURPOSE: To determine the effects of X-linked and autosomal recessive Alport syndrome on retinal basement membranes and how these result in the characteristic perimaular dot and fleck retinopathy, 'lozenge', and macular hole.

METHODS: The type IV collagen chains present in the normal retina were determined immunohistochemically. Ten patients with Alport syndrome underwent retinal photography and optical coherence tomography (OCT< Topcon OCT-1000, Topcon, Tokyo; and Cirrus HD-OCT and Stratus OCT< Carl Zeiss Meditec, CA) to determine the thickness of the internal limiting membrane (ILM) by segmentation analysis, the layers affected by the retinopathy and any correlates of the lozenge and macular hole. Bruch's membrane was examined directly by electron microscopy in a donated Alport eye.

RESULTS: The alpha3alpha4alpha5 type IV collagen network was present in the normal ILM as well as the retinal pigment epithelium membrane of Bruch's membrane. In Alport syndrome the ILM/nerve fibre layer and Bruch's membrane were both thinned. The dot and fleck retinopathy corresponded to hyperreflectivity of the ILM/ nerve fibre layer in the distribution of the nerve fibre layer. The lozenge and macular hole corresponded to temporal macular thinning. The whole retinal thinning was principally due to thinning of the ILM/ nerve fibre layer and inner nuclear layer.

CONCLUSIONS: ILM/nerve fibre layer rather than the Bruch's membrane. Thinning of the ILM/nerve fibre layer contributes to the retinopathy, lozenge and macular hole possibly through interfering with nutrition of the overlying retina or the clearance of metabolic by-products.

Nick Mamalis, M.D., Ph.D.

Femtosecond-assisted lamellar keratoplasty in atypical Avellino corneal dystrophy of Indian origin.

Agarwal A, Brubaker JW, Mamalis N, Kumar DA, Jacob S, Chinnamuthu S, Nair V, Prakash G, Meduri A, Agarwal A.

Journal: Eye Contact Lens. 2009 Sep;35(5):272-4.

PURPOSE: To report a case of Avellino corneal dystrophy (ACD) in a patient of Indian origin treated with femtosecond-assisted lamellar keratoplasty (FALK).

METHODS: A 6-year-old male patient presented with severe photophobia with decreased visioni for 2 months. A clinical diagnosis of Avellino dystrophy was made after complete examination under anesthesia and FALK was performed.

RESULTS: The postoperative period was uneventful with good symptomatic improvement and graft clarity. HIstopathological study with special staining, namely Masson trichrome and Congo red stain, of the patient's corneal button showed features of both granular and lattice lesions suggestive of ACD. Genetic analysis showed absence of R124H mutation in BIGH3 gene. No recurrence or exacerbation was noted at 19-month follow-up.

CONCLUSIONS: To our knowledge, this is the first case report of clinical, histopathological, miscroscopic features of ACD in young patient of Indian origin with absence of BIGH3 gene treated with FALK with IntraLase Femtosecond Laser for donor and recipient cuts.

Nepafenac-associated bilateral corneal melt after photorefractive keratectomy.

Author: Feiz V, Oberg TJ, Kurz CJ, Mamalis N, Moshirfar M.

Journal: Cornea. 2009 Sep;28(8):948-50.

PURPOSE: We are reporting a case of bilateral corneal melt after photorefractive keratectomy requiring bilateral corneal transplantations.

RESULTS: A 35-year-old man underwent uncomplicated photorefractive keratectomy and was treated postoperatively with topical nepafenac, one drop in both eyes every 2 hours. Three days into this course of treatment, the patient developed bilateral irritation and the dose was decreased to one drop every 4 hours. The next day, he developed stromal melting in both eyes. Although nepafenac was discontinued at this point, the ulcerative kertolysis progressed in both eyes requiring penetrating keratoplasty.

CONCLUSIONS: We report a case of sterile ulceration after photorefractive keratectomy surgery, which we believe was caused by frequent postoperative dosing of nepafenac.

Endophthalmitis rates after implantation of the intraocular Collamer lens: survey of users between 1998 and 2006.

Author: Allan BD, Argeles-Sabate I, Mamalis N.

Journal: J Cataract Refract Surg. 2009 Apr;35(4):766-9.

ABSTRACT: An anonymous on-line survey was sent to 234 intraocular Collamer lens (ICL) (Staar Surgical) surgeons in 21 countries to determine how many of their ICL cases had been complicated by endophthalmitis between January 1998 and December 2006. A second questionnaire about the infection details and treatment outcome was sent to those who reported cases of endophthalmitis. Ninety-five (40%) surgeons responded to the survey. They had implanted 17954 ICLs during the study period. Three surgeons reported 1 case of endophthalmitis each, a rate of 0.0167% (95%) confidence interval 0 to 0.036% or approximately 1 case of endophthalmitis per 6000 ICL implantations. Follow-up details were available in 2 cases. Staphylococcus epidermidis was cultured in both cases, and both were treated without loss of vision. Endophthalmitis may be less common after ICL implantation than after cataract surgery. Further studies are required to define the rate and prognosis for endophthalmitis after ICL implantation to assist in accurate preoperative patient counseling.

Intraoperative floppy iris syndrome.

Author: Abdel-Aziz S, Mamalis N.

Journal: Curr Opin Ophthalmol. 2009 Jan;20(1):37-41.

PURPOSE OF REVIEW: To describe the condition known as intraoperative floppy iris syndrome in association with systemic alpha-1 blocker use in patients undergoing cataract surgery and techninques to prevent related complications.

RECENT FINDINGS: In recent years, an unexpected complication of progressive intraoperative miosis, iris billowing, and prolapse was noted during routine phacoemulsification in patients with current or previous use of alpha-1 adrenergic receptor antagonists. The syndrome is particularly prevalent among patients treated ith tamsulosin, an alpha-1A blocker prescribed for the treatment of benign prostatic hyperplasia. This condition is also seen, in smaller numbers, in patients treated with nonspecific alpha-1 blockers.Intraoperative floppy iris syndromm was noted to occur even when patients discontinued alpha-1blocker use. However, the risk remains in patients who do not disclose current or prior use of these medications.

SUMMARY: There are several clinical concerns, such as most effective methods of managing intraoperative floppy iris syndrome, increasing awareness among physicians and patient about potential risk associated with this class of drug, and importance of disclosure of use prior to cataract surgery.

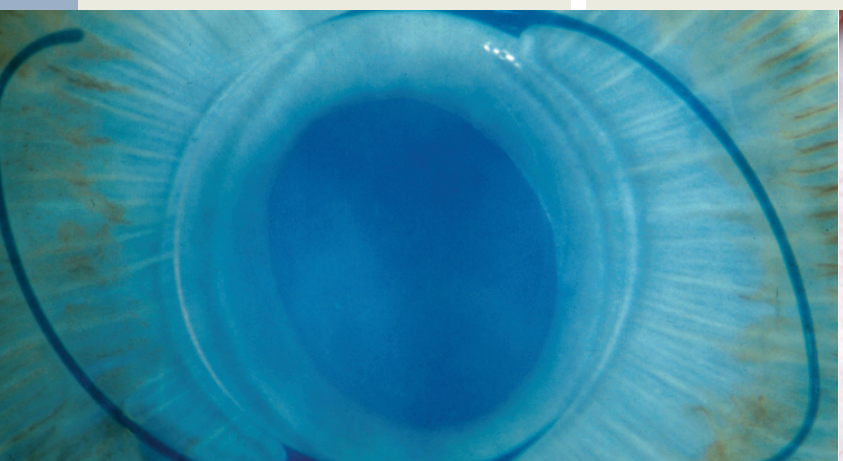

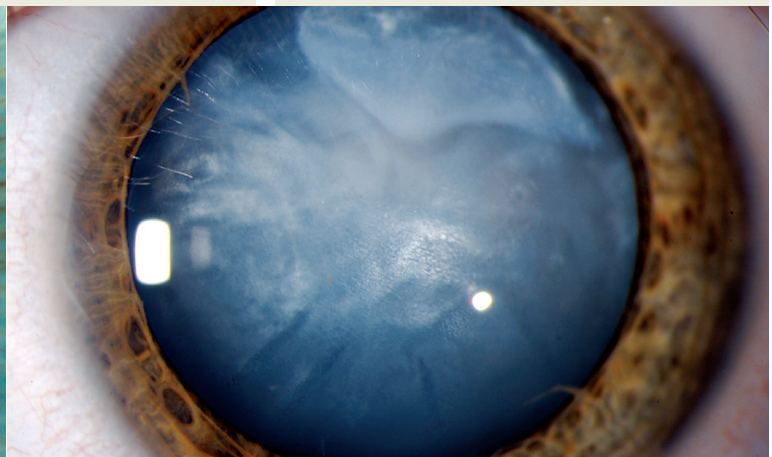

Clinical Research: Anterior Segment

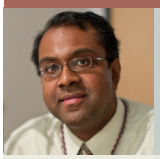

Balamurali Ambati, M.D., Ph.D.

Corneal transparency: genesis, maintenance and dysfunction.

Authors: Qazi Y, Wong G, Monson B, Stringham J, Ambati BK.

Journal: Brain Res Bull. 2010 Feb 15;81(2-3):198-210. Epub 2009 May 27.

ABSTRACT: Optimal vision is contingent upon transparency of the cornea. Corneal neovascularization, trauma and, surgical procedures such as photorefractive keratectomy and graft rejection after penetrating keratoplasty can lead to corneal opacification. In this article we identify the underlying basis of corneal transparency and factors that compromise the integrity of the cornea. With evidence from work on animal models and clinical studies, we explore the molecular mechanisms of both corneal avascularity and its dysfunction. We also seek to review therapeutic regimens that can safely salvage and restore corneal transparency.

Corneal stroma PDGF blockade and myofibroblast development.

Author: Kaur H, Chaurasia SS, de Medeiros FW, Agrawal V, Salomao MQ, Singh N, Ambati BK, Wilson SE.

Journal: Exp Eye Res. 2009 May;88(5):960-5. Epub 2008 Dec 24.

ABSTRACT: Myofibroblast development and haze generatin in the corneal stroma is mediated by cytokines, including transforming growth factor-beta (TGF-beta), and possibly other cytokines. This study examined the effects of stromal PDGF-beta blockade on the development of myofibroblasts in response to -9.0 diopter photorefractive keratectomy in the rabbit. Rabbits that had haze generating photorefractive keratectomy (PRK, for 9 diopters of myopia) in one eye were divided into three different gropus: stromal application of plasmid pCMV. PDGFRB.23KDEL expressing a subunit of PDGF receptor b (domains 2-3, which bind PDGF-B) stromal application of empty plasmid pCMV, or stromal application of balanced salt solution (BSS). The plasmids (at a concentration 1000ng/microl) or BSS was applied to the exposed stroma immediately after surgery and every 24h for 45 days until the epithelium healed. The gropu treated with pCMV.PDGFRB.23KDEL showed lower alphaSMA+ myofibroblast density in the anterior stroma compared to either control group (P<or=0.001). Although there was also lower corneal haze at the slit lamp at one month after surgery, the difference in haze after PDGF-B blockade was not statistically significant compared to either control group. Stromal PDGF-B blockade during the early postoperative period following PRK decreases stromal alphaSMA+ myofibroblast generation. PDGF is an important modulator of myofibroblast development in the cornea.

Alan Crandall M.D.

Pseudoexfoliation and the cataract surgeon: preoperative, intraoperative, and postoperative issues related to intraocular pressure, cataract, and intraocular lenses.

Author: Shingleton BJ, Crandall AS, Ahmed II.

Journal: J Cataract Refract Surg. 2009 Jun;35(6):1101-20.

ABSTRACT: This review provides a comprehensive assessment of intraocular pressure (IOP), phacoemulsification techniques, and intraocular lenses (IOLs) in pseudoexfoliation (PXF) eyes having cataract surgery. Pseudoexfoliation is ubiquitous and the most common cause for open-angle glaucoma worldwide. Cataracts occur with increased frequency in PXF eyes, and surgery is potentially complicated by the presence of small pupils and zonule laxity and significantly affects IOP in these eyes. Preoperative evaluation and the options for intraoperative management of cataract are presented with recommendations for the use of adjunctive pupil and zonule support devices. Postoperative complications such as capsule contraction and IOL instability are discussed and laser and surgical options to manage these special problems presented.

Mark D. Mifflin, M.D., specializes in the medical and surgical treatment of corneal and anterior segment eye diseases. His expertise includes all types of corneal transplantation, cataract surgery, and vision correction using lasers, intra-ocular lenses, and conductive keratoplasty.

Endothelial cell density to predict endothelial graft failure after penetrating keratoplasty.

Authors: Lass JH, Sugar A, Benetz BA, Beck RW, Dontchev M, Gal RL, Kollman C, Gross R, Heck E, Holland EJ, Mannis MJ, Raber I, Stark W, Stulting RD; Cornea Donor Study Investigator Group. Collaborators (281) Mifflin M.

Journal: Arch Ophthalmol. 2010 Jan;128(1):63-9.

OBJECTIVE: To determine whether preoperative and/or postoperative central endothelial cell density (ECD) and its rate of decline postoperatively are predictive of graft failure caused by endothelial decompensation following penetrating keratoplasty to treat a moderate-risk condition, prin-

Majid Moshirfar, M.D., F.A.C.S., is the director of the Moran Eye Center's Refractive Surgery Program. Dr. Moshirfar specializes in refractive surgery, medical and surgical management of corneal disorders, cataract removal and inflammatory eye diseases.

Dr. Moshirfar lectures extensively around the country on a variety of vision correction procedures and has become a community spokesperson on the benefits and risks of vision correction surgery.

cipally, Fuchs dystrophy or pseudophakic corneal edema. METHODS: In a subset of Cornea Donor Study participants, a central reading center determined preoperative and postoperative ECD from available specular images for 17 grafts that failed because of endothelial decompensation and 483 grafts that did not fail.

RESULTS: Preoperative ECD was not predictive of graft failure caused by endothelial decompensation (P = .91). However, the 6-month ECD was predictive of subsequent failure (P < .001). Among those that had not failed within the first 6 months, the 5-year cumulative incidence (+/-95% confidence interval) of failure was 13% (+/-12%) for the 33 participants with a 6-month ECD of less than 1700 cells/mm(2) vs 2% (+/-3%) for the 137 participants with a 6-month ECD of 2500 cells/mm(2) or higher. After 5 years' follow-up, 40 of 277 participants (14%) with a clear graft had an ECD below 500 cells/mm(2).

CONCLUSIONS: Preoperative ECD is unrelated to graft failure from endothelial decompensation, whereas there is a strong correlation of ECD at 6 months with graft failure from endothelial decompensation. A graft can remain clear after 5 years even when the ECD is below 500 cells/mm(2).

A comparison of three methods for trephining donor corneal buttons: endothelial cell loss and microscopic ultrastructural evaluation.

Authors: Moshirfar M, Meyer JJ, Kang PC

Journal: Curr Eye Res. 2009 Nov;34(11):939-44.

PURPOSE: To evaluate the ultrastructure of the cut edge and associated endothelial cell loss following donor cornea trephination with a standard punch, vacuum punch, and vacuum trephine and artificial anterior chamber system.

MATERIALS AND METHODS: This laboratory investigation compared trephinations (8.0 mm) performed on human corneas using either a standard posterior punch (n = 12), vacuum posterior punch (n = 12), or vacuum trephine and artificial anterior chamber system (n = 12). Specular microscopy was performed before and after trephination to determine central endothelial cell density. Light and scanning electron microscopy were performed to evaluate the structure of the trephined edge. Endothelial cell-free distances from the trephinated edges were measured on light microscopy sections.

RESULTS: Central endothelial cell loss (cells/mm(2)) after trephination was -14.0 +/- 49.9 (SD) for the standard posterior punch, -85.6 +/- 87.0 for the vacuum posterior punch, -116.0 +/- 223.1 for the vacuum trephine and artificial anterior chamber system. Endothelial cell-free distances from the trephined margin were 63 +/- 22 microm, 85 +/- 13 microm, and 123 +/- 48 microm for the three respective methods. The edges of grafts cut with anterior trephination were inward sloping from the epithelial to endothelial surfaces, while both posterior punches created outward sloping edges. Increased fibrillar disruption at edges was seen following anterior trephination.

CONCLUSION: Different trephination methods produce distinct cut morphologies with the anterior trephination approach, resulting in more irregular margins. The anterior approach was associated with increased variability and greater endothelial cell loss than the studied posterior approaches. The use of corneal scissors may contribute to the morphologic features of the corneal button seen following anterior trephination.

Cataract surgery following phakic intraocular lens implantation.

Authors: Moshirfar M, Mifflin M, Wong G, Chang JC.

Journal: Curr Opin Ophthalmol 2010 Jan;21(1):39-44.

PURPOSE OF REVIEW: To review the most recent literature regarding the incidence and pathophysiology of phakic intraocular lens (pIOL) associated cataracts, surgical issues and outcomes of combined pIOL explantation/cataract surgery, and the prevention of cataract formation secondary to pIOLs.

RECENT FINDINGS: The overall rate of cataracts secondary to pIOLs is low, but a disproportionate number is associated with posterior chamber pIOLs. All combination pIOL explantation/cataract surgeries resulted in the successful implantation of a posterior chamber intraocular lens in the capsular bag. We present several theories regarding the pathophysiology of anterior subcapsular cataracts secondary to posterior chamber pIOLs. In addition, we present general strategies in performing combination pIOL explantation/cataract surgery. Several methods of preoperative assessment show promise in helping prevent cataracts secondary to pIOLs, including new ultrasound methods for sulcus imaging and preoperative simulations.

SUMMARY: Although the incidence of cataracts secondary to pIOLs is low, more studies regarding the pathophysiology of this phenomenon and improvement of preoperative assessment are needed, especially for posterior chamber pIOLs.

Contact lens-induced keratitis resembling central toxic keratopathy syndrome.

Authors: Moshirfar M, Kurz C, Ghajarnia M.

Journal: Cornea. 2009 Oct;28(9):1077-80.

PURPOSE: To document a case of contact lens-induced keratitis resembling central toxic keratopathy syndrome.

METHODS: A 23-year-old female developed an acute, central, stromal haze subsequent to soft contact lens overwear. Slit lamp examination revealed corrugated stromal "mud cracks," as seen in stage IV diffuse lamellar keratitis (DLK). This was accompanied by relative corneal thinning and flattening with a hyperopic shift of approximately 6 diopters.

RESULTS: Eight weeks after discontinuing contact lens wear and after a 2-week tapering regimen of topical steroids, she had partial resolution of the central haze, partial increase in corneal thickness, steepness, and decrease in hyperopic shift.

CONCLUSION: The authors present a case with a history of soft contact lens overwear and a clinical presentation notably similar to the central toxic keratopathy syndrome, which has recently been reported after laser refractive surgery.

Effect of iris registration on outcomes of LASIK for myopia with the VISX CustomVue platform.

Authors: Moshirfar M, Chen MC, Espandar L, Meyer JJ, Christensen D, Christiansen SM, Dave SB, Bedke B, Kurz C.

Journal: J Refract Surg. 2009 Jun;25(6):493-502.

PURPOSE: To compare visual outcomes after LASIK using the VISX STAR S4 CustomVue, with and without Iris Registration technology.

METHODS: In this retrospective study, LASIK was performed on 239 myopic eyes, with or without astigmatism, of 142 patients. Iris registration LASIK was performed on 121 eyes and non-iris registration LASIK was performed on 118 eyes. Primary outcome measures were uncorrected visual acuity (UCVA), best spectacle-corrected visual acuity (BSCVA), and manifest refraction.

RESULTS: At 6 months, the mean values for UCVA (logMAR) were 0.00 +/- 0.09 in the iris registration group and -0.01 +/- 0.11 in the non-iris registration group (P = .587). Seventy-nine percent of eyes in the iris registration group had UCVA of 20/20 or better compared to 78% in the non-iris registration group (P = .518). Ninety-two percent of eyes in the iris registration group and 90% in the non-iris registration group were within +/- 0.50 diopters (D) of emmetropia (P = .999). Mean postoperative absolute change in total root-mean-square higher order aberrations in the iris registration group and non-iris registration group was 0.22 microm and 0.19 microm, respectively (P = .6). At 3 months, the mean magnitude of error of surgically induced astigmatism was -0.09 in the iris registration group and -0.04 in the non-iris registration group (P = .25).

CONCLUSIONS: Wavefront-guided LASIK with the VISX STAR S4 CustomVue laser system, independent of iris registration status, is effective, safe, and predictable. Under well-controlled surgical conditions, this study did not find any statistical significance supporting the better achievement of visual acuity, astigmatism correction, or the lesser induction of higher order aberrations using iris registration in comparison to a non-iris registration system.

Inadvertent pigmentation of the limbus during cosmetic blepharopigmentation.

Authors: Moshirfar M, Espandar L, Kurz C, Mamalis N.

Journal: Cornea. 2009 Jul;28(6):712-3.

PURPOSE: To present a case of perilimbal pigmentation as a complication of cosmetic blepharopigmentation.

METHODS: Interventional case report.

RESULTS: A 54-year-old white woman underwent bilateral upper and lower eyelid cosmetic blepharopigmentation. After the procedure, the patient noted a small area of black pigmentation of the surface of her right eye. Slit-lamp examination revealed perilimbal pigmentation involving the conjunctiva and the superficial cornea of the right eye. The affected conjunctiva was excised, and a diamond burr used to remove the underlying pigmented superficial cornea and sclera. The excised conjunctiva was analyzed by standard light microscopy. Hematoxylin and eosin-stained sections of the surgical specimen showed a thin ribbon of pigmentation just under the conjunctival epithelium without obvious inflammatory cell reaction around the extracellular pigment. The patient tolerated the surgical removal of the pigmentation without any complications and was pleased with the cosmetic result.

CONCLUSIONS: Possible complications of blepharopigmentation include pigment deposition into the conjunctiva and the superficial cornea and sclera as was seen in this case report. This case of inadvertent pigmentation did not cause any significant chronic inflammation, although acute and chronic inflammatory reactions of the conjunctiva and surrounding structures have been reported as complications after cosmetic blepharopigmentation. Surgical removal of the affected tissue is a treatment option and was successful in removing the pigment in this case.

Randall J Olson, M.D., is the CEO of the John A. Moran Eye Center. He is the author of more than 300 professional publications and a worldwide lecturer. Dr. Olson specializes in research dealing with intra-ocular lens complications, teleophthalmology and corneal transplantation techniques. He was selected as one of the 15 best cataract surgeons in the United States in a peer survey conducted by Ophthalmology Times. Cataract and Refractive Surgery Today named Dr. Olson as one of 50 international opinion leaders. He has appeared in the last three editions of Best Doctors in America.

Scanning Electron Microscopy Visualization of Methicillin-resistant Staphylococcus aureus After Contact With Gatifloxacin With and Without Preservative.

Authors: Monson BK, Stringham J, Jones BB, Abdel-Aziz S, Cutler Peck CM, Olson RJ.

Journal: J Ocul Pharmacol Ther. 2010 Mar 24 (Epub ahead of print)

PURPOSE: To test a visual model by looking at the differences in effect of Zymar ® (gatifloxacin plus benzalkonium chloride [BAK]) When compared to gatifloxacin and a normal saline (NS) control upon a methicillin and gatifloxacin-resistant Staphylococcus aureus (MRSA) species.

METHODS: An ocular isolate of gatifloxacin-resistant (minimal inhibitory concentration >2 to 4 mircrog/mL) MRSA was grown to confluency. Chambered slides were prepared ith bacterial culture smears, and then incubated with either gatifloxacin at the concentrations of 1 and 10 microg/mL, Zymar ® containing equivalent concentrations of gatifloxacin, or NS. Bacterial cultures were fixed after 10, 30, and 60 min. Fixed slides were coated in gold sputter for examination. Bacteria were visually evaluated with scanning electron microscopy (SEM) at 50,000x. Blinded review of SEM images compared structural changes and mitotic activity across samples.

RESULTS: MRSA exposed to 10 microg Zymar(® for 60 min showed significantly greater pleomorphism and cell wall surface changes when compared to gatifloxacin ($P < 0.0001$), and significantly less mitotic activity than NS ($P = 0.002$).

CONCLUSION: Using SEM, the topical formulation of gatifloxacin 0.3% (Zymar(®, which contains BAK, had greater antibacterial activ ity than did gatifloxacin alone in gatifloxacin and methicillin-resistant S. aureus, thereby illustrating potential advantages of the preservative in the commercial formulation. We further show that these effects canbe visualized and quantified.

The Risk of Capsular Breakage from Phacoemulsification Needle Contact with the Lens Capsule: A Laboratory Study.

Authors: Meyer JJ, Kuo AF, Olson RJ.

Journal: Am J Ophthalmol. 2010 Mar 13. (Epub ahead of print)

PURPOSE: To determine capsular breakage risk from contact by phacoemulsification needles by machine and tip type.

DESIGN: Experimental laboratory investigation.

METHODS: Infiniti (Alcon, Inc., Fort Worth, Texas, USA) with Intrepid cartridges and Signature (Abbott Medical Optics, Inc., Santa Ana, California, USA) phacoemulsification machines were tested using 19- and 20-gauge sharp and rounded tips Actual and unoccluded flow vacuum were determined at 550 mm Hg, bottle height of 75 cm, and machine-indicated flow rate of 60 mL/minute. Breakage from brief tip contact with a capsular surrogate and human cadaveric lenses was calculated.

RESULTS: Nineteen-gauge tips had more flow and less unoccluded flow vacuum than 20-gauge tips for both machines, with highest unoccluded flow vacuum in the Infiniti. The 19-gauge sharp tip was more likely than the 20-gauge sharp tip to cause surrogate breakage for Signature with micropulse and Ellips (Abbott Medical Optics, Inc) ultrasound at 100% power. For Infiniti using OZil (Alcon, Inc) ultrasound, 20-gauge sharp tips were more likely than 19-gauge sharp tips to break the membrane. For cadaveric lenses, using rounded 20-gauge tips at 100% power breakage rates were micropulse (2.3%), Ellips (2.3%), OZil (5.3%). Breakage rates for sharp 20-gauge Ellips tips were higher than for rounded tips.

CONCLUSION: Factors influencing capsular breakage may include active vacuum at the tip, flow rate, needle gauge, and sharpness. Nineteen-gauge sharp tips were more likely than 20-gauge tips to cause breakage in lower vacuum methods. For higher-vacuum methods, breakage is more likely with 20-gauge than with 19-gauge tips. Rounded-edge tips are less likely than sharp-edged tips to cause breakage.

Thermal Comparison of Infiniti OZil and Signature Ellips Phacoemulsification Systems.

Authors: Schmutz JS, Olson RJ.

Journal: Am J Ophthalmol. 2010 Mar 3 (Epub ahead of print)

PURPOSE: To determine thermal characteristics of Signature Ellips (Abbot Medical Optics, Inc., Santa Ana, California, USA) and Infiniti OZil (Alcon, Inc, Fort Worth, Texas, USA) transverse ultrasound and compare both with longitudinal ultrasound in clinically relevant scenarios.

DESIGN: Laboratory investigation.

METHODS: Temperature increase over baseline after 60 seconds was mea-

sured in water at positions in 90-degree increments around the sleeve near the proximal needle shart in an artificial chamber for Ellips and OZil on continuous ultrasound with aspiration blocked and unblocked. This as also done with Signature using longitudinal ultrasound, with and without micropulse (6 ms on, 12 ms off), with aspiration blocked and unblocked, and at the OZil sleeve tip on continuous transverse mode with aspiration unblocked.

RESULTS: OZil (8.1 ± 0.3 C) had greater temperature increase than Ellips (5.2 ± 0.3 C; P < .0001) with aspiration unblocked and blocked (29.3 ± 1.0 C vs 12.2 ± 0.7 C; P < .0001). OZil had uneven distribution of heat around the shaft (30.1 ± 0.5 C vs 28.5 ± 0.6 C; P < .0001), whereas Ellips did not (P = .57). OZil was cooler at the tip (6.6 ± 0.2 C; P < .0001). Friction in a cadaver eye incision only increased these numbers by 10% (OZil, irrigation blocked).

CONCLUSION: Metal stress probably creates heat at the proximal needle junction for both transverse methods. Heat generation differences between OZil and Ellips result from t manner in which they create needle motion. Incision burns may occur, especially for OZil under non-pulsed settings during fragment removal with occlusion when reaching across the anterior chamber such that the proximal needle shaft came near the wound.

Dysphotopsia outcomes analysis of two truncated acrylic 6.0-mm intraocular optic lenses.

Authors: Jin Y, Zabriskie N, Olson RJ.

Journal: Ophthalmologica. 2009;223(1):47-51.

BACKGROUND/AIMS: To determine the incidence of pseudophakic dysphotopsia complaints in patients successfully implanted with two 6.0-mm acrylic intraocular optic lenses (IOL) with treated edges: the Sensar AR-40-e (Advanced Medical Optics, Santa Ana, Calif., USA) and the SA-60AT (Alcon, Fort Worth, Tex., USA).

METHODS: A patient history and telephone survey at least 1 year after uncomplicated surgery at an academic eye hospital. Patients operated on for cataract with no pathology noted that the procedure could have an impact upon vision. At least 20/25 best corrected vision was documented after surgery, and patients were asked to rate specific dysphotopsia complaints. A single relevant case study is also presented.

RESULTS: Case study: the patient had unremitting dysphotopsia with an SA-60AT IOL and had an AR-40-e implanted in the second eye. She went on to have the SA-60AT exchanged with an AR-40-e IOL with relief of symptoms. Main study: the survey showed both 6.0-mm optic acrylic IOL were similar, except there was significantly more midday dysphotopsia with the SA-60AT in a subgroup (p = 0.014). Both were generally superior to the MA-30 with the SA-30AT between the two extremes. The control group did better than all IOL in general, except in overall satisfaction where the AR-40-e and SA-60AT were better.

CONCLUSION: Pseudophakia induces dysphotopsia which can be minimized by a 6.0-mm optic and treated IOL edge.

Norm A. Zabriskie, M.D., specializes in the medical and surgical treatment of glaucoma and cataracts. He is the Vice-Chairman of Clinical Operations and the Medical Director of the John A. Moran Eye Center. He has a research interest in the genetics of glaucoma.

2010 ASCRS Awards, Boston, April 9-14

Honorable Mention to the poster P173 (Category of Intraocular Surgery, Cataract & Refractive, with 181 entries): Liliana Werner, Jack Stringham, Bryan Monson, Raymond Theodosis, Nick Mamalis. Calcification of different designs of silicone IOLs in eyes with asteroid hyalosis.

Best-Paper-of-Session Award (Session 1-F) to the presentation: Nick Mamalis, Peter Ness, Henry Edelhauser. Toxic anterior segment syndrome: Analysis of recent outbreaks.

Runner up in the Category of New Producers, AND Amazing Outtake Award to the video (ASCRS Film Festival; 182 entries): Kandon Kamae, Bala Ambati, Paul Bernstein, JoAnn Chang. To boldly go where no cornea has gone before: Pars plana DSEKtomy.

From left to right, Spencer Thornton, Jack Singer, John Vukich, Kandon Kamae, Liliana Werner, William Fishkind.

Clinical Research: Posterior Segment

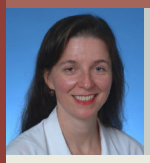

Mary Elizabeth Hartnett, M.D.

Aqueous vascular endothelial growth factor as a predictor of macular thickening following cataract surgery in patients with diabetes mellitus.

Authors: Hartnett ME, Tinkham N, Paynter L, Geisen P, Rosenberg P, Koch G, Cohen KL.
Journal: Am J Ophthalmol. 2009 Dec;148(6):895-901.e1. Epub 2009 Oct 17

PURPOSE: To study associations between serum and aqueous vascular endothelial growth factor (VEGF) and insulin-like growth factor 1 (IGF-1) and macular edema measured with optical coherence tomography (OCT) following phacoemulsification in diabetic patients.

DESIGN: Cohort study.

METHODS: A pilot study of 36 consecutive diabetic patients undergoing planned phacoemulsification with IOL in 1 eye by one surgeon at the University of North Carolina consented to preoperative and postoperative OCT central subfield (CSF) thickness measurements and aqueous and blood samples for VEGF and IGF-1. Four patients with clinically significant macular edema (CSME) received laser preoperatively. Spearman-rank correlations were performed between growth factors and mean CSF or a clinically meaningful percent change in CSF (>11% of preoperative measurement) at 1 and 6 months postoperatively.

RESULTS: There were no surgical complications or new cases of CSME following surgery. Mean aqueous VEGF in patients with retinopathy, determined preoperatively, increased with increasing level of severity. Patients with preoperative CSME also had severe or worse retinopathy and the greatest mean aqueous VEGF. Significant preoperative correlations existed between aqueous VEGF and more severe retinopathy whether CSME was present or absent ($r = 0.49$; $P = .007$), and between aqueous VEGF and CSME ($r = 0.41$; $P = .029$). At 1 month postoperative, aqueous VEGF was positively correlated with >11% change from preoperative CSF regardless of CSME status ($r = 0.47$; $P = .027$). No noteworthy associations existed between CSF and IGF-1 values.

CONCLUSIONS: Aqueous VEGF was significantly positively associated with a clinically meaningful change in CSF in diabetic patients 1 month following cataract surgery. Accounting for preoperative CSF was important. Further study is indicated.

Development of an instrument to measure glaucoma medication self-efficacy and outcome expectations.

Authors: Sleath B, Blalock SJ, Robin A, Hartnett ME, Covert D, Devellis B, Giangiacomo A.

Journal: Eye (Lond). 2009 Jul 17.

PURPOSE: The purpose of this study was to develop and evaluate the psychometric properties of (a) a glaucoma medication self-efficacy scale and (b) a glaucoma outcome expectations scale.

PATIENTS AND METHODS: Two instruments were developed: a glaucoma medication self-efficacy scale and a glaucoma outcome expectations scale. Packets containing (a) the instruments and patient demographic questions and (b) a letter explaining the study were distributed to 225 glaucoma patients from three ophthalmology practices between August and December 2007. The instrument was completed by 191 patients for a response rate of 85%. Principal components factor analysis with a varimax rotation and Cronbach's alpha reliability were used to analyse the data. To assess discriminant validity, we administered the scales and two self-reported measures of adherence in a separate sample of 43 glaucoma patients who were currently using at least one glaucoma medication.

RESULTS: Our results yielded a 21-item self-efficacy in overcoming barriers that might interfere with the use of glaucoma medications scale, a 14-item self-efficacy in carrying out specific tasks required to use eye drops correctly scale, and a four-item glaucoma outcome expectations scale. Results of the Cronbach's alpha reliability indicated that the scales are internally consistent. The self-efficacy scales were both significantly associated with two patient self-reported measures of glaucoma medication adherence, which show discriminant validity.

CONCLUSIONS: Eye care providers and researchers can use these scales to identify patients with low self-efficacy in using their glaucoma medications and patients who do not believe that following their eye care providers' advice can help their vision.

A randomized trial comparing the efficacy and safety of intravitreal triamcinolone with standard care to treat vision loss associated with macular Edema secondary to branch retinal vein occlusion: the Standard Care vs Corticosteroid for Retinal Vein Occlusion (SCORE) study report 6.

Authors: Scott IU, Ip MS, VanVeldhuisen PC, Oden NL, Blodi BA, Fisher M, Chan CK, Gonzalez VH, Singerman LJ, Tolentino M; SCORE Study Research Group (Hartnett ME).

Journal: Arch Ophthalmol. 2009 Sep;127(9):1115-28. Erratum in: Arch Ophthalmol. 2009 Dec;127(12):1655.

OBJECTIVE: To compare the efficacy and safety of 1-mg and 4-mg doses of preservative-free intravitreal triamcinolone with standard care (grid photocoagulation in eyes without dense macular hemorrhage and deferral of photocoagulation until hemorrhage clears in eyes with dense macular hemorrhage) for

eyes with vision loss associated with macular edema secondary to branch retinal vein occlusion (BRVO).

METHODS: Multicenter, randomized clinical trial of 411 participants. Main Outcome Measure Gain in visual acuity letter score of 15 or more from baseline to month 12.

RESULTS: Twenty-nine percent, 26%, and 27% of participants achieved the primary outcome in the standard care, 1-mg, and 4-mg groups, respectively. None of the pairwise comparisons between the 3 groups was statistically significant at month 12. The rates of elevated intraocular pressure and cataract were similar for the standard care and 1-mg groups, but higher in the 4-mg group.

CONCLUSIONS: There was no difference identified in visual acuity at 12 months for the standard care group compared with the triamcinolone groups; however, rates of adverse events (particularly elevated intraocular pressure and cataract) were highest in the 4-mg group. Application to Clinical Practice Grid photocoagulation as applied in the SCORE Study remains the standard care for patients with vision loss associated with macular edema secondary to BRVO who have characteristics similar to participants in the SCORE-BRVO trial. Grid photocoagulation should remain the benchmark against which other treatments are compared in clinical trials for eyes with vision loss associated with macular edema secondary to BRVO.

A randomized trial comparing the efficacy and safety of intravitreal triamcinolone with observation to treat vision loss associated with macular edema secondary to central retinal vein occlusion: the Standard Care vs Corticosteroid for Retinal Vein Occlusion (SCORE) study report 5.

Authors: Ip MS, Scott IU, VanVeldhuisen PC, Oden NL, Blodi BA, Fisher M, Singerman LJ, Tolentino M, Chan CK, Gonzalez VH; SCORE Study Research Group (Hartnett ME).

Journal: Arch Ophthalmol. 2009 Sep;127(9):1101-14. Erratum in: Arch Ophthalmol. 2009 Dec;127(12):1648.

OBJECTIVE: To compare the efficacy and safety of 1-mg and 4-mg doses of preservative-free intravitreal triamcinolone with observation for eyes with vision loss associated with macular edema secondary to perfused central retinal vein occlusion (CRVO).

METHODS: Multicenter, randomized, clinical trial of 271 participants.

MAIN OUTCOME MEASURE: Gain in visual acuity letter score of 15 or more from baseline to month 12.

RESULTS: Seven percent, 27%, and 26% of participants achieved the primary outcome in the observation, 1-mg, and 4-mg groups, respectively. The odds of achieving the primary outcome were 5.0 times greater in the 1-mg group than the observation group (odds ratio [OR], 5.0; 95% confidence interval [CI], 1.8-14.1; P = .001) and 5.0 times greater in 4-mg group than the observation group (OR, 5.0; 95% CI, 1.8-14.4; P = .001); there was no difference identified between the 1-mg and 4-mg groups (OR, 1.0; 95% CI, 0.5-2.1; P = .97). The rates of elevated intraocular pressure and cataract were similar for the observation and 1-mg groups, but higher in the 4-mg group.

CONCLUSIONS: Intravitreal triamcinolone is superior to observation for treating vision loss associated with macular edema secondary to CRVO in patients who have characteristics similar to those in the SCORE-CRVO trial. The 1-mg dose has a safety profile superior to that of the 4-mg dose. Application to Clinical Practice Intravitreal triamcinolone in a 1-mg dose, following the retreatment criteria applied in the SCORE Study, should be considered for up to 1 year, and possibly 2 years, for patients with characteristics similar to those in the SCORE-CRVO trial.

SCORE Study Report 7: incidence of intravitreal silicone oil droplets associated with staked-on vs luer cone syringe design.

Authors: Scott IU, Oden NL, VanVeldhuisen PC, Ip MS, Blodi BA, Antoszyk AN; SCORE Study Investigator Group. (Hartnett ME)

Journal: Am J Ophthalmol. 2009 Nov;148(5):725-732.e7. Epub 2009 Aug 11.

PURPOSE: To evaluate the incidence of intravitreal silicone oil (SO) droplets associated with intravitreal injections using a staked-on vs luer cone syringe design in the SCORE (Standard Care vs COrticosteroid in REtinal Vein Occlusion) Study.

DESIGN: Prospective, randomized, phase III clinical trial.

METHODS: The incidence of intravitreal SO was compared among participants exposed to the staked-on syringe design, the luer cone syringe design, or both of the syringe designs in the SCORE Study, which evaluated intravitreal triamcinolone acetonide injection(s) for vision loss secondary to macular edema associated with central or branch retinal vein occlusion. Injections were given at baseline and 4-month intervals, based on treatment assignment and study-defined retreatment criteria. Because intravitreal SO was observed following injections in some participants, investigators were instructed, on September 22, 2006, to look for intravitreal SO at all study visits. On November 1, 2007, the luer cone syringe design replaced the staked-on syringe design.

RESULTS: A total of 464 participants received a total of 1,205 injections between November 4, 2004 and February 28, 2009. Intravitreal SO was noted in 141 of 319 participants (44%) exposed only to staked-on syringes, 11 of 87 (13%) exposed to both syringe designs, and 0 of 58 exposed only to luer cone syringes (P < .0001). Among participants with first injections after September 22, 2006, intravitreal SO was noted in 65 of 114 (57%) injected only with staked-on syringes compared with 0 of 58 injected only with luer cone syringes. Differential follow-up is unlikely to explain these results.

CONCLUSION: In the SCORE Study, luer cone syringe design is associated with a lower frequency of intravitreal SO droplet occurrence compared with the staked-on syringe design, likely attributable to increased residual space in the needle hub with the luer cone design.

The following individuals and organizations contributed to the Moran Eye Center from January 1, 2009 through December 31, 2009

Gifts of $1 Million and Above
Janice and Thomas D. Dee, II

Gifts of $100,000 and above
Alcon Research, Ltd.
Allergan, Inc.
Gayle L. Eschmann
Alan E. and Drue B. Huish
Research to Prevent Blindness, Inc.
Steve and Sharon Steele McGee

Gifts of $50,000 and above
Val A. and Edith D. Green Foundation
Calvin S. and JeNeal N. Hatch
Randall and Ruth Olson
John P. and Louise Tracy

Gifts of $25,000 and above
Larry S. and Marilyn A. Larkin
The Semnani Family Foundation

Gifts of $10,000 and above
Albert E. and Margaret M. Bradbury
Nicholas and Courtney Gibbs
John B. and Geraldine W. Goddard
Thomas R. and Susan C. Hodgson
Monterey Peninsula Foundation
Marcia and Gordon M. Olch
Noel and Florence Rothman Family
Denise R. Sobel
Utah Lions Foundation
James W. and Jeanne Welch

Gifts of $5,000 and above
American Endowment Foundation
G.W. and Ida Lee Anderson
Bamberger-Allen Foundation
Gainor and Joseph Bennett
Bingham Canyon Lions Club
Burningham Foundation
Margaret D. Hicks
Johnson Foundation - Jamestown, New York
James M. and Alison Luckman
Ralph and Marge Neilson
Hazel M. Robertson
Richard and Carmen Rogers

Gifts of $1,000 and above
LaRee and Richard Aldous, MD
Anonymous
Marvin L. and Lynn Arent
Richard E. Ashworth
Jeanne F. and Wolfgang Baehr
Bonnie Barry
Bettilyon Realty
Rodney H. & Carolyn Hansen Brady Foundation
Jackie Brinkerhoff
Robert S. Carter Foundation
Joel and Rita Cohen
In Honor of David Cooper
Alan S. Crandall, Jr., MD and Family
Janice and Thomas D. Dee, II
David M. Diamond
Larry A. Donoso, MD, Ph.D., JD, MBA
Henry W. and Leslie M. Eskuche Foundation
Joan B. and John H. Firmage
Cecelia H. Foxley, PhD
S. Sedonia Grant
Paul E. Griffin
Leah Hatziathanasiou and Family
Lisette and C. Charles Hetzel, III
Brad, Tracey, Sam, Jonah and Zev Katz
Geraldine and Peter Kypreos
Allan M. and Kay W. Lipman
Cullen McCarty
Richard McCarty
William and Julie McCarty
G. Mitchell and June M. Morris
Edward N. and Carol Scott Robinson
William L. Rogers Foundation
Bertram H. and Janet M. Schaap
Peter and Jutta Scholla
Tueng T. Shen, MD
Howard S. and Carolyn A. Spurrier
James and Rolande Vaughn
Theodore Waddell and Lynn Campion
Robert and Luree Welch
The Wuliger Foundation
Louise and Norman A. Zabriskie, MD

Gifts of $100 and above
Hans and Martha Ahrens
Anita and Sylvan Alcabes
Milton and Dianne Anderson
Anonymous
Anonymous
Keyhan F. Aryah, MD
Ralph L. and Virginia W. Ashton
Robert K. Avery, Ph.D.
Stella Barton
Lloyd and Nancy Beacom

John Bendixen
David and Margaret Bernhardt
John and Dee Bianucci
Emmy Blechmann
Bloomington Utah Lions Club
Linda and John Bonar
Charles Boswell and Amanda Manatt
Bryce Point Bed and Breakfast
Laura Byrne
In Memory of Basil and Virginia Byrne
William L. and Sheral L. Calvin
Robert Camp
Irene G. Casper
Pauline and George Childs
Don and Anne Christensen
Thayer S. and Sue D. Christensen
Kristeen Church
Blaine and Jacquelyn Clements
Drury W. Cooper
Margaret Anne Cragin
Marilyn and Joseph F. Cronin, Jr.
Paul B. Crookston
Richard and Lois Cunningham
Peter A. D'Arienzo, MD
Craig W. Dayhuff
Nancy and Bruce Deifik
Christopher J. Dirkes
Gaye and R. Michael Duffin, MD
Helen B. Duncan
George H. and Joan D. Earl
Robert D. and Danna Earl
Karen Ehresman
Lavon and Richard Erickson
Christine and Fred W. Fairclough, Jr.
Spencer P. and Barbara S. Felt
Peter Q. Freed
Roger C. Furlong, MD
Alice Gartman
William and Claudia Gislason
Stephen and Leslie Goddard
Rachel M. Goldberg
Dee Ann Gornichec
Shari Gowers
Robert and Joyce Graham
James and Sandra Grice
J. Darwin and Dorothy Gunnell
Frank J. and Gloria Gustin
William B. Hale
Hansen Construction, Inc.
Leonard Clark Hardy
Anne and Eastman Hatch
Ruth A. Hensel
Doris and Martin Hoffman Family Foundation
Kalen P. Holmes
Lois Horvitz
Michael Horvitz
Peter Horvitz
Edward and Roberta Hughes
Ruthanne Humphrey
Gil and Thelma Iker
Edward and Juanita Jenkins
Jerry J. and Roslyn Jensen
Jewish Community Endowment Fund
Frank J. and Sally Johnson
Robert G. Jones
David and Connie Katz
Laurel D. and Charles Kay
Charles and Patria Kerrick
Drs. Robert M. and Jeryl D. Kershner
Tae S. Kim, MD
William M. Kleinschmidt and Julia J. Kleinschmidt, Ph.D.
Thomas C. Laucomer and Eve LeClaire
Dixie and Larry Lehman
Norma and N. Richard Lockmiller
Richard S. Lord
Jeffrey Lyons
M H Finance Company
Willard Z. Maughan, MD and Rona Lee Maughan, Ph.D.
Beth and Edward M. McGill, MD
Leslie A. McLachlan
Corey A. and Nancy J. Miller
Ruth A. Morey
Morgan Lions Club
Marilyn Mott, RN
David and Jann Nelson
Joan J. and Charles W. Odd
Donna L. and Ferron A. Olson, PhD
Donald E. and Mildred L. Olsson
Eugene and Jean Overfelt
Deborah S. Park
Kim and Philip Parr
Sally Allen Potvin
Janice and Keith Poulsen
Jacqueline Kim Pullos
Maria Estela and Guillermo Ramirez
Mervin J. and Verna B. Rasmussen
J. Scott Raymond, MD
Reese Henry and Company, Inc.
Rita and Ralph Reese
Carol A. and Stanley J. Riemer
David and Lois P. Salisbury
Helen F. and A. Wally Sandack
Milton and Pam Schneider
Elaine and Paul Schwanebeck
Marilyn Schwartz
Nicola M. and Michael H. Scott, MD
Michael A. and LaDonna Shea
Neil S. Shifrin
Gregory J. Skedros
Albert H. Small
Star Foundry & Machine
Suzanne and Ralph Stern
Carlton T. Sumsion
Barbara Tingey
Nicholas and Deanna Volpe
Jon P. Wagnild
Judith S. and Douglas G. Waters
West Jordan Lions Club
Vernil West
Bart and Marlene Wheelwright
Michael B. Wilcox, MD, PC
Veronica and Evan Wolf, MD, PhD
Donna and Carl T. Woolsey, Sr., MD
Betty S. Wuliger
Myrna and Steven Robert Young, MD
Gerard and Dominique Yvernault
Robert C. and Patience Ziebarth
Susan and Robert Zohlman

In Memory of

Those in whose memory gifts were made to the Moran Eye Center from January 1, 2009 through December 31, 2009

Alice Adams
Ronald Beacom
Virginia and Basil Byrne
Michael Cooper
Mariann Corcoran
Donna Cunningham
Henry J. Desz
Lyman G. Fussell
Cleon Garritson
Kathryn Goodfellow
Paul E. Griffin
Mildred M. Groves
Ray and Ruth Hudson
Reed C. Jensen
Viola B. Jensen
Heidi Linge
Violet McGrath
Becky McKenzie
Robert Dale Moss
Oscar W. Moyle III
Steven J. Nichols
Sid Nordenschild
Anna Krajnc Picco
Jamie-Lynn Ratheal
Shirley Susaeta
Mel Thompson
Jean Wertz
Shirley J. Wertz

In Honor of

Those in whose honor gifts were made to the Moran Eye Center from January 1, 2009 through December 31, 2009

Neil Anderson
John A. Moran
Rex Rushton
Barbara Tingey
Neil L. Warren
Steve Wynn

The Moran Eye Center is very grateful for the contributions made to support our mission and goals. We have made every effort to ensure that this 2009 Donor Report is as accurate as possible. Should you find an error or wish to change your listing, please feel free to contact us at (801) 585-9700.

John A. Moran Eye Center
65 Mario Capecchi Drive
Salt Lake City, UT 84132

Telephone 801.581.2352
Fax 801.581.3357